12-2012

A STUDY ON THE FUNCTION OF 14-3-3SIGMA IN REGULATING CANCER ENERGY METABOLISM

Liem M. Phan

Liem M. Phan

A STUDY ON THE FUNCTION OF 14-3-3SIGMA IN REGULATING CANCER ENERGY METABOLISM

by

Liem Minh Phan, B.S.

APPROVED

Mong-Hong Lee, Ph.D.
Supervisory Professor

Sai-Ching Yeung, M.D., Ph.D.

Honami Naora, Ph.D.

Peng Huang, M.D., Ph.D.

Hui-Kuan Lin, Ph.D.

APPROVED

Dean, The University of Texas
Graduate School of Biomedical Sciences at Houston

A STUDY ON THE FUNCTION OF 14-3-3SIGMA IN REGULATING CANCER ENERGY METABOLISM

A

DISSERTATION

Presented to the Faculty of

The University of Texas

Health Science Center at Houston

and

The University of Texas

M. D. Anderson Cancer Center

Graduate School of Biomedical Sciences

in Partial Fulfillment

of the Requirements

for the Degree of

DOCTOR OF PHILOSOPHY

by

Liem Minh Phan, B.S.

Houston, Texas

December 2012

Dedication

To all my family, my mentors, my teachers, and my friends

for their love, teaching, and support.

I couldn’t have done this without you.

Acknowledgements

I would like to express my deepest gratitude to the many people who have helped me throughout my PhD education. Without their teaching, advice, encouragement and support, I would not have been able to complete my dissertation.

I would like to offer my special thank to my mentor, Dr. Mong-Hong Lee for his patient guidance, very kind support, enthusiastic encouragement and extremely valuable advice during my study. He is truly an inspirational teacher and a formidable mentor. He is a role model of integrity, honesty, and diligence for me as well as many other students. He has taught me not only about science but also the ethical concepts to become a dedicated and successful scientist. His encouragement has tremendously helped me overcome all challenges to pursue the dream of my life – finding a cure for cancer. I have learned a lot from my mentor and sincerely thank him for his very kind help and outstanding teaching.

In addition, I would like to extend my grateful appreciation to my co-mentor, Dr. Sai-Ching Yeung for his advice, instructions and assistance in advancing my research. His innovative ideas, dedicated working ethics, and constant passion for research have inspired me to continuously make progress every day in my career and explore new horizons in science and technology. I also particularly appreciate his kind willingness to take care of my lab fellows and me during our study.

Furthermore, I wish to offer my special thanks to the Members of my Advisory, Examining and Supervisory Committees. I am deeply grateful to Dr.

Honami Naora, Dr. Hui-Kuan Lin, Dr. Peng Huang, Dr. Xin Lin, Dr. Dos Sarbassov and Dr. Pierre McCrea for their very helpful advice, valuable suggestions and outstanding guidance. Without their support, I would not have been able to complete this PhD study.

I also sincerely thank my previous mentor, Dr. Hector Martinez-Valdez, for his excellent teaching, and very kind help. In addition, I highly appreciate and thank the support and guidance of my previous lab members, Dr. Morgan McKeller, Dr. Blanca Ortiz-Quintero, Dr. Bon Trinh, Dr. Sara Herrera-Rodriguez, Dr. Wenbin Ma, Cristina Kashi and Ramon Garcia.

My gratitude is also extended to all my friends and collaborators. It is truly a great privilege to have the opportunity to work with them and become their friends. I sincerely thank Ping-Chieh (Ben) Chou, Guermarie Velazquez-Torres, Dr. Ismael Samudio, Kenneth Parreno, Yaling Huang, Chieh Tseng, Thuy Vu, Dr. Chris Gully, Dr. Chun-Hui Su, Edward Wang, Dr. Jian Chen, Hyun-Ho Choi, Dr. Enrique Fuentes-Mattei[1], Ji-Hyun Shin, Christine Shiang, Dr. Brian Grabiner, Dr. Marzenna Blonska, Dr. Yiping Shao, Dr. Dianna Cody, Jorge Delacerda, Charles Kingsley, Douglas Webb, Colin Carlock, Dr. Zhongguo Zhou, Nibal Rizk, Dr. Yun-Chih Hsieh, Dr. Jaehyuk Lee, Dr. Andrew Elliott, Dr. Marc Ramirez, Dr. Jim Bankson, Dr. Yongxing Wang, Dr. Lei Li, Dr. Shaofan Weng, Dr. Hua Wang, Dr. Huamin Wang, Dr. Aijun Zhang, Dr. Xuefeng Xia, Dr. Yun Wu, Dr. Wei Yang, Dr. Lajos Pusztai, Dr. Ngo Vu, Dr. Louis Staudt, Dr. Ngoc Phan, Dr. Nhut Duong, Dr.

Duong Ho, Dr. Thuoc Linh, Dr. Su Pham, Mr. Ghe Tran, Dr. Phuc Pham, Dr. Thang Nguyen, Dr. Yu-Ye Wen, and Dr. Ruiying Zhao. I also very much appreciate the expert support from Dr. Zhenbo Han and Su Zhang. The assistance and encouragement from my friends and collaborators are indispensable for the success of my PhD thesis. From the bottom of my heart, I am very grateful and sincerely thank all my friends and other people who have helped me along the way of my research career and life.

Moreover, I would like to extend my special thanks to all my teachers, professors and friends who have given me excellent teaching, valuable advice and offered very strong suppport. I am very grateful to every one in my graduate school (The University of Texas Graduate School of Biomedical Sciences) and my department (MD Anderson Cancer Center, Department of Molecular and Cellular Oncology) for providing me with the education, training and helping me in my study. I especially thank Vietnam Education Foundation, Rosalie B. Hite Foundation, Department of Defense Breast Cancer Research Program, Andrew Sowell-Wade Huggins Foundation, Sylvan Rodriguez/Cancer Answers Foundation and many other fellowship foundations and sponsors for giving me the opportunity to pursue my graduate study and my dream to find a cure for cancer.

Last but not least, I am deeply grateful to everyone in my family, especially my parents, my brother, my wife, my parents-in-law, my grand parents, my

uncles, my aunts, and cousins for their unconditional love, care, advice, encouragement, and strong support. They shared my successes, happiness, and challenges along the way of my career and life. Without them, I would not have been able to complete this project and pursue my dream. There are not enough words or ways to express my deepest gratitude to each and every one of my family. From the bottom of my heart, I would like to let them know that I am very grateful.

ABSTRACT

Metabolic reprogramming has been shown to be a major cancer hallmark providing tumor cells with significant advantages for survival, proliferation, growth, metastasis and resistance against anti-cancer therapies. Glycolysis, glutaminolysis and mitochondrial biogenesis are among the most essential cancer metabolic alterations because these pathways provide cancer cells with not only energy but also crucial metabolites to support large-scale biosynthesis, rapid proliferation and tumorigenesis. In this study, we find that 14-3-3σ suppresses all these three metabolic processes by promoting the degradation of their main driver, c-Myc. In fact, 14-3-3σ significantly enhances c-Myc poly-ubiquitination and subsequent degradation, reduces c-Myc transcriptional activity, and down-regulates c-Myc-induced metabolic target genes expression. Therefore, 14-3-3σ remarkably blocks glycolysis, decreases glutaminolysis and diminishes mitochondrial mass of cancer cells both *in vitro* and *in vivo*, thereby severely suppressing cancer bioenergetics and metabolism. As a result, a high level of 14-3-3σ in tumors is strongly associated with increased breast cancer patients' overall and metastasis-free survival as well as better clinical outcomes. Thus, this study reveals a new role for 14-3-3σ as a significant regulator of cancer bioenergetics and a promising target for the development of anti-cancer metabolism therapies.

GRAPHICAL ABSTRACT

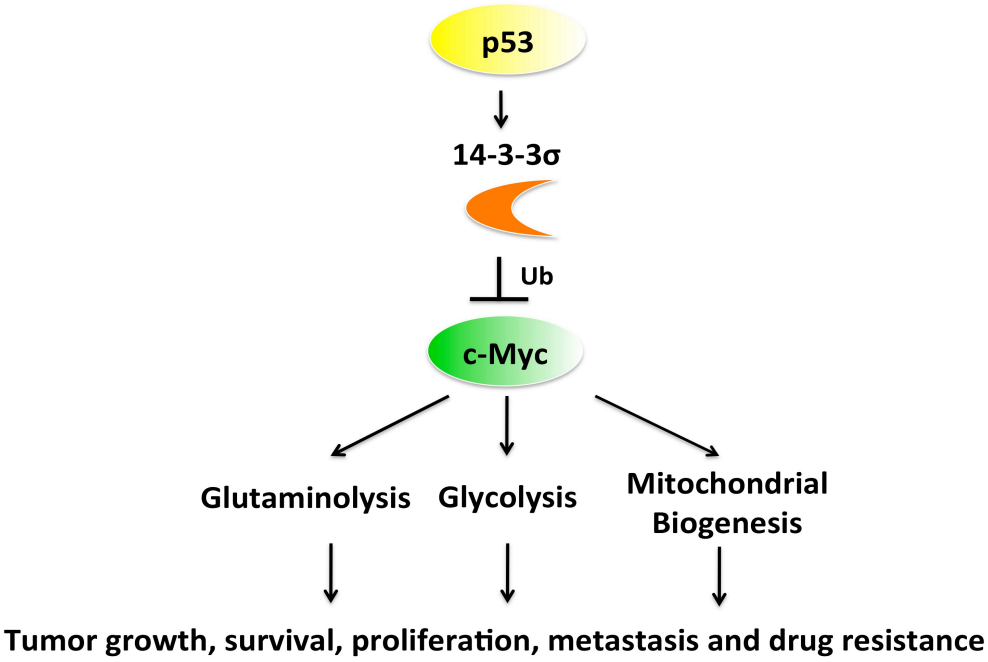

Figure 1

Figure 1. 14-3-3σ suppresses cancer glycolysis, glutaminolysis and mitochondrial biogenesis by targeting c-Myc. Glycolysis, glutaminolysis and mitochondrial biogenesis are essential metabolic alterations for cancer cells because they provide not only the necessary energy but also vital metabolites for rapid cell division and large-scale biosynthesis, for instance amino acid, lipid, nucleotide syntheses. Therefore, these metabolic processes are important for tumor growth, survival, proliferation, metastasis and resistance to anti-cancer therapies. Myc has been characterized as a main driver of these three metabolic pathways. In fact, Myc induces the expression of many target genes that are crucial for glycolysis, glutaminolysis and mitochondrial biogenesis. On the other hand, 14-3-3σ is a tumor suppressor that is directly transactivated by p53. In this study, we find that 14-3-3σ suppresses glycolytic pathway, reduces glutaminolysis and decreases mitochondrial mass in cancer cells by promoting the ubiquitination and degradation of Myc. Furthermore, metabolomics analysis additionally suggests that 14-3-3σ may also control phospholipid metabolism, as well as nucleotide and amino acid biosynthesis, which indicates a broad impact of 14-3-3σ on cancer metabolism. Thus, 14-3-3σ severely affects cancer bioenergetics and may ultimately decrease tumor growth, survival, proliferation, metastasis as well as resistance to anti-cancer therapies.

TABLE OF CONTENTS

List of Figures

List of Tables

List of Abbreviations

2-NBDG	2-(N-(7-nitrobenz-2-oxa-1,3-diazol-4-yl)amino)-2-deoxyglucose
ACTB	Beta actin
Ad-14-3-3σ	Adenovirus carrying 14-3-3σ gene
Ad-βgal	Adenovirus carrying beta galactosidase gene
ADP	Adenosine diphosphate
ASCT2	Anti-Neutral amino acid transporter 2 (synonym of SLC1A5)
ATCC	American Type Culture Collection
ATP	Adenosine triphosphate
BCL-2	B-cell Chronic lymphocytic leukemia/lymphoma 2
BCL-XL	BCL2-like 1
CAD	Carbamoyl-phosphate synthetase 2
CDC2 or CDK1	Cyclin-dependent kinase 1
CDK2	Cyclin-dependent kinase 2
cDNA	complementary deoxyribonucleic acid
Chx	Cycloheximide
CI	Confidence interval
CMV	Cytomegalo virus
CMV/TO	Cytomegalo virus / Tetracycline Repressor Operator
DHFR	Dihydrofolate reductase
DMEM	Dulbecco's Modified Eagle Medium
DMSO	Dimethyl sulfoxide

DNA	Deoxyribonucleic acid
DNP	Dynamic nuclear polarisation
DSB	Double strand break
ECAR	Extracellular Acidification Rate
ENO1	Enolase 1
FADH2	reduced flavin adenine dinucleotide
FCCP	Carbonyl cyanide 4-(trifluoromethoxy)phenylhydrazone
FDG	Fluorodeoxyglucose
GAPDH	Glyceraldehyde 3-phosphate dehydrogenase
GLS1	Glutaminase 1
GPI	Glucose-6-phosphate Isomerase
GSEA	Gene Set Enrichment Analysis
HIF1A	Hypoxia-inducible factor 1
HK2	Hexokinase 2
HLH	Helix-loop-helix
ID	inner diameter
IHC	Immunohistochemistry
IKK	I-kappa-B kinase
k_{PL}	rate constant of ^{13}C pyruvate-to-^{13}C lactate reaction
LDHA	Lactate Dehydrognease
LPL	Lipoprotein lipase
LZ	Leucine zipper

MDACC	M.D. Anderson Cancer Center
MDM2	Murine double minute 2, p53 E3 ubiquitin protein ligase homolog (mouse)
miR	micro RNA
MrDb or DDX18	DEAD (Asp-Glu-Ala-Asp) box polypeptide 18
MRI	Magnetic Resonance Imaging
mRNA	messenger ribonucleic acid
MRSI	Magnetic Resonance Spectroscopy Imaging
MT-CO1	mitochondrial cytochrome c oxidase I
MT-ND1	NADH dehydrogenase
mtDNA	mitochondrial DNA
NAD	nicotinamide adenine dinucleotide
NAO	10-Nonyl Acridine Orange
NDAH	reduced nicotinamide adenine dinucleotide
NDAPH	reduced nicotinamide adenine dinucleotide phosphate
NF-κB	Nuclear Factor KB
NIMA	(never in mitosis gene a)-related kinase 1
NMR	Nuclear Magnetic Resonance
NP-40	Nonidet P40
OCR	Oxygen Consumption Rate
PARP-1	poly(ADP-ribose) polymerase
PDH	Pyruvate Dehydrogenase

PDK1	Pyruvate Dehydrogenase Kinase
PET	Positron Emission Tomography
PET SUV	Positron Emission Tomography Standardized Uptake Value
PFK1	Phosphofructose kinase 1
PFK2	Phosphofructose kinase 2
PGK1	Phosphoglycerate kinase 1
PGM1	Phosphoglucomutase-1
Pi	inorganic Phosphate
Pin1	peptidylprolyl cis/trans isomerase, NIMA-interacting 1
PKM2	Pyruvate Kinase M2 isoform
PPP	Pentose phosphate pathway
PPRC1	Peroxisome proliferator-activated receptor gamma
qRT-PCR	quantitative Realtime Polymerase Chain Reaction
RCC1	Regulator of chromosome condensation 1
RNA	Ribonucleic acid
SCO2	Synthesis of cytochrome c oxidase-2
shRNA	short hairpin ribonucleic acid
SLC1A5 or ASCT2	Solute carrier family 1 (neutral amino acid transporter), member 5 [Homo sapiens]
SLC2A1 or Glut1	Solute carrier family 2 (facilitated glucose transporter), member 1
SLC2A2 or Glut2	Solute carrier family 2 (facilitated glucose transporter), member 2
SLC2A3 or Glut3	Solute carrier family 2 (facilitated glucose transporter), member 3

SLC2A4 or Glut4	Solute carrier family 2 (facilitated glucose transporter), member 4
SN2 or SLC38A5	Solute carrier family 38, member 5 (a high-affinity glutamine importer)
TCA	Tricarboxylic Acid cycle
TERT	Telomerase Reverse Transcriptase
TetR BSR	Tetracycline Repressor - Blasticidine Resistance Fusion Protein
TFAM	Transcription Factor A, Mitochondrial
TIGAR	TP53-induced glycolysis and apoptosis regulator
TK	Thymidine kinase 1, soluble
TPI	Triosephosphate isomerase 1
wt	wild type
α-KG	alpha ketoglutarate

Chapter 1. Introduction

1.1 Cancer metabolic reprogramming

Cancer metabolic reprogramming has been shown to be a major emerging hallmark of cancer providing tumor cells with significant advantages in proliferation, growth, metastasis, survival and resistance to anti-cancer therapies (Hanahan and Weinberg, 2011; Yeung et al., 2008). Among the most significant alterations of cancer cells bioenergetics, increase in glycolysis, glutaminolysis and mitochondrial biogenesis is essential for tumor formation and progression. These metabolic processes are crucial because they provide not only energy but also important metabolites to support large-scale biosynthesis and rapid proliferation of tumor cells.(Dang, 2010a; Hanahan and Weinberg, 2011; Wallace, 2012; Yeung et al., 2008).

a. Cancer glycolysis

Glycolysis is an important cellular metabolic process that sequentially catabolizes D-glucose ($C_6H_{12}O_6$) into pyruvate (CH_3COCOO^-). Glycolysis includes 10 sequential reactions that produce 10 intermediate metabolites. The energy from glycolysis is used to produce ATP (adenosine triphosphate) and also NADH (reduced nicotinamide adenine dinucleotide). The general reaction of glycolysis is listed as below:

$$C_6H_{12}O_6 + 2\ NAD^+ + 2\ ADP + 2\ P_i \rightarrow 2\ CH_3COCOO^- + 2\ NADH + 2\ H^+ + 2\ ATP + 2\ H_2O$$

There is a significant difference between normal and tumor cells regarding their preference for glycolysis. In aerobic conditions, normal cells prefer mitochondrial

oxidative phosphorylation. These healthy cells use glycolysis to convert glucose to pyruvate and then to Acetyl-CoA to fuel the Tricarboxylic Acid Cycle (TCA cycle) and electron transport chain in mitochondria. Only under hypoxic conditions, glycolysis is prioritized and most of pyruvate is processed to lactate in healthy cells. Interestingly, in 1930 and 1956, the Nobel Laureate Otto Warburg reported that even in the presence of ample amount of oxygen, cancer cells preferentially utilized glycolysis rather than mitochondrial respiration (Warburg, 1930, 1956a, b). In addition, most of pyruvate produced from glycolysis is converted to lactate in the cytosol rather than to Acetyl-CoA. This phenomenon is aerobic glycolysis and often referred as the Warburg effect (Hanahan and Weinberg, 2011; Yeung et al., 2008).

To compensate for the 18-fold lower ATP production yield by glycolysis compared to mitochondrial oxidative phosphorylation, cancer cells frequently upregulate glucose transporters, especially Glut1 (*SLC2A1*), which significantly increases glucose uptake into cytosol. Cancer cells also increase the expression of glycolytic enzymes to speed up the glycolytic rate. In some cases, malignant fast growing cells may have a glycolytic rate that is 200 times faster than that of normal tissue of the same origin (DeBerardinis et al., 2008a; Hsu and Sabatini, 2008; Jones and Thompson, 2009; Wise et al., 2008). In fact, this substantial elevation in glucose import and usage has been found in many cancer types and is the basis for Positron Emission Tomography (PET) Scan with ^{18}Fluorodeoxyglucose, a radio-labeled glucose analog, to visualize tumors.

The shift from an oxidative to a glycolytic metabolism in cancer cells confers a

significant survival advantage under hypoxic and harsh conditions. In fact, since glycolysis does not require oxygen, this metabolic pathway enables cancer cells to survive hypoxia, which occurs frequently in solid tumors. Furthermore, by shifting to glycolysis, cancer cells are able to suppress apoptosis, promote cell division, radio/chemotherapy resistance, and facilitate invasion (Gatenby and Gillies, 2004; Hanahan and Weinberg, 2011; Yeung et al., 2008). In addition, glycolysis with upregulated Lactate Dehydrogenase A (*LDHA*) also facilitates the conversion of pyruvate to lactate, which significantly reduces oxidative stress because there is less pyruvate entering mitochondria for oxidative phosphorylation (Bonnet et al., 2007; Chen, 1988). Moreover, lactate produced by cancer glycolysis is released into tumor microenvironment, lowers pH and promotes the breaking down of Extra Cellular Matrix, thereby facilitating cancer cell invasion and metastasis. Secreted lactate is also used by other neighboring cancer cells as their main energy source via the TCA cycle (Feron, 2009; Kennedy and Dewhirst, 2010; Semenza, 2008).

Interestingly, over-expression of Hexokinase 2, a glycolytic enzyme that catalyzes the phosphorylation of glucose into glucose-6-phosphate, significantly suppresses apoptosis by preventing cytochrome c release from mitochondria (Pastorino et al., 2005). More importantly, increased glycolysis enables the diversion of glycolytic metabolites into many other important biosynthetic pathways to generate nucleotides, nicotinamide adenine dinucleotide phosphate (NADPH), amino acids and other macromolecules that are important for cell growth and division (Potter, 1958; Vander Heiden et al., 2009; Yeung et al., 2008). Notably, elevated glycolysis is also present in

stem cells, which suggests a role of this metabolic pathway in promoting survival and proliferation of cancer progenitors (Hanahan and Weinberg, 2011).

Glycolytic metabolism is also crucial for cancer cells to survive and resist anti-cancer therapies. In fact, glycolysis promotes the production of NADPH by fueling pentose phosphate pathway (Mazurek et al., 1997). NADPH is an important reducing factor that is crucial for cytochrome P-450-mediated drug detoxification. Moreover, glycolytic pathway also regenerates NAD^+ that is essential for DNA damage repair. In this reaction, poly(ADP-ribose) polymerase (PARP-1) breaks down NAD^+ into ADP-ribose and nicotinamide. Then, ADP-ribose is further polymerized by PARP-1 and transferred to nuclear proteins. Therefore, PARP-1 activation uses a large amount of NAD^+ to repair DNA damage (Ying et al., 2005). In addition, ATP from glycolysis is also an important material for DNA reparation and a major energy source for Multi Drug Resistance 1 to discard toxic chemotherapeutic agents (Yeung et al., 2008).

In addition to generating ATP, glycolysis supplies cancer cells with important precursors for crucial biosynthetic pathways. For example, glucose-6-phosphate of glycolysis can fuel pentose phosphate pathway for subsequent nucleotide synthesis, an important process required for cell proliferation (Hsu and Sabatini, 2008). Dihydroxyacetone phosphate, another glycolysis intermediate, can be converted to glycerol-3-phosphate to form triglycerides and lipids (Gruning et al., 2011; Wallace, 2012).

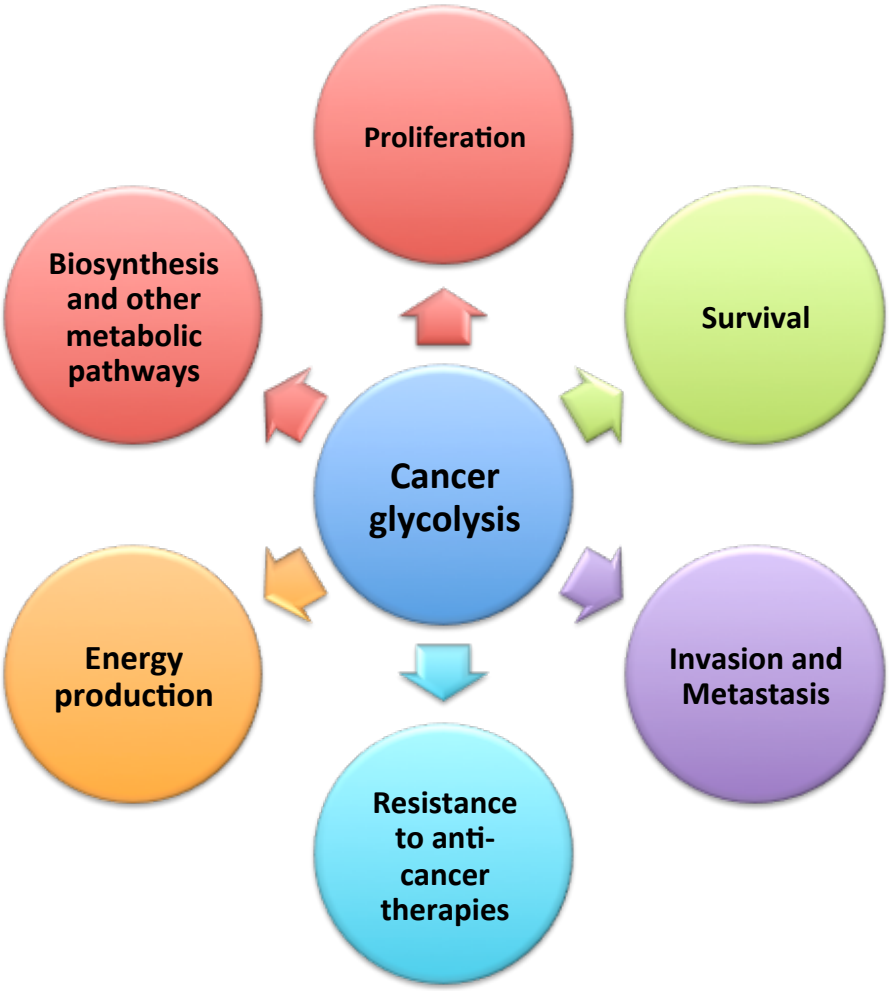
Proliferation
Survival
Invasion and Metastasis
Resistance to anti-cancer therapies
Energy production
Biosynthesis and other metabolic pathways
Cancer glycolysis

Figure 2

Figure 2. Cancer glycolysis is essential for tumor cells. Increased glycolysis has been shown to be a common and very important feature of cancer bioenergetics. In fact, this metabolic pathway provides cancer cells with energy and metabolites to support cell growth, proliferation, biosynthesis and metabolism. In addition, glycolysis significantly increases survival, promotes metastasis and enhances resistance to anti-cancer therapies.

At the molecular level, aerobic glycolysis in cancer cells has been shown to be driven by activated oncogenes as *Myc, HIF1a, Ras* and suppressed by tumor suppressors, e.g., *TP53* (DeBerardinis et al., 2008a; Deberardinis et al., 2008b; Jones and Thompson, 2009; Yeung et al., 2008). The important role of Myc in inducing aerobic glycolysis has been well documented in many studies. Hexokinase 2 (*HK2*), Phosphatefructose Kinase (*PFK1*), Glucose-6-phosphate Isomerase (*GPI*), Enolase 1 (*ENO1*), Lactate Dehydrogenase A (*LDHA*) and glucose transporter Glut1 (*SLC2A1*) are direct targets of Myc. Conserved canonical E box (5'-CACGTG-3') has been found in 31-111 base pair islands of *ENO1, HK2*, and *LDHA*. Non-conserved canonical E boxes also occur in *GPI*, pyruvate kinase 2 (*PKM2*), phosphoglycerate kinase 1 (*PGK1*), glyceraldehyde 3-phosphate dehydrogenase (*GAPDH*) and triose phosphate isomerase 1 (*TPI1*). Nuclear run-on and Chromatin Immunoprecipitation assays in multiple independent studies additionally confirmed the upregulation of these glycolytic enzymes due to Myc and the binding of Myc to these target genes (Dang, 2009; Kim et al., 2004; Li et al., 2005; Yeung et al., 2008).

While Myc is important to induce glycolysis in aerobic condition, HIF-1 is the major driver of glycolysis in hypoxia. Indeed, HIF-1 directly transactivates the majority of glucose transporters and glycolytic enzymes in hypoxic condition. These glycolytic genes contain HIF-1 regulatory element (Dang et al., 1997; Dang and Semenza, 1999). The list of HIF-1 glycolytic targets is presented in Figure 3. Among HIF-1-induced glycolytic genes, *LDHA* is crucial for aerobic glycolysis in cancer cells. LDHA catalyzes the reaction to convert pyruvate to lactate and regenerates NAD^+ to accelerate

glycolytic flux. Lactate is also very important for cancer cell metabolism and metastasis as discussed above. Another enzyme that is induced by both HIF-1 and Myc is pyruvate dehyrogenase kinase 1 (*PDK1*). PDK1 functionally inactivates pyruvate dehydrogenase by phosphorylation, thereby blocking the biochemical reaction that converts pyruvate to Acetyl-CoA and facilitating glycolysis (Kim et al., 2007).

In addition to its tumor suppressing ability, p53 is also a major regulator that controls the balance between glycolysis and mitochondrial oxidative phosphorylation through inducing two important target genes: TP53-induced glycolysis and apoptosis regulator **(***TIGAR*) and synthsis of cytochrome c oxidase-2 (*SCO2*) (Bensaad et al., 2006; Matoba et al., 2006). TIGAR is a fructose-bisphosphatase-2 that converts fructose-2,6-bisphosphate to fructose-6-phosphate. Since fructose-2,6-bisphosphate is a strong allosteric activator of Phosphofructose Kinase 1, an important glycolytic enzyme, TIGAR expression and activity can significantly slow down glycolytic flux. On the other hand, SCO2 is critical for cytochrome c oxidase complex of mitochondrial electron transport chain. ATP from mitochondrial respiration has been shown to inhibit Hexokinase function, thereby decelerating glycolysis (Matoba et al., 2006).

Furthermore, p53 directly binds to promoter regions of Glut1 and Glut4 to suppress the transcription of these two glucose transporters, causing a significant decrease in glucose uptake (Schwartzenberg-Bar-Yoseph et al., 2004). Additionally, p53 inhibits I-kappa-B kinase (IKK)-mediated NF-κB activation, thereby reducing the expression of Glut3, an NF-κB target gene involved in glucose transport

(Schwartzenberg-Bar-Yoseph et al., 2004).

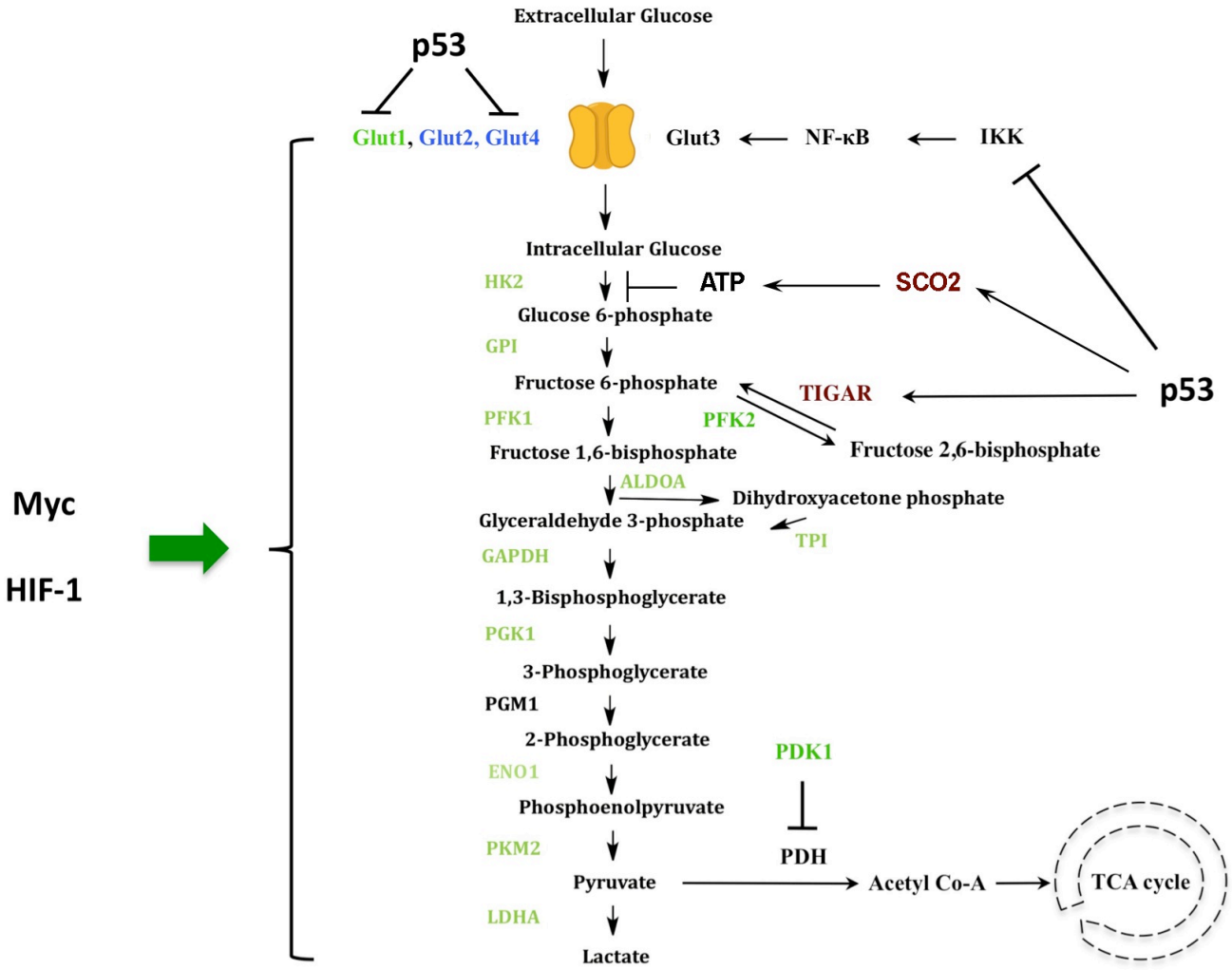
Extracellular Glucose
p53
Glut1, Glut2, Glut4
Glut3
NF-κB
IKK
Intracellular Glucose
HK2
ATP
SCO2
Glucose 6-phosphate
GPI
Fructose 6-phosphate
TIGAR
p53
PFK1
PFK2
Fructose 1,6-bisphosphate
Fructose 2,6-bisphosphate
ALDOA
Dihydroxyacetone phosphate
Glyceraldehyde 3-phosphate
TPI
GAPDH
1,3-Bisphosphoglycerate
PGK1
3-Phosphoglycerate
PGM1
2-Phosphoglycerate
PDK1
ENO1
Phosphoenolpyruvate
PKM2
PDH
Pyruvate
Acetyl Co-A
TCA cycle
LDHA
Lactate
Myc
HIF-1

Figure 3

Figure 3. Cancer glycolysis is regulated by three master regulators, Myc, HIF1 and p53. Myc and HIF-1 are strong inducers of glycolysis by transactivating the majority of glucose transporters and glycolytic enzymes. In contrast, p53 is a suppressor of this metabolic pathway by elevating the expression of TIGAR, SCO2 and suppresses the expression of important glucose transporters Glut1, Glut3, Glut4. This figure is modified from Yeung et al. 2008. The gene names that are printed in green are the common target genes of Myc and HIF1. Glut2 and Glut4 are only induced by Myc.

b. Glutaminolysis

b. Glutaminolysis

Beside glycolysis, cancer cells also depend on glutaminolysis. Glutaminolysis is a multi-step biochemical reaction sequence that converts glutamine into various metabolites. Glutaminolysis provides tumor cells with not only energy but also carbon and nitrogen sources to support their large-scale biosynthesis and rapid proliferation (Dang, 2010a). In fact, glutaminolysis plays a significant role in fueling the Tricarboxylic Acid (TCA) cycle and mitochondrial respiration. The intermediates of TCA cycle can be then further used to synthesize amino acids, nucleotides, lipids, and many other important building blocks to support the accelerated proliferation of tumor cells (Dang, 2010a; DeBerardinis et al., 2007).

Glutaminolysis is crucial for tumor growth and proliferation. In 2008, DeBerardinis et al. reported that glioma cells had a high rate of glutaminolysis to provide anaplerotic α-ketoglutarate to fuel the TCA Cycle and mitochondrial respiration, resulting in increased metabolic intermediates for active lipid, amino acid and nucleotide biosynthesis (DeBerardinis et al., 2007). The importance of glutaminolysis is also demonstrated by the multifaceted and key role of glutamine in cancer metabolism. After being imported into cytoplasm by glutamine transporters, glutamine can be used to synthesize protein, glucosamine, nucleotide, or converted by mitochondrial glutaminase (GLS) into glutamate and urea (Dang, 2010a; Wise et al., 2008). Glutamate can be then processed into α-ketoglutarate through transamination or oxidative deamination reactions (Dang, 2010a; Meng et al., 2010). In addition, glutamine is also crucial to activate TOR (target of rapamycin) kinase, a master switch of cell growth (Blommaart et

al., 1995; Dann and Thomas, 2006; Fox et al., 1998; Hara et al., 1998; Nicklin et al., 2009; Xu et al., 1998). The uptake process of essential amino acids also needs glutamine (Nicklin et al., 2009). Furthermore, glutamine is required to maintain mitochondrial membrane integrity and potential and is needed to produce NADPH, which is often used to control redox balance and synthesize macromolecules (Vander Heiden et al., 2009). Because of the importance of glutamine and glutaminolysis, a number of cancer cells are addicted to glutamine and this addiction could be exploited as a therapeutic target for cancer treatment (Wise and Thompson, 2010).

Myc is the primary inducer of glutaminolysis in cancer cells. Indeed, Myc elevates the expression of Glutaminase 1 (*GLS1*) by suppressing miR-23a/b, and transactivates glutamine importers *ASCT2* and *SN2* (Dang, 2010a; Dang et al., 2009; Gao et al., 2009). ChIP and quantitative RT-PCR data show that Myc directly induces the expression of high-affinity glutamine importers *ASCT2* and *SN2,* leading to a significant influx of glutamine (Dang, 2010a; Dang et al., 2009; Gao et al., 2009).

Interestingly, Myc-induced glutaminolysis renders many cancer cells addicted to exogenous glutamine as nitrogen and carbon sources for mitochondrial membrane potential maintenance and biosynthesis. Therefore, glutamine depletion causes apoptosis and eliminates cancer cells in a Myc-dependent manner (Wise et al., 2008; Yuneva et al., 2007). This programmed cell death due to glutamine deprivation could be reversed by overexpressing BCL-2, BCL-X_L as well as a dominant negative caspase-9 mutant (Wise et al., 2008; Yuneva et al., 2007). Supplying cancer cells with pyruvate, α-

ketoglutarate, and oxaloacetate also prevents this cell death, indicating the importance of glutamine in mitochondrial anaplerosis (Yuneva et al., 2007). In fact, glutamine deprivation of cancer cells that have a high Myc level results in a significant decrease in TCA cycle intermediates concentrations. Importantly, excessive glucose abundance still can't reverse this reduction, which implies that Myc may abolish the ability of cancer cells to use glucose for mitochondrial anaplerosis by upregulating LDHA to convert pyruvate to lactate (Wise and Thompson, 2010; Yuneva et al., 2007). Thus, glutaminolysis is crucial for cancer cells in terms of energy production and biosynthesis.

c. Mitochondrial biogenesis

In contrast to common thinking, mitochondrial biogenesis is essential for the tumor cells because mitochondria are the key nexus of the majority of biosynthetic pathways and energy production. Furthermore, mitochondria also regulate redox status and Ca^{2+} concentration (Wallace, 2012). Therefore, lack of mitochondria severely reduces tumorigenesis, tumor growth and colony formation (Cavalli et al., 1997; Desjardins et al., 1985; King and Attardi, 1989; Magda et al., 2008; Morais et al., 1994; Wallace, 2012; Weinberg et al., 2010). Moreover, compared to normal and differentiated cells, cancer cells reprogram their mitochondria to change from a maximal energy production by mitochondrial respiration to a balance between energy demands with large-scale biogenesis and rapid cell division (Wallace, 2012). Therefore, mitochondria in general and mitochondrial biogenesis in particular are very important for tumor cells.

It has been well documented that Myc is a major inducer of mitochondrial biogenesis. Indeed, Myc promotes the expression of many nuclear-encoded mitochondrial genes and directly transactivating Transcription Factor A, Mitochondrial (*TFAM)*, a transcription factor that is essential for mitochondrial genes transcription and mitochondrial DNA replication (Li et al., 2005). Since the synthesis of new mitochondrial components and mitochondrial DNA is crucial for mitochondrial biogenesis, Myc plays a critical role in increasing mitochondria number. Consequently, lack of Myc severely diminishes mitochondrial mass and mitochondrial biogenesis, leading to a negative impact on many metabolic pathways of cancer cells (Li et al., 2005).

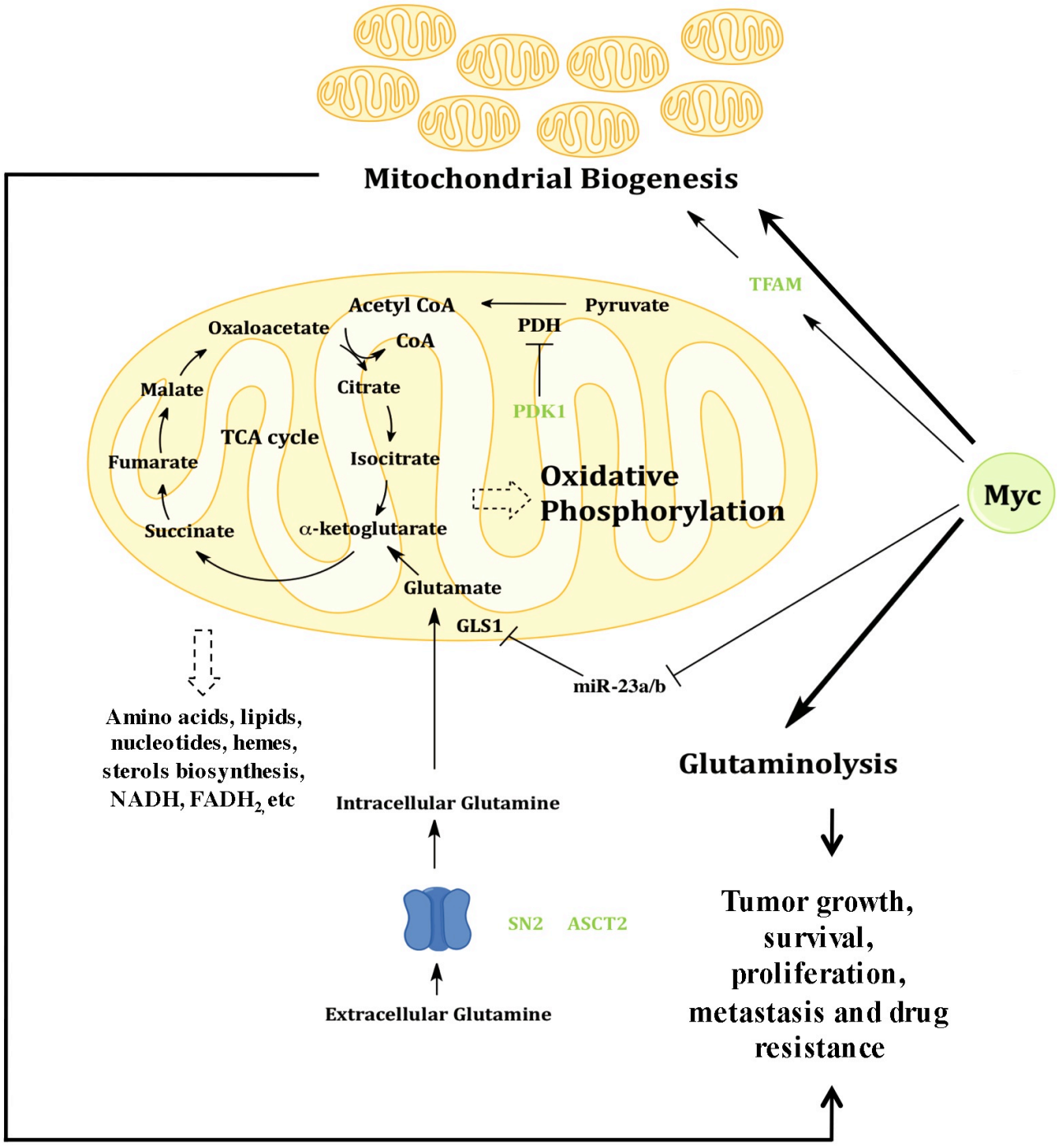
Mitochondrial Biogenesis
TFAM
Acetyl CoA
Pyruvate
PDH
Oxaloacetate
CoA
Citrate
Malate
PDK1
TCA cycle
Isocitrate
Fumarate
Oxidative Phosphorylation
Myc
Succinate
α-ketoglutarate
Glutamate
GLS1
miR-23a/b
Amino acids, lipids, nucleotides, hemes, sterols biosynthesis, NADH, FADH2, etc
Glutaminolysis
Intracellular Glutamine
SN2
ASCT2
Tumor growth, survival, proliferation, metastasis and drug resistance
Extracellular Glutamine

Figure 4

Figure 4. Glutaminolysis and mitochondrial biogenesis provide important energy and metabolites for cancer cells to support tumor growth, survival, proliferation, metastasis and resistance to anti-cancer therapies. In glutaminolytic pathway, glutamine is imported into cytoplasm by glutamine transporters, mostly by ASCT2 and SN2. Glutamine is then converted to glutamate by glutaminase. Glutamate is then processed into α-ketoglutarate that participates in TCA cycle. TCA cycle generates NADH and $FADH_2$ that donate electrons to mitochondrial respiratory chain to produce ATP. In addition, TCA cycle intermediates can also be used to synthesize amino acids, lipids, nucleotides, sterols, among other important molecules, to support rapid proliferation of cancer cells. On the other hand, mitochondrial biogenesis is also vital for cancer cells because mitochondria play a key role in producing energy and synthesizing many crucial macromolecules and metabolites for cell growth and division. Myc has been shown to induce glutaminolysis by up-regulating glutaminase, ASCT2 and SN2 expression. Myc also transactivates the genes that encode mitochondrial components. In addition, Myc induces the expression of Transcription Factor A, Mitochondrial (*TFAM*). TFAM bends mitochondrial DNA and facilitates mitochondrial gene transcription and mitochondrial DNA replication, which is required for mitochondrial biogenesis. Thus, Myc is an important inducer of both glutaminolysis and mitochondrial biogenesis that are crucial for cancer cell metabolism.

1.2 Myc

c-*myc* (Myc) is the cellular equivalent of the v-*myc* oncogene from retroviruses (Bishop, 1982, 1985; Bishop et al., 1978; Bister and Jansen, 1986; Sheiness et al., 1978). The proto-oncogene c-*myc* is a member of myc family consisting of L-*myc*, B-*myc*, N-*myc*, and s-*myc*. Nevertheless, c-*myc*, L-*myc*, and N-*myc* are the only isoforms that induce aberrant proliferation (Facchini and Penn, 1998; Henriksson and Luscher, 1996; Lemaitre et al., 1996; Marcu et al., 1992; Spencer and Groudine, 1991). Deletion of c-*myc* results in embryonic lethality, indicating the essential role of c-*myc* in development and survival (Davis et al., 1993).

Myc is an important transcription factor regulating multiple essential signaling pathways (Dang, 1999; Yeung et al., 2008) (Figure 5). Myc contains a transactivation/repression domain in its N-terminus as well as a helix-loop-helix leucine zipper (HLH/LZ) domain at the C-terminus (Figure 6). The canonical DNA binding site of Myc is 5′-CACGTG-3′ but Myc can also bind to non-canonical sequences to transactivate or suppress its target genes expression (Blackwell et al., 1993; Blackwell et al., 1990; Prendergast and Ziff, 1991). By dimerizing with Max, Myc transactivates its target genes. Myc is also able to repress transcription by associating with other transcriptional activators, for instance Miz-1 (Amati, 2004). On the other hand, Myc is frequently overexpressed in many human cancers. Myc is a major oncogenic transcription factor that can induce tumorigenesis by promoting cell proliferation, causing genome instability, and blocking cell differentiation (Adhikary and Eilers, 2005).

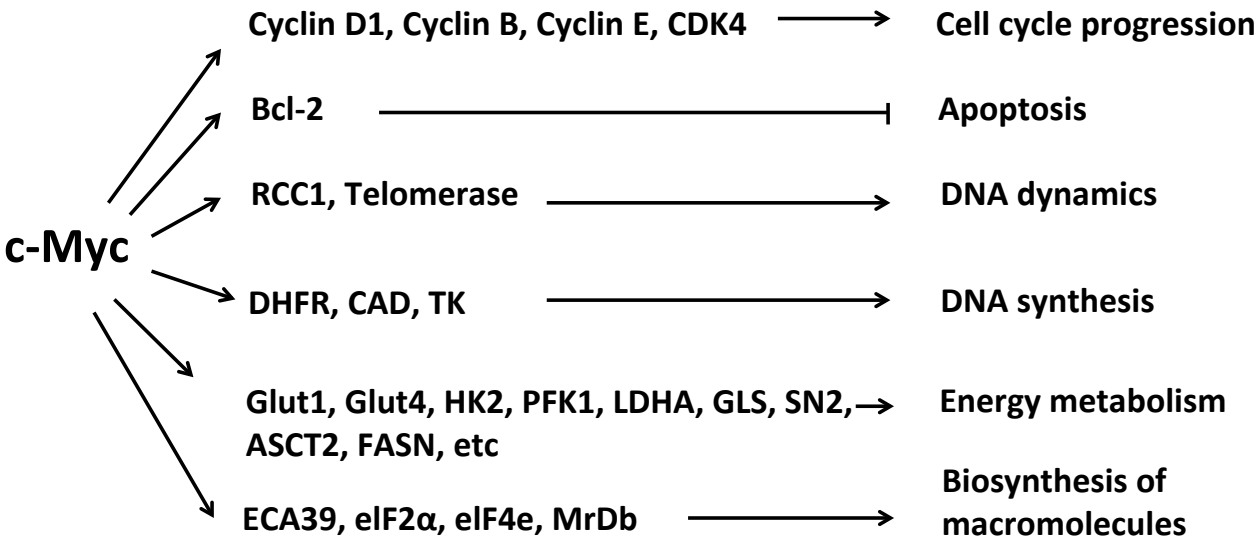
c-Myc
Cyclin D1, Cyclin B, Cyclin E, CDK4
Cell cycle progression
Bcl-2
Apoptosis
RCC1, Telomerase
DNA dynamics
DHFR, CAD, TK
DNA synthesis
Glut1, Glut4, HK2, PFK1, LDHA, GLS, SN2, ASCT2, FASN, etc
Energy metabolism
ECA39, elF2α, elF4e, MrDb
Biosynthesis of macromolecules

Figure 5

Figure 5. Myc plays an important role in controlling multiple essential cellular processes, for instance cell cycle progression, apoptosis, DNA dynamics, DNA synthesis, energy metabolism, and biosynthesis of macromolecules. This figure is modified from Dang, 1999. All full gene names are listed in the List of Abbreviations (pages xxi – xxv).

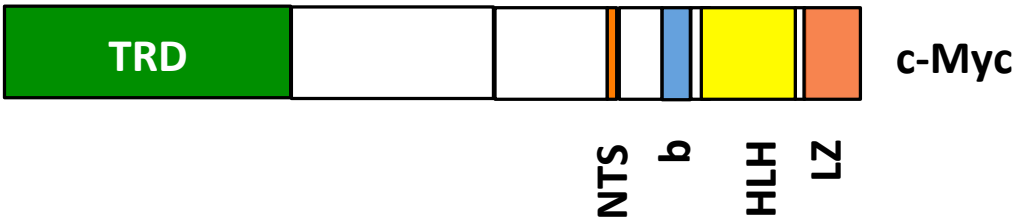

Figure 6

Figure 6. The domains and motifs of Myc protein. TRD: Transcriptional Regulatory Domain; HLH-LZ: Helix-Loop-Helix/Leucine Zipper motif; b: basic region; NTS: nuclear target signal.

In particular, it has been well documented that Myc is a strong inducer of important metabolic alterations in cancer cells (Dang, 2010a; Dang et al., 2009; Li et al., 2005; Yeung et al., 2008). Indeed, Myc is one of the master regulators that remarkably upregulates the majority of glycolytic genes, thereby promoting glucose consumption and glycolysis (Dang, 2010b; Yeung et al., 2008). The upregulation of these glycolytic enzymes is due to Myc binding to its target genes for transcriptional activation (Dang et al., 2009; Kim et al., 2004; Li et al., 2005; Yeung et al., 2008). Myc also elevates the expression of glutaminase and glutamine transporters ASCT2 and SN2, thereby increasing glutaminolysis in cancer cells (Dang, 2010a, b). Moreover, Myc stimulates mitochondrial biogenesis by up-regulating the expression of *TFAM* and mitochondrial components (Li et al., 2005). On the other hand, Myc also induces the expression of important genes involved in nucleotide synthesis and amino acid transport (Dang et al., 1997). Thus the broad impact of Myc on multiple metabolic pathways makes Myc one of the master regulators of cancer metabolism and gives the Myc-highly-expressing cancer cells the ability to effectively adapt to various conditions and the versatility to use different nutrient sources to support rapid tumor growth, proliferation and metastasis.

1.3 14-3-3σ

14-3-3σ has been widely known for its function in cell cycle regulation and apoptosis. This protein is a unique member of 14-3-3 family, which consists of 7 members (Benzinger et al., 2005a; Benzinger et al., 2005b). While other 14-3-3 family members form both hetero and homo-dimers, 14-3-3σ has a strong preference in forming homo-dimers. In addition, compared to other 14-3-3 isoforms, 14-3-3σ contains a different C terminus structure, which allows it to associate with a distinct set of interacting partners (Benzinger et al., 2005b; Wilker et al., 2005).

It is notable that 14-3-3σ is a phospho Serine/Threonine binding protein with two consensus binding motifs RxxpSxP and RxxxpSxP (Benzinger et al., 2005a; Benzinger et al., 2005b) that are found on the C terminus of c-Myc. This implies a potential physical interaction between 14-3-3σ and c-Myc. The binding of 14-3-3σ to its interacting partners often results in significant changes in stability, localization, interaction and activity of these target proteins (Lee and Lozano, 2006; Verdoodt et al., 2006).

Among 14-3-3 family members, only 14-3-3σ is induced by p53 after DNA damage (Hermeking et al., 1997). After being induced by p53, 14-3-3σ generates a positive feed back loop by protecting p53 from MDM2-mediated ubiquitination and degradation. 14-3-3σ sequesters MDM2 to cytoplasm and promotes MDM2 self-ubiquitination. In addition, 14-3-3σ also enhances p53 tetramerization and transactivational activity (Yang et al., 2003; Yang et al., 2007). 14-3-3σ is also known to cause cell cycle arrest at G1 phase by inhibiting CDK2/CyclinE, and at G2 phase by sequestering CDC2/CyclinB (Lee and Lozano, 2006).

14-3-3σ is commonly down-regulated in many common types of cancer. This loss can be caused either by excessive methylation of the promoter region of 14-3-3σ gene (Ferguson et al., 2000) or by enhanced ubiquitin-mediated degradation of 14-3-3σ (Choi et al., 2011; Urano et al., 2002). The loss of 14-3-3σ expression provides a growth advantage to cancer cells and leads to poor prognosis (Lee and Lozano, 2006), as 14-3-3σ has been demonstrated to have tumor suppressive qualities (Yang et al., 2006; Yang et al., 2003).

In spite of all this information, how 14-3-3σ suppresses tumorigenesis is not fully understood and whether 14-3-3σ involves in the regulation of cancer metabolism remains unknown. In this study, we demonstrate that 14-3-3σ is a strong inhibitor of cancer glycolysis, glutaminolysis and mitochondrial biogenesis by promoting Myc degradation. Thus, our data not only provides an additional insight into the regulation of cancer metabolism but also discovers a new function of the potent tumor suppressor 14-3-3σ and holds the potential to unlock a door to the development of anti-cancer metabolism therapies.

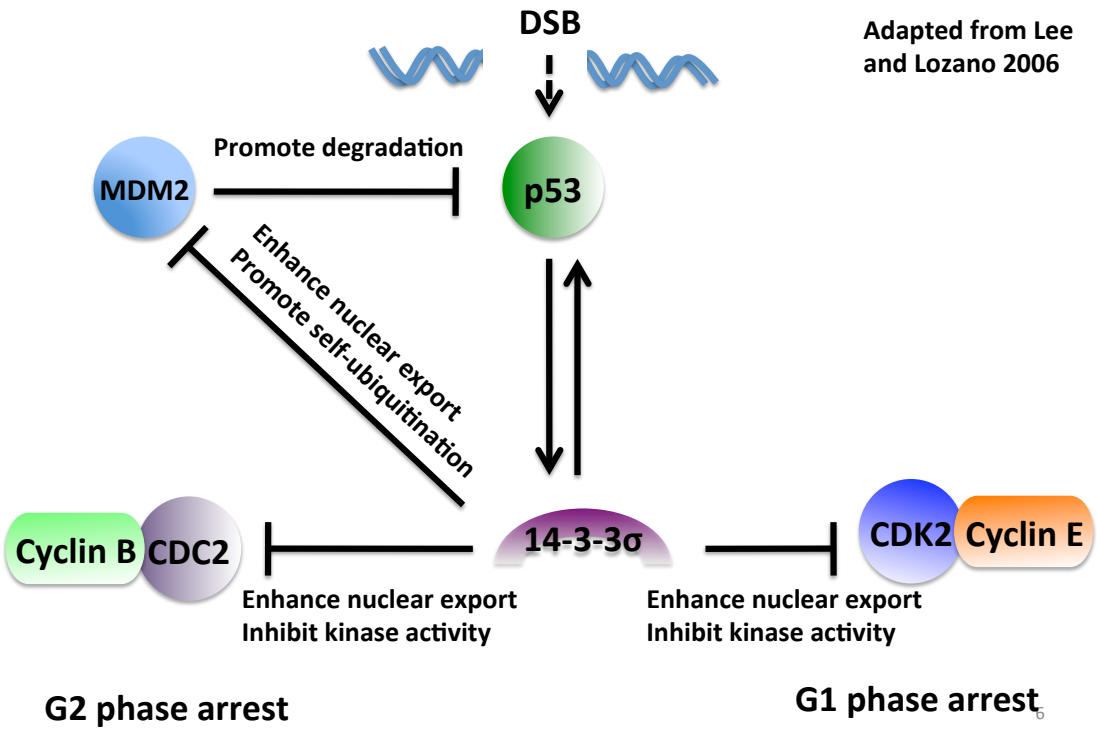
DSB
Adapted from Lee and Lozano 2006
MDM2
Promote degradation
p53
Enhance nuclear export
Promote self-ubiquitination
Cyclin B
CDC2
14-3-3σ
CDK2
Cyclin E
Enhance nuclear export
Inhibit kinase activity
Enhance nuclear export
Inhibit kinase activity
G2 phase arrest
G1 phase arrest

Figure 7

Figure 7. 14-3-3σ stabilizes p53 and induces cell cycle arrest. Upon DNA damage or double strand break (DSB), p53 is activated. p53 directly transactivates 14-3-3σ. 14-3-3σ exerts a positive feedback stabilizing p53 by causing MDM2 nuclear export and enhancing MDM2 self-ubiquitination. 14-3-3σ also promotes the nuclear export of CyclinB/CDC2 and CDK2/Cyclin E complexes. 14-3-3σ suppresses kinase activity of CDK2 and CDC2. As a result, cell cycle progression will stop at G1 and G2 phases when 14-3-3σ is transactivated.

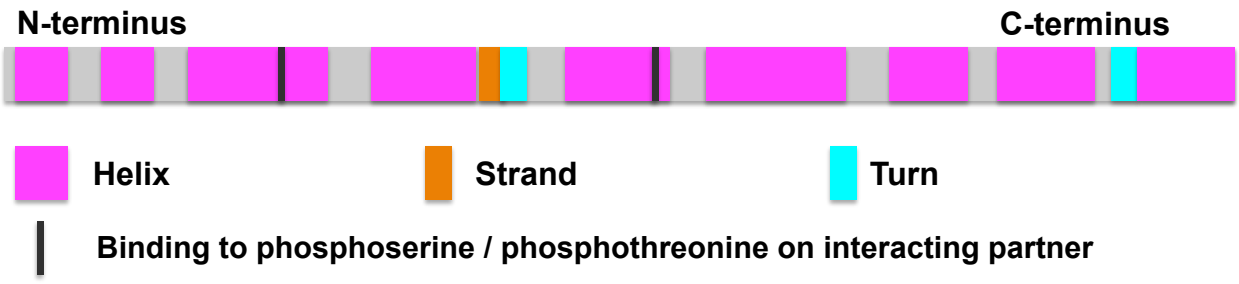

Source: UniProt KB Database, (identifier: P31947-1)

Figure 8

Figure 8. Domain mapping of 14-3-3σ protein. 14-3-3σ contains 9 helices, 1 strand and 2 turns in its structure. 14-3-3σ uses its N-terminus to form homo-dimers and its C-terminus to interact with its partners. 14-3-3σ is a phosphoserine/phosphothreonine binding protein. The unique structure of 14-3-3σ C-terminus enables 14-3-3σ to interact with a distinct set of target proteins compared to other 14-3-3 family members.

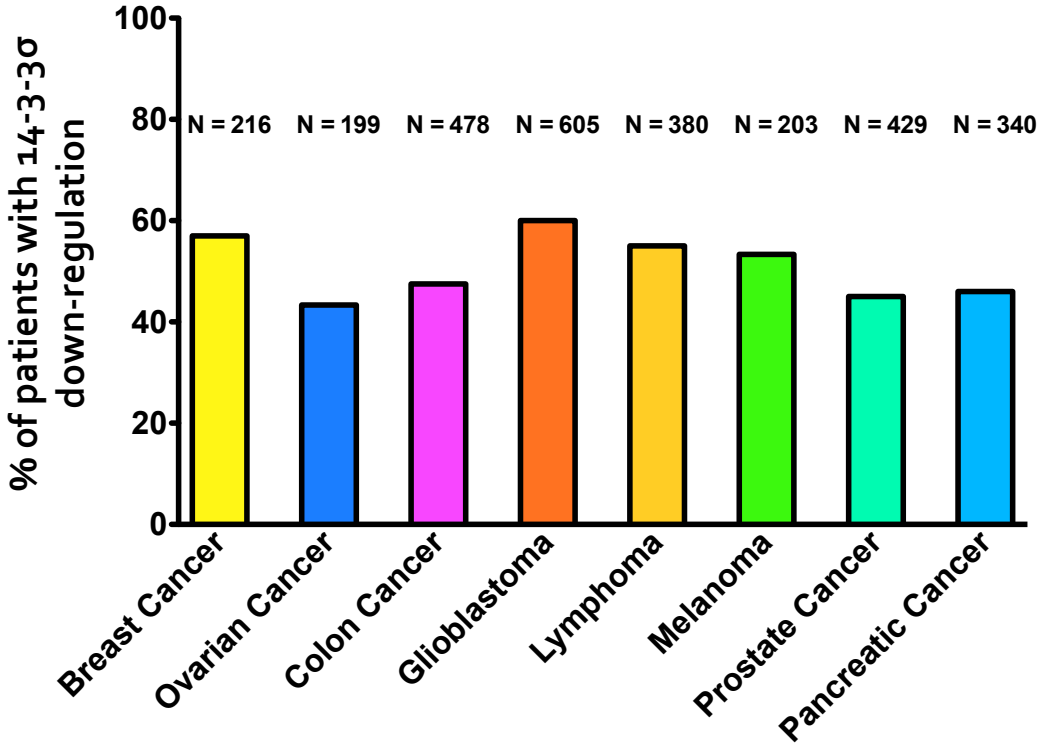
% of patients with 14-3-3σ down-regulation
100
80
60
40
20
0
N = 216
N = 199
N = 478
N = 605
N = 380
N = 203
N = 429
N = 340
Breast Cancer
Ovarian Cancer
Colon Cancer
Glioblastoma
Lymphoma
Melanoma
Prostate Cancer
Pancreatic Cancer

Figure 9

Figure 9. 14-3-3σ expression is commonly suppressed in many common cancers. 14-3-3σ level was determined by analyzing transcriptomics profiles of cancer patients that were retrieved from public databases such as Oncomine, The Cancer Genome Atlas, Gene Expression Omnibus. For each type of cancer, N indicates the number of patients included in our analysis. The patients that have more than 60% decrease in 14-3-3σ mRNA expression level compared to corresponding normal tissues were considered as having 14-3-3σ down-regulation.

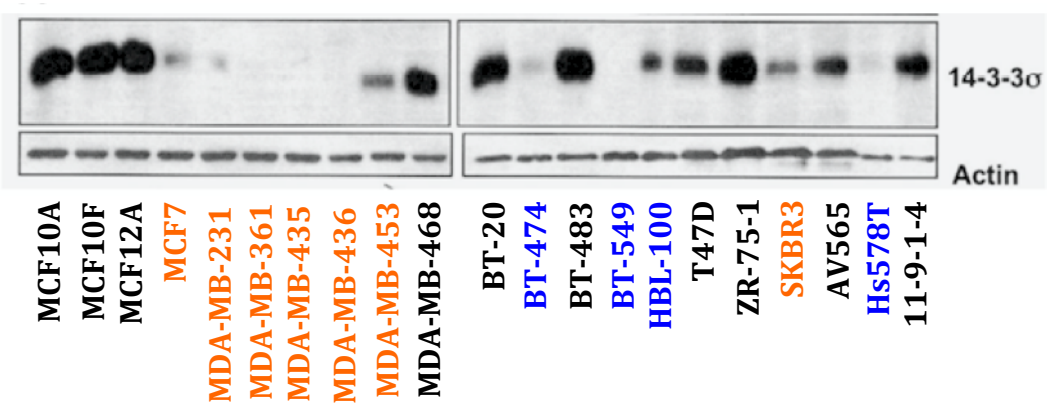
14-3-3σ
Actin
MCF10A
MCF10F
MCF12A
MCF7
MDA-MB-231
MDA-MB-361
MDA-MB-435
MDA-MB-436
MDA-MB-453
MDA-MB-468
BT-20
BT-474
BT-483
BT-549
HBL-100
T47D
ZR-75-1
SKBR3
AV565
Hs578T
11-9-1-4

Figure 10

Figure 10. 14-3-3σ expression is frequently down-regulated in metastatic (orange printed) and invasive (blue printed) breast cancer cell lines. MCF10A, MCF10F, MCF12A are non-tumorigenic epithelial cells having high level of 14-3-3σ. MCF-7, MDA-MB-231, MDA-MB-361, MDA-MB-435, MDA-MB-436, MDA-MB-453 and SKBR3 are metastatic breast cancer cell lines with very low 14-3-3σ expression. BT474, BT549, HBL-100 and Hs578T are invasive breast carcinoma cell lines with low 14-3-3σ amounts. BT20, BT483, T47D, ZR-75-1, and 11-9-1-4 are weakly invasive breast carcinoma cell lines that have moderate or abundant 14-3-3σ presence. The high level of 14-3-3σ in early/non-invasive breast cancer cells and down-regulation of 14-3-3σ in advanced, metastatic and invasive breast cancer cells suggest the role of 14-3-3σ as a checkpoint that cancer cells need to bypass during tumorigenesis.

1.4 Rationale and hypothesis:

Our transcriptomics analysis and tissue micro array screening of more than 700 tumors from breast cancer patients indicated an inverse correlation between 14-3-3σ level and metabolic enzymes expression, which suggests a role of 14-3-3σ in controlling cancer metabolism. Furthermore, our previous studies showed that 14-3-3σ decreased c-Myc stability while increasing p53 expression (Wen et al., 2012; Yang et al., 2003). Since c-Myc and p53 are two major regulators of cancer bioenergetics, these observations prompt us to hypothesize that **14-3-3σ may play an important role in regulating essential cancer energy metabolic pathways that are controlled by c-Myc and p53, such as glycolysis, glutaminolysis and mitochondrial biogenesis.**

Chapter 2. Materials and Methods

2.1 Tissue Culture

MDA-MB-231, MDA-MB-435, T47D, MCF10A, H1299 cancer cell lines were pruchased from the ATCC (Manassas, VA, USA) and grown in DMEM High glucose medium which is supplemented with 10% fetal bovine serum (FBS) (Sigma-Aldrich, Atlanta Biologicals), 2 mM L-glutamine (Cellgro, Manassas, VA) as well as 1% antibiotic-antimycotic solution (Invitrogen, Grand Island, NY). HCT116 wt, 14-3-3$\sigma^{-/-}$, and $p53^{-/-}$ colon cancer cells (a kind gift from Dr. Bert Vogelstein's Lab) were also cultured in DMEM High glucose medium containing 10% fetal bovine serum (Sigma-Aldrich, Atlanta Biologicals), 2 mM L-glutamine from Cellgro (Manassas, VA) and 1% antibiotic-antimycotic solution from Invitrogen (Grand Island, NY). All cells were grown in humidified 37^{o}C incubator with 5% CO_2. MDA-MB-231, MDA-MB-435, HCT116 wt, 14-3-3$\sigma^{-/-}$, $p53^{-/-}$ cell lines that carry a Tet On Flag-14-3-3σ system were grown in DMEM High glucose medium containing 10% Tetracycline-free fetal bovine serum (Atlanta Biologicals), 2 mM L-glutamine from Cellgro (Manassas, VA) and 1% antibiotic-antimycotic solution from Invitrogen (Grand Island, NY).

2.2 Western Blot analysis

Cells were lysed using a standard lysis buffer containing NP-40 and 0.1% TritonX-100. The antibodies used were: from Sigma-Aldrich: anti-Flag, anti-Actin; from Cell Signaling: anti-Hexokinase 2, anti-Aldolase, anti-Pyruvate Kinase M2, anti-Lactate Dehydrogenase A, anti-Pyruvate Dehydrogenase Kinase 1, anti-Enolase 1, anti-

Glutaminase; from Novus Biologicals: anti-Phosphofructose Kinase 1, from Fitzgerald International Industry: anti-14-3-3σ; from Abcam and Epitomics: anti-c-Myc.

2.3 Lactate production and glucose consumption assays

Lactate concentration was measured with an Accutrend Lactate Analyzer (Roche). Glucose consumption was determined by measuring the difference in glucose concentrations at the beginning and the end of experiments. Glucose level was quantified using a Freestyle Glucose Meter (Abbott). Lactate production and glucose consumption were normalized to final cell number and culture time.

2.4 Establishment of retroviral Tet On 14-3-3σ system

Flag-14-3-3σ cDNA was amplified by PCR from a pCMV5-Flag-14-3-3σ plasmid in Dr. Lee's lab and cloned into a pRetro-CMV/TO retroviral plasmid (kindly provided by Dr. Staudt's lab, National Cancer Institute (NCI)). After sequence verification, the pRetro/CMV-TO-Flag-14-3-3σ plasmid was co-transfeted with VSVg and Gag/Pol plasmids into 293T cells to produce 14-3-3σ Tet On retroviruses. Tet Repressor retroviruses were produced from the 293T cells after co-transfection of p-BMN-TetR-BSR, VSVg and Gag/Pol plasmids (kindly provided by Dr. Staudt's lab, NCI).

Target cells were first infected with TetR-BSR retroviruses and then selected with a medium containing 20 μg/ml Blasticidin for 1 week. After that, the cells were infected with retroviruses carrying Flag-14-3-3σ and followed by a selection with 5 μg/ml

Puromycin for 1 week. Target cells with established Tet On Flag-14-3-3σ system were maintained in a regular medium containing 10% Tetracycline-free fetal bovine serum, 2 μg/ml Puromycin, 10 μg/ml Blasticidin, 2 mM L-glutamine and 1% antibiotic-antimycotic solution. To induce 14-3-3σ's expression *in vitro*, Doxycycline (a stable derivative of Tetracycline) was added to the culture medium at final concentration of 5 ng/ml for 48 hours. To induce 14-3-3σ's expression *in vivo*, Doxycycline was added to drinking water at a final concentration of 200 μg/ml of Doxycycline for 2 weeks. Drinking water that contains Doxycycline was replaced every 48 hours because of the short half-life of Doxycycline.

2.5 Experiment plan for microPET Scan and hyperpolarized ^{13}C-pyruvate-based Magnetic Resonance Spectroscopy Imaging to examine the impact of 14-3-3σ on glucose uptake and pyruvate-lactate flux *in vivo*.

^{18}Fluorodeoxyglucose (^{18}FDG) microPET Scan experiment design

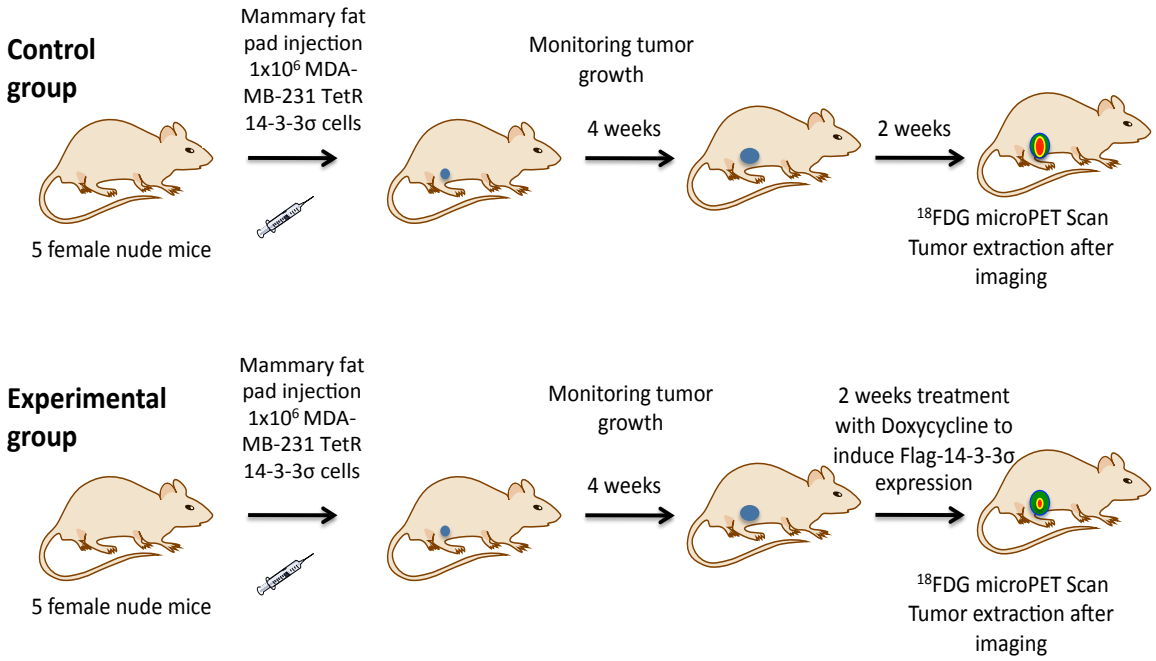

Hyperpolarized ^{13}C-pyruvate Magnetic Resonance Spectroscopy Imaging (MRSI) experiment design

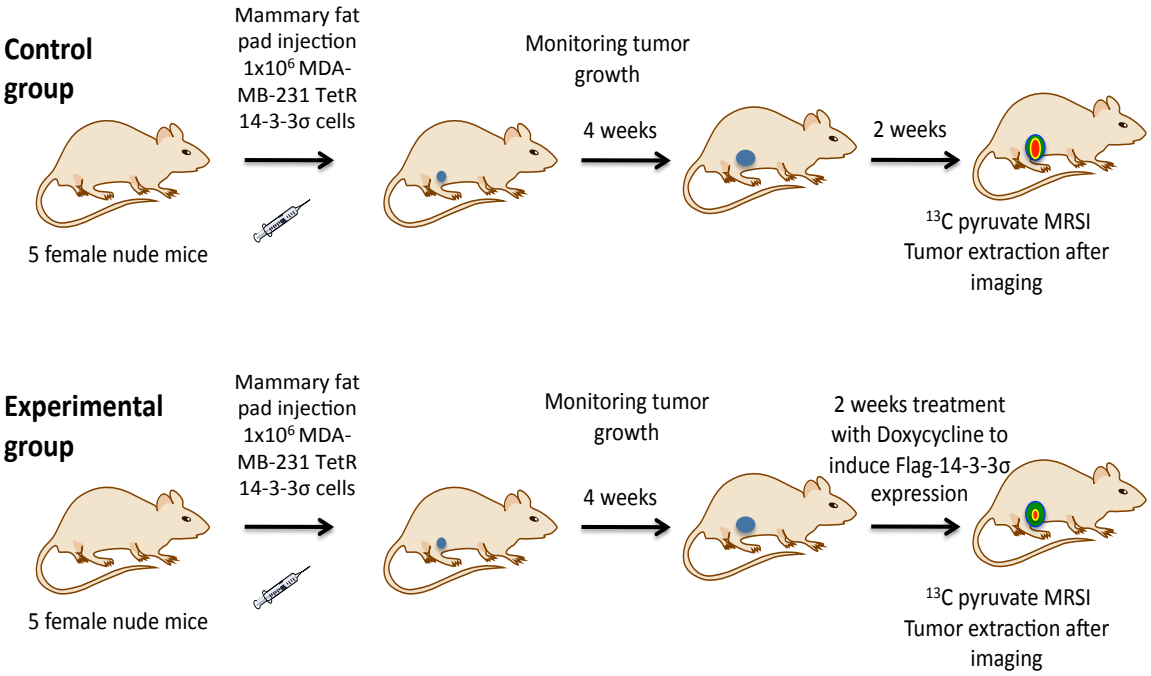

Figure 11

Figure 11. The *in vivo* experiment plan to study the impact of 14-3-3σ on cancer metabolism. $1x10^6$ MDA-MB-231 TetR 14-3-3σ cells were injected into mammary fat pad of each 7-week old female nude mouse. Tumor growth was monitored for 4 weeks. All mice were then divided into two groups with 5-10 mice in each group. The experimental group received drinking water containing 200 μg/ml Doxycycline for 2 weeks to induce Flag-14-3-3σ expression in the xenografted breast tumors. The control group received normal drinking water. The 1^{st} batch of mice with both the control and experimental groups were subjected to a microPET Scan with ^{18}FDG to measure the negative impact of 14-3-3σ on glucose uptake *in vivo*. Similarly, the 2^{nd} batch of mice with both the control and experimental groups were imaged with hyperpolarized ^{13}C-pyruvate-based Magnetic Resonance Spectroscopy Imaging (MRSI) to evaluate the suppressive influence of 14-3-3σ on pyruvate-lactate flux in xenograft tumors. All tumors were extracted after imaging and used for further analyses.

2.6 Glucose uptake assay and microPET Scan

Glucose uptake in cells was examined using (2-(*N*-(7-nitrobenz-2-oxa-1,3-diazol-4-yl)amino)-2-deoxyglucose (2-NBDG)), a green fluorescent glucose analog, from Molecular Probes (Invitrogen). Experimental cells were incubated in glucose-free 10% FBS DMEM containing 120 μM 2-NBDG for 0 minute, 1 minute, 10 minutes, 30 minutes, 1 hour, 2 hours and 3 hours. 2-NBDG uptake was analyzed using a fluorescent microscope (Olympus) and BD Flow Cytometer.

For glucose uptake in mice, 7-week-old female nude mice carrying MDA-MB-231 TetR 14-3-3σ breast cancer cells were imaged with a Micropet Rodent–R4 scanner 30 minutes after injection with 400 μCi ^{18}FDG according to imaging protocol from the Small Animal Imaging Facility (SAIF) of M.D. Anderson Cancer Center (MDACC). Tumors were also visualized with a Burker 7.0 Tesla Magnetic Resonance Imaging (MRI) at SAIF following SAIF standard imaging procedures.

2.7 Hyperpolarized ^{13}C-pyruvate Magnetic Resonance Spectroscopy Imaging

^{13}C Hyperpolarization

A mixture containing 20 μL (26 mg) of [1-^{13}C] pyruvic acid (Cambridge Isotopes) with 15 mM of trityl radical OX063 (GE Healthcare) was combined with 0.6 μL 50mM Prohance (Bracco Diagnostic Inc.) and polarized using a Hypersense DNP system (Oxford Instruments). In brief, the solution was frozen to approximately 1.4°K and irradiated at 94.154 GHz for 45 - 60 minutes in a 3.35T magnetic field (Ardenkjaer-

Larsen et al., 2003; Golman et al., 2006). When the solid-state polarization reached a plateau, the solution was dissolved in 4 mL of a heated (180°C) solution containing 80 mM NaOH and 50 mM NaCl. The final solution containing 80 mM hyperpolarized pyruvate at a nominal temperature of 37°C and pH of 7.6 was flushed into a receptacle from which 200 μL was drawn for injection. The injection was administered over 10 seconds beginning within 12 seconds of sample dissolution.

Magnetic Resonance Spectroscopy

Animals were anesthetized using 0.5%-5% isoflurane in oxygen and then placed on a positioning sled with built-in channels for distribution of anesthesia gases and circulation of warm water to maintain animal temperature. All experiments and procedures involved animals were approved by MD Anderson Cancer Center Institutional Animal Care and Use Committee. This committee is accredited by the Association for the Assessment and Accreditation of Laboratory Animal Care International.

The chemical fate of the hyperpolarized [1-13C]-pyruvate was monitored using a 7T Biospec USR7030 system (Bruker Biospin MRI, Inc) using a dual-tuned ^{1}H-^{13}C volume coil with 72 mm inner diameter (ID) and a custom-built ^{13}C surface coil (12 mm ID) placed over the tumor. Animal position was confirmed using a 3-plane gradient-echo proton MRI sequence (TE = 3.6 ms, TR = 100 ms, 30° excitation angle) and the location of the tumor was confirmed in T2-weighted axial and coronal spin-echo images (TE = 50ms, TR = 2500ms, 1 mm slice thickness, 4 cm x 3 cm field-of-view encoded

over a 256 x 192 matrix in 1 mm sections). Field homogeneity was maximized over the tumor volume using a point-resolved spectroscopy sequence.

For ^{13}C measurements, a signal was generated by the volume coil and detected using the surface coil. Dynamic spectra were acquired using a slice-selective single-pulse sequence (SW = 5000 Hz over 2048 points, 10° excitation, 8 mm slice thickness) that was repeated every 2 seconds for 3 minutes beginning just prior to the injection of ^{13}C via tail-vein catheter. The spectra were phase-adjusted, and the area under the spectral peaks corresponding to the C1 of pyruvate and lactate were integrated to generate curves describing the arrival of hyperpolarized pyruvate and its conversion into hyperpolarized lactate. These curves were fit to kinetic models that account for chemical conversion (Harris et al., 2009). The model we used is a modification from the one described by Harris et al., 2009. Our model had two physical compartments to separate the effects of tracer circulation, extravasation, and activity. All modeling was performed using Matlab (The Mathworks) and statistical analysis was performed using GraphPad Prism 5.0d.

2.8 Measurement of Extracellular Acidification Rate (ECAR) and Oxygen Consumption Rate (OCR)

Cells and Compounds:

All cancer cell lines with retroviral 14-3-3σ Tet On system such as MDA-MB-231, HCT116, and H1299 were maintained in a growth medium: DMEM High glucose supplemented with 10% Tetracycline-free fetal bovine serum, 2 μg/ml Puromycin, 10

μg/ml Blasticidin, 2 mM L-glutamine and 1% antibiotic-antimycotic solution. The other cancer cell lines were maintained in a different growth medium: DMEM High glucose containing 10% normal fetal bovine serum, 2 mM L-glutamine as well as 1% antibiotic-antimycotic solution.

Oligomycin (an inhibitor of ATP Synthase) was prepared as 1000X stock at 10 mM in DMSO. FCCP (an ionophore and strong mitochondrial depolarizer) was diluted as 1000X stock at 5 mM in DMSO. Rotenone (a potent inhibitor of mitochondrial complex I) and Antimycin A (a strong suppressor of mitochondrial complex III) were solubilized as 1000X stock at 10 mM in DMSO.

Assay

To measured ECAR and OCR, $3x10^4$ cells from each cell line were seeded per well of a XF24 microplate 16 hours before the experiment. Right before the Seahorse XF assay, the cells were changed from a culture medium to an assay medium (low-buffered DMEM containing 25 mM D-glucose, 1 mM of sodium pyruvate and 1 mM of L-glutamine) and incubated for 1 hour at 37^{o}C. After a baseline measurement, 75 μl of the above-mentioned inhibitors prepared in assay medium was sequentially injected into each well to reach the final working 1X concentrations. After 5 minutes of mixing to equally expose cancer cells to the chemical inhibitors, OCR and ECAR were measured. OCR was reported in pmole/minute, ECAR was recorded in mpH/minute. Results were analyzed using Seahorse XF software. Statistical analysis was done with GraphPad Prism and Sigma Plot programs. OCR and ECAR measurements were normalized to either final cell number or protein concentration.

2.9 Metabolomics analysis by Nuclear Magnetic Resonance (NMR)

HCT116 14-3-3σ$^{+/+}$, HCT116 14-3-3σ$^{-/-}$, HCT116 14-3-3σ$^{-/-}$ infected with Ad-βgal, and HCT116 14-3-3σ$^{-/-}$ infected with Ad-14-3-3σ were grown under normal culture conditions for 48 hours. 20x10^{6} cells per cell line were collected and snap-frozen with liquid nitrogen. Total metabolites were then extracted from cell pellets using freezing/thawing extraction and filtration protocols provided by Chenomx Inc. (Alberta, Canada). Metabolite extracts were then snap-frozen with liquid nitrogen and shipped to Chenomx Inc. (Canada) on dry ice for NMR analysis.

2.10 Real-time PCR

For quantitative Real-time PCR (qRT-PCR), total RNA was collected using Trizol Reagents (Invitrogen) and cDNA was synthesized using an iScript cDNA Synthesis Kit (BioRad). qRT-PCR was performed with an iQ-SYBR Green Supermix (BioRad), an Applied Biosystems StepOnePlus Realtime PCR system and an iCycler CFX96 Real-Time PCR Detection System (BioRad). Actin mRNA and 18S rRNA were used for normalization.

qRT-PCR primers used to measure mRNA level:

HK2-5’ ATGAGGGGCGGATGTGTATCA

HK2-3’ GGTTCAGTGAGCCCATGTCAA

GPI-5’	GGTACACAGGCAAGACCATC
GPI-3’	GTTTTGGCAATGTGAGTTCC
PFK1-5’	GGGCGCCAAGGCTATGAACTG
PFK1-3’	GCTCCCACCCACTGCCTGCTC
ALDOA-5’	GGGTGTCATCCTCTTCCATGA
ALDOA-3’	GACCACGCCCTTGTCTACCTT
ALDOB-5’	GGAGGCTTTTATGAAGCGGG
ALDOB-3’	TGAAGAGCGACTGGGTGGAA
TPI-5’	GCACTCAGAGAGAAGGCATGT
TPI-3’	CAATGCAGGCGATTACTCCGA
PGK1-5’	GGGCAAGGATGTTCTGTTCT
PGK1-3’	TCTCCAGCAGGATGACAGAC
PGM1-5’	ACCCACTCCCTTCATACAATC
PGM1-3’	CTCCTCACTGGTCATGGCTTA
ENO1-5’	AAAGCTGGTGCCGTTGAGAAG
ENO1-3’	AGCATGAGAACCGCCATTGAT
PKM2-5’	CGCCCACGTGCCCCCATCATTG

PKM2-3’	CAGGGGCCTCCAGTCCAGCATTCC
LDHA-5’	TTCAAGGTTTATTGGGGGTTT
LDHA-3’	AGTTCTGCCACCTCTGACG
PDK1-5’	CCGCTCTCCATGAAGCAGTT
PDK1-3’	TTGCCGCAGAAACATAAATGAG
SLC2A1-5’	CCAGCTGCCATTGCCGTT
SLC2A1-3’	GACGTAGGGACCACACAGTTGC
SLC2A2-5’	GCGGCTGCGGGGCTATGATGAT
SLC2A2-3’	CGGGGGCCCTGGGAGAAGAACT
SLC2A4-5’	CTGGGCCTCACAGTGCTAC
SLC2A4-3’	GTCAGGCGCTTCAGACTCTT
TFAM-5’	AAGATTCCAAGAAGCTAAGGGTGA
TFAM 3’	CAGAGTCAGACAGATTTTTCCAGTTT
MT-CO1-5’	TCGCATCTGCTATAGTGGAG
MT-CO1-3’	ATTATTCCGAAGCCTGGTAGG
PPRC1-5’	ACAGGCAGCAAAGCGGTGTG
PPRC1-3’	AGGAATGGCCGTAGAGACGC

C17-5’ CTTTAACTTGGCTGCTTAGAC

C17-3’ CATAGTTTAGAGGGGACTCC

MT-ND1-5’ CCCATTCGCGTTATTCTT

MT-ND1-3’ AAGTTGATCGTAACGGAAGC

LPL-5’ GGATGGACGGTAAGAGTGATTC

LPL-3’ ATCCAAGGGTAGCAGACAGGT

GLS1-5’ TGGTGGCCTCAGGTGAAAAT

GLS1-3’ CCAAGCTAGGTAACAGACCCTGTTT

2.11 Dual Luciferase Reporter Assay

c-Myc transactivational activity was measured using a Dual-Luciferase Reporter Assay System from Promega with a Luciferase reporter plasmid containing a TERT (telomerase reverse transcriptase) promoter. TERT is a c-Myc target gene and its promoter contains an E-box c-Myc binding site.

2.12 Lentiviral shRNA

14-3-3σ shRNA lentiviral plasmids were purchased from Sigma-Aldrich. 14-3-3σ shRNA lentiviruses were then produced from 293T cells following the virus production protocol that is similar to the protocol described in 2.4. Infection efficiency was

enhanced using 8 µg/ml Polybrene and centrifugation at 2000 rotation per minute for 60 minutes at 32^{o}C. Knockdown efficiency was verified by Western Blot.

2.13 Bioinformatics analysis:

14-3-3σ expression level in human cancers is was analyzed using Oncomine database and Nexus Expression 3.0 (BioDiscovery). The analysis of transcriptomics landscapes of human cancer patients was done using data sets GSE5847, GSE2109, GSE11121, and GSE20194 that were downloaded from Oncomine and Gene Expression Omnibus databases. These data sets were then analyzed by Gene Set Enrichment Analysis (GSEA) (Broad Institute), Oncomine, Nexus Expression 3.0 (BioDiscovery), and Gene Spring 12 (Agilent Technologies). The Myc glycolytic target gene geneset was built by our lab. The Myc target genes geneset was made by Benporath et al. (GSEA Molecular Signature Database). (http://www.broadinstitute.org/gsea/msigdb/cards/BENPORATH_MYC_TARGETS_WITH_EBOX.html). Pearson correlation analysis was done using Prism and Sigma Plot programs. Retrospective analysis of patients' information was done under approved clinical protocols at MDACC.

2.14 Immunohistochemistry staining

Breast cancer tissue microarrays were provided by the Department of Pathology at M.D. Anderson Cancer Center (MDACC). The xenograft breast tumor slides were

constructed by the MDACC Histology Facility Core. Immunohistochemistry Hematoxylin and Eosin and cleaved Caspase 3 staining was done by the MD Anderson Cancer Center Tissue Core Lab. Other IHC staining was performed following the IHC staining protocols provided by the MDACC Department of Pathology. Tissue microarrays and tumor slides were stained with anti Pyruvate Kinase M2 antibodies (1:300 dilution, Cell Signaling), anti-Phosphofructose kinase 1 antibodies (1:300 dilution, Novus Biologicals), anti-14-3-3σ (1:200 dilution, Fitzgerald Industry International), anti-Myc (1:50 dilution, Epitomics). IHC staining results were analyzed by pathologists of the MDACC Department of Pathology and quantified using a Dako ChromaVision System ACIS III at MDACC Department of Molecular and Cellular Oncology.

2.15 Supplemental Information

All experiments involved cancer patients' samples and information have been done under approved clinical protocols at M.D. Anderson Cancer Center. All experiments and procedures involved animals were approved by M.D. Anderson Cancer Center Institutional Animal Care and Use Committee, which is accredited by the Association for the Assessment and Accreditation of Laboratory Animal Care International. All *in vitro* experiments have been repeated at least 5 times. Statistical analyses and representative pictures are shown in figures.

2.16 Biostatistics analysis

All bar graphs and line graphs are represented as mean ± 95% confidence intervals (CI) unless otherwise stated. All error bars in this thesis also represent 95% CI unless otherwise stated. The error bars of line graphs from Seahorse Extracellular Flux Analyzer are standard deviations.

Student t-test has been used to compare the difference between two groups. One-way analysis of variance (ANOVA) has been employed for comparison if there are more than two groups unless otherwise stated. * indicates p value less than 0.05. Log-rank (Mantel-Cox) test has been used to compare survival times of breast cancer patients. All experiments have been independently repeated at least 4 times.

Chapter 3. Results

3.1 High 14-3-3σ expression is associated with good clinical outcomes and negatively correlated with Myc-induced metabolic genes expression in breast cancer patients.

By correlating 14-3-3σ protein expression level in breast tumors with clinical data of breast cancer patients, we found that this tumor suppressor is associated with a positive impact on these patients' prognosis. High 14-3-3σ presence in breast tumors is correlated with a long overall and recurrence-free survival times. 95.7% of breast cancer patients with high expression of 14-3-3σ in their breast tumors have survived more than 14 years without local or distant metastasis (Figures 12A and 12B). Elevated 14-3-3σ level was also inversely correlated with tumor grade (Table 2). Thus, these data suggest a role of 14-3-3σ in suppressing tumorigenesis.

Interestingly, we noticed that high-14-3-3σ breast tumors had very low ^{18}Fluorodeoxyglucose Positron Emission Tomography Standardized Uptake Values (^{18}FDG PET SUV) (Figure 13, Table 3). PET Scan with ^{18}FDG is a powerful nuclear medicine imaging technique that relies on the high glucose uptake of cancer cells to detect local and metastatic tumors. Thus, from a metabolic standpoint, this observation suggested that 14-3-3σ might reduce the ability of tumors to uptake glucose, a vital nutrient for cancer cells.

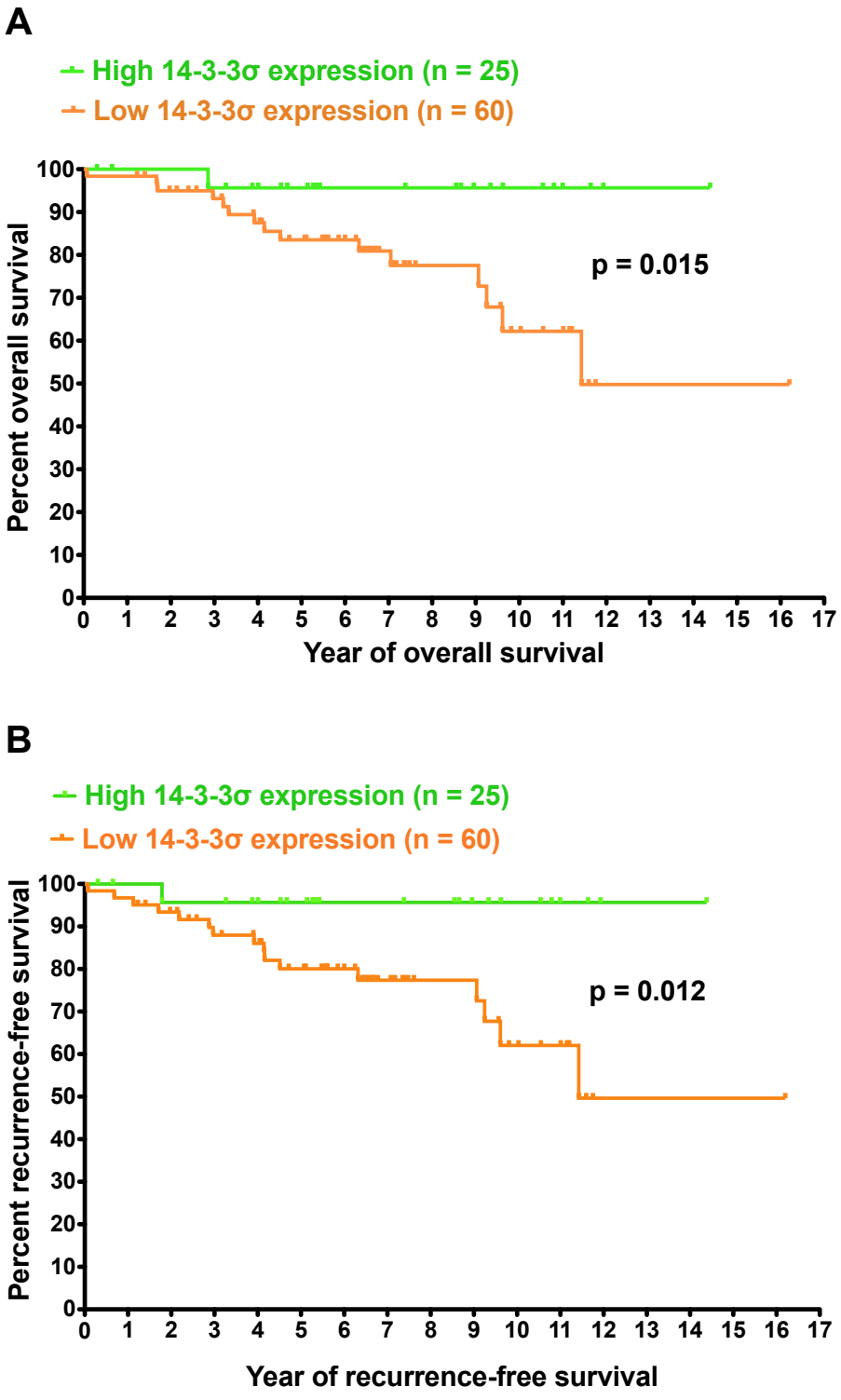
A
High 14-3-3σ expression (n = 25)
Low 14-3-3σ expression (n = 60)
Percent overall survival
p = 0.015
Year of overall survival
B
High 14-3-3σ expression (n = 25)
Low 14-3-3σ expression (n = 60)
Percent recurrence-free survival
p = 0.012
Year of recurrence-free survival

Figure 12

Figure 12. High 14-3-3σ expression is associated with prolonged overall survival and metastasis-free survival of breast cancer patients.

(A) High 14-3-3σ expression in tumors is correlated with significantly increased breast cancer patients' overall survival. 14-3-3σ protein expression in tumors was quantified based on immunohistochemistry staining of breast cancer patients' tumors tissue microarrays. The average of 14-3-3σ protein expression level of normal breast tissues was used as a reference to classify cancer patients into high and low 14-3-3σ groups. If 14-3-3σ protein level in tumors of a cancer patient was higher than the average of 14-3-3σ protein levels in normal breast tissues, that patient was considered as having a "high 14-3-3σ expression". In contrast, if 14-3-3σ protein level in tumors of a cancer patient was lower than the average of 14-3-3σ protein levels in normal breast tissues, that patient was considered as having a "low 14-3-3σ expression".

(B) Recurrence-free survival of breast cancer patients is considerably improved when 14-3-3σ expression is elevated in tumors. The 14-3-3σ classification standard was the same as in Figure 12A.

Table 1. Demographic and clinical information of breast cancer patient cohort analyzed in Figure 12

		High 14-3-3σ expression group (N=25)	Low 14-3-3σ expression group (N=60)
Race	White	19 (76%)	43 (71.6%)
	Asian	1 (4%)	4 (6.7%)
	Asian Pacific	1 (4%)	0 (0%)
	Black	1 (4%)	9 (15%)
	Hispanic	3 (12%)	4 (6.7%)
Age at diagnosis	21-40	2 (8%)	5 (8.33%)
	41-60	15 (60%)	35 (58.33%)
	61-80	8 (32%)	18 (30%)
	>81	0 (0%)	2 (3.33%)
Pathology stage at diagnosis	1	12 (48%)	22 (36.67%)
	2	7 (28%)	21 (35%)
	3	6 (24%)	17 (28.33%)
	4	0 (0%)	0 (0%)
Estrogen Receptor status	Positive	11 (44%)	34 (56.67%)
	Negative	14 (56%)	26 (43.33%)
Progesterone Receptor status	Positive	14 (56%)	27 (45%)
	Negative	11 (44%)	33 (55%)
Human epidermal growth factor receptor 2 status	Positive	11 (44%)	46 (76.67%)
	Negative	14 (56%)	14 (23.33%)
Triple Negative Breast Cancer status	Yes	8 (32%)	12 (20%)
	No	17 (68%)	48 (80%)

Table 2. 14-3-3σ's expression is inversely correlated with breast tumor grade.

		Tumor Grade			Total Number	Chi-square Test
		1	2	3		
14-3-3σ Expression	Low	7 (70%)	62 (58.5%)	**84 (67.7%)**	153	p < 0.0001
	High	3 (30%)	44 (41.5%)	**40 (32.3%)**	87	p < 0.0001
Total		10 (100%)	106 (100%)	124 (100%)	240	

Table 2. 14-3-3σ's expression is inversely correlated with breast tumor grade.

Tumor grade is determined by pathological histology. 14-3-3σ mRNA expression in the tumors was determined by transcriptomics analysis of breast cancer patients tumors' fine needle aspirates (microarrays analysis) and normalized to β-actin (*ACTB*) mRNA level. The average of 14-3-3σ/β-actin mRNA ratios of normal breast tissues was used as a reference to classify cancer patients into high and low 14-3-3σ groups. If 14-3-3σ/β-actin mRNA ratio in tumors of a cancer patient was at least 60% higher than the average of 14-3-3σ/β-actin mRNA ratios in normal breast tissues, that patient was considered as having a "high 14-3-3σ expression". In contrast, if 14-3-3σ/β-actin mRNA ratio in tumors of a cancer patient was at least 60% lower than the average of 14-3-3σ/β-actin mRNA ratios in normal breast tissues, that patient was considered as having a "low 14-3-3σ expression".

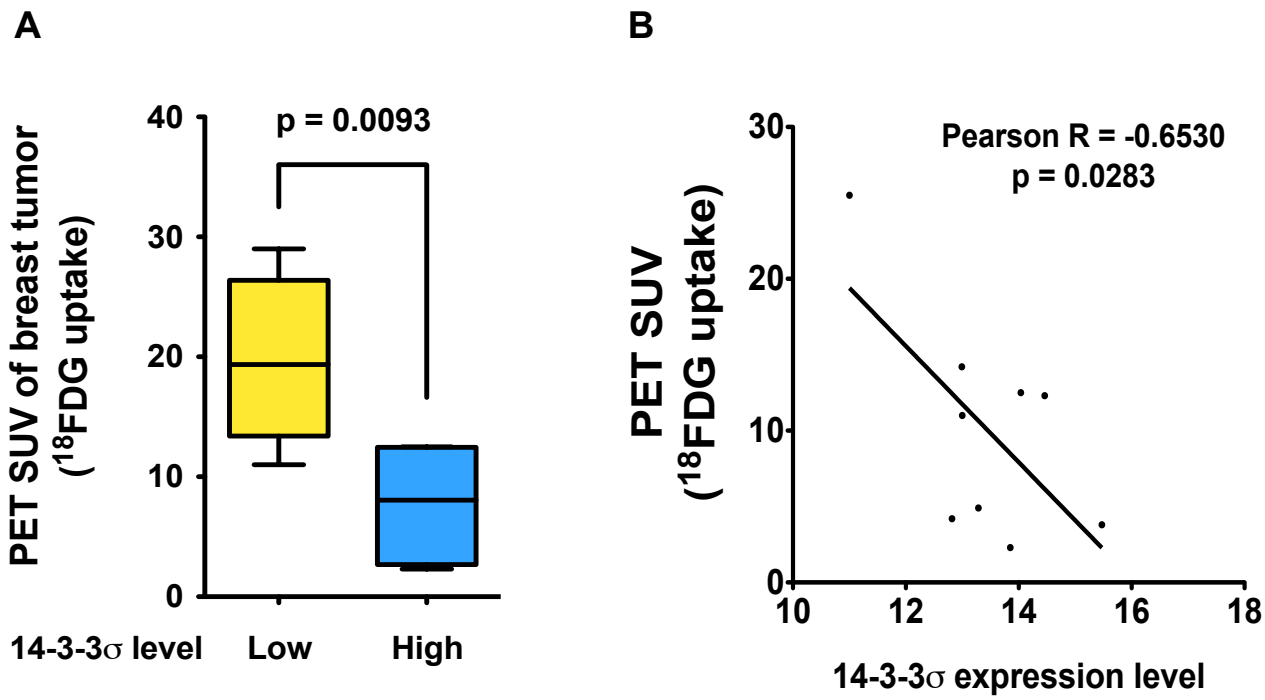
A
B
p = 0.0093
PET SUV of breast tumor
(18FDG uptake)
40
30
20
10
0
14-3-3σ level
Low
High
Pearson R = -0.6530
p = 0.0283
PET SUV
(18FDG uptake)
30
20
10
0
10
12
14
16
18
14-3-3σ expression level

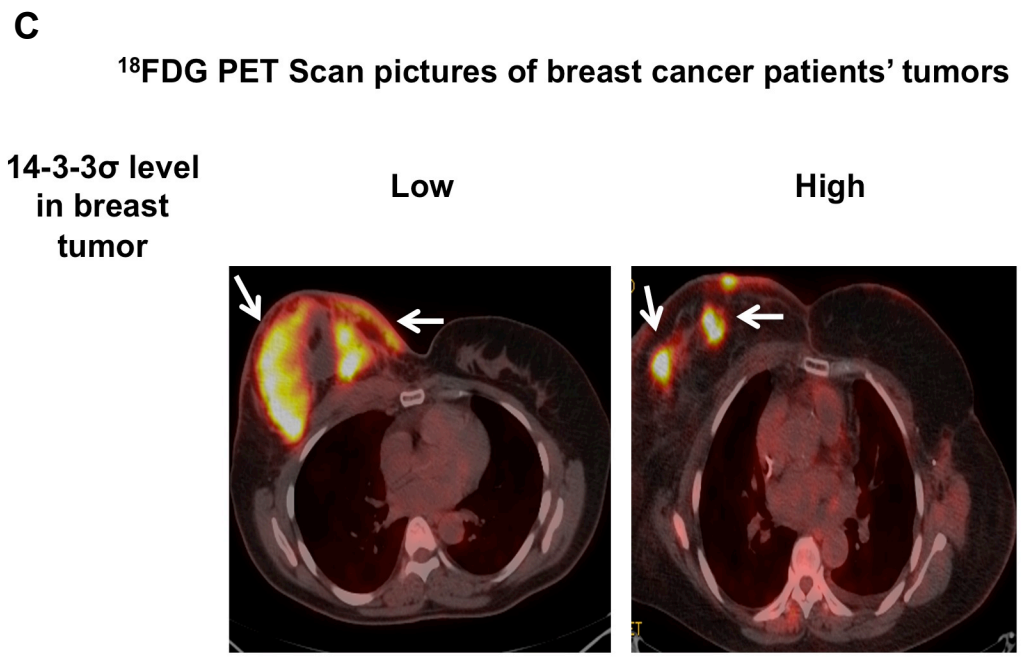
C
18FDG PET Scan pictures of breast cancer patients' tumors
14-3-3σ level in breast tumor
Low
High

Figure 13

Figure 13. High 14-3-3σ expression is associated with decreased ^{18}FDG uptake in tumors of breast cancer patients.

(A) Box plot graph implied a negative influence of 14-3-3σ on ^{18}FDG uptake of breast cancer patients' tumors. ^{18}FDG PET SUVs of breast cancer patients were measured and graphed with the expression score of 14-3-3σ, which was determined by transcriptomics analysis. Data is represented as mean ± 95% confidence intervals (CI). 14-3-3σ mRNA expression in the tumors was determined by transcriptomics analysis of breast cancer patients tumors' fine needle aspirates (microarrays analysis) and normalized to β-actin (*ACTB*) mRNA level. The average of 14-3-3σ/β-actin mRNA ratios of normal breast tissues was used as a reference to classify cancer patients into high and low 14-3-3σ groups. If 14-3-3σ/β-actin mRNA ratio in tumors of a cancer patient was at least 60% higher than the average of 14-3-3σ/β-actin mRNA ratios in normal breast tissues, that patient was considered as having a "high 14-3-3σ expression". In contrast, if 14-3-3σ/β-actin mRNA ratio in tumors of a cancer patient was at least 60% lower than the average of 14-3-3σ/β-actin mRNA ratios in normal breast tissues, that patient was considered as having a "low 14-3-3σ expression".

(B) Pearson correlation test showed an inverse correlation between 14-3-3σ mRNA expression and ^{18}FDG uptake.

(C) Representative ^{18}FDG PET Scan pictures indicated the negative impact of 14-3-3σ on ^{18}FDG uptake in breast cancer patients' tumors. The 14-3-3σ classification standard was the same as in Figure 13A.

Table 3. 14-3-3σ's expression is inversely correlated with ^{18}FDG PET Standardized Uptake Value in breast cancer patients' tumors.

		PET Standardized Uptake Value		Total	Chi-squate Test
		Low	**High**		
14-3-3σ Expression	**Low**	28.6%	**71.4%**	100%	$p < 0.0001$
	High	**75%**	25%	100%	$p < 0.0001$

Table 3. 14-3-3σ's expression is inversely correlated with ^{18}FDG PET Standardized Uptake Value in breast cancer patients' tumors.

PET Standardized Uptake Value = c(t) / (injected dose t_0/body weight).

c(t) is the tissue radioactivity concentration at time t.

Injected dose t_0 is the amount of radioactivity injected at the beginning (t=0)

Body weight is the weight of patient in kg.

14-3-3σ mRNA expression in the tumors was determined by transcriptomics analysis of breast cancer patients tumors' fine needle aspirates (microarrays analysis) and normalized to β-actin (*ACTB*) mRNA level. The 14-3-3σ classification standard was the same as in Table 2.

To further understand these correlations, we compared the transcriptomics landscapes of breast cancer patients having low 14-3-3σ levels (loss of >60% of 14-3-3σ expression compared to normal breast tissues) with those who exhibited upregulation of 14-3-3σ (gain >60% of 14-3-3σ expression compared to normal breast tissues) in cohorts GSE20194, GSE5847, GSE11121 and GSE2109. We noticed that breast cancer patients with low 14-3-3σ levels have a significant upregulation of Myc-induced target genes, including the genes involved in glycolysis, glutaminolysis and mitochondrial biogenesis (Figures 14A, 14B, 15A, 15B).

In addition, statistic analyses and Pearson correlation tests showed a negative correlation between 14-3-3σ expression and the levels of Myc–induced target genes genes involved in glycolysis, glutaminolysis and mitochondrial biogenesis, for instance, Glut1 (*SLC2A1*), Glut2 (*SLC2A2*), Glut4 (*SLC2A4*), Hexokinase 2 (*HK2*), Phosphofructose kinase 1 (*PFK1*), Aldolase A (*ALDOA*), Enolase (*ENO1*), Pyruvate Kinase M2 (*PKM2*), Lactate Dehydrogenase A (*LDHA*), Glutaminase 1 (*GLS1*), glutamine transporter *ASCT2* (*SLC1A5*), *TFAM*, among others (Figures 15, 16 and 17). In addition, tissue microarray analysis showed a significant inverse correlation between 14-3-3σ level and Myc protein expression in breast cancer patients' tumors (Figures 18A and 18B). Thus, these results suggested that 14-3-3σ could suppress cancer glycolysis, glutaminolysis and mitochondrial biogenesis through the regulation of Myc.

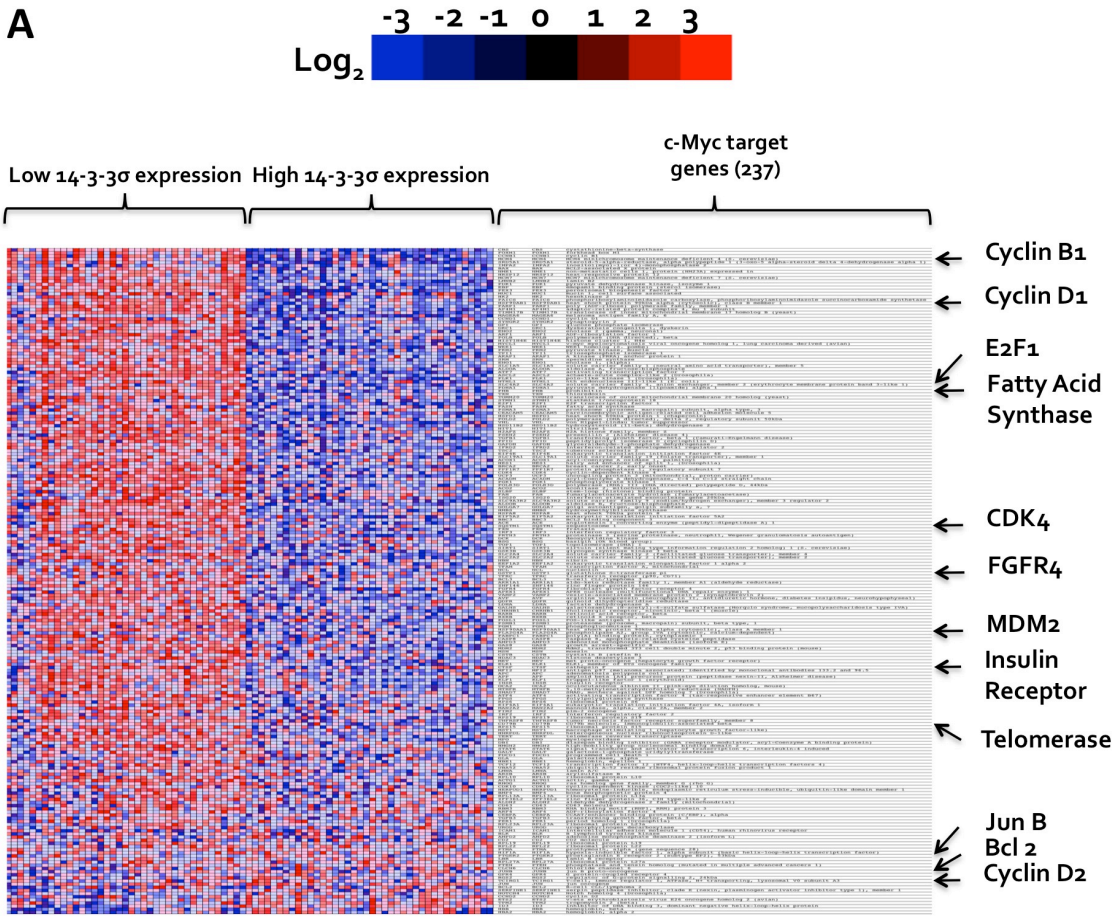
A
Log2
-3 -2 -1 0 1 2 3
Low 14-3-3σ expression
High 14-3-3σ expression
c-Myc target genes (237)
Cyclin B1
Cyclin D1
E2F1
Fatty Acid Synthase
CDK4
FGFR4
MDM2
Insulin Receptor
Telomerase
Jun B
Bcl 2
Cyclin D2

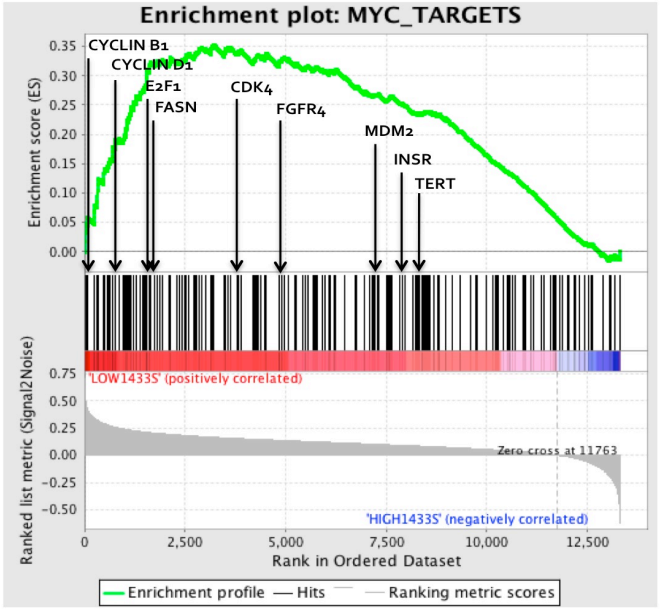
B
Enrichment plot: MYC_TARGETS
CYCLIN B1
CYCLIN D1
E2F1
FASN
CDK4
FGFR4
MDM2
INSR
TERT
Enrichment score (ES)
'LOW1433S' (positively correlated)
Zero cross at 11763
'HIGH1433S' (negatively correlated)
Ranked list metric (Signal2Noise)
Rank in Ordered Dataset
Enrichment profile
Hits
Ranking metric scores

Figure 14

Figure 14. Myc-induced target genes expression increases in breast tumors that have low levels of 14-3-3σ.
(A) Heat map from Gene Set Enrichment Analysis (GSEA) indicates an up-regulation of Myc-induced target genes in breast cancer patients that have a low 14-3-3σ level.
(B) GSEA Enrichment score graph shows the enhancement of Myc target gene expression in breast cancer patients that have a low 14-3-3σ level. The 14-3-3σ classification standard was the same as in Table 2.

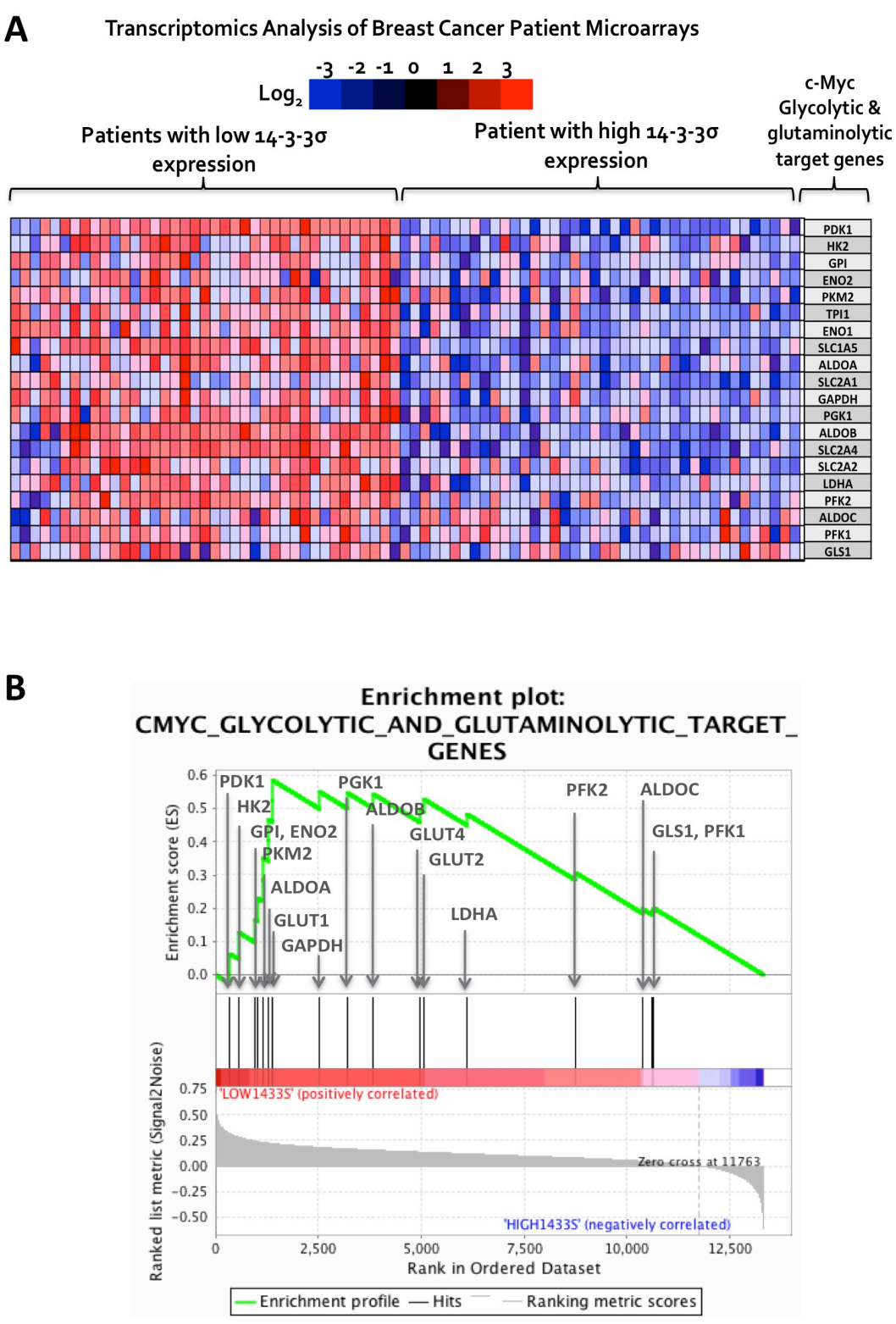
A
Transcriptomics Analysis of Breast Cancer Patient Microarrays
Log2
-3 -2 -1 0 1 2 3
Patients with low 14-3-3σ expression
Patient with high 14-3-3σ expression
c-Myc Glycolytic & glutaminolytic target genes
PDK1
HK2
GPI
ENO2
PKM2
TPI1
ENO1
SLC1A5
ALDOA
SLC2A1
GAPDH
PGK1
ALDOB
SLC2A4
SLC2A2
LDHA
PFK2
ALDOC
PFK1
GLS1
B
Enrichment plot: CMYC_GLYCOLYTIC_AND_GLUTAMINOLYTIC_TARGET_GENES
Enrichment score (ES)
PDK1
HK2
GPI, ENO2
PKM2
ALDOA
GLUT1
GAPDH
PGK1
ALDOB
GLUT4
GLUT2
LDHA
PFK2
ALDOC
GLS1, PFK1
'LOW1433S' (positively correlated)
Zero cross at 11763
'HIGH1433S' (negatively correlated)
Ranked list metric (Signal2Noise)
Rank in Ordered Dataset
Enrichment profile
Hits
Ranking metric scores

Figure 15

Figure 15. Elevation of Myc-induced metabolic target genes expression in breast tumors that have low levels of 14-3-3σ.

(A) Heat map from Gene Set Enrichment Analysis (GSEA) indicates an up-regulation of Myc-induced metabolic target genes in breast cancer patients that have a low 14-3-3σ level.

(B) GSEA Enrichment score graph shows the enhancement of Myc metabolic target gene expression in breast cancer patients that have a low 14-3-3σ level. The 14-3-3σ classification standard was the same as in Table 2.

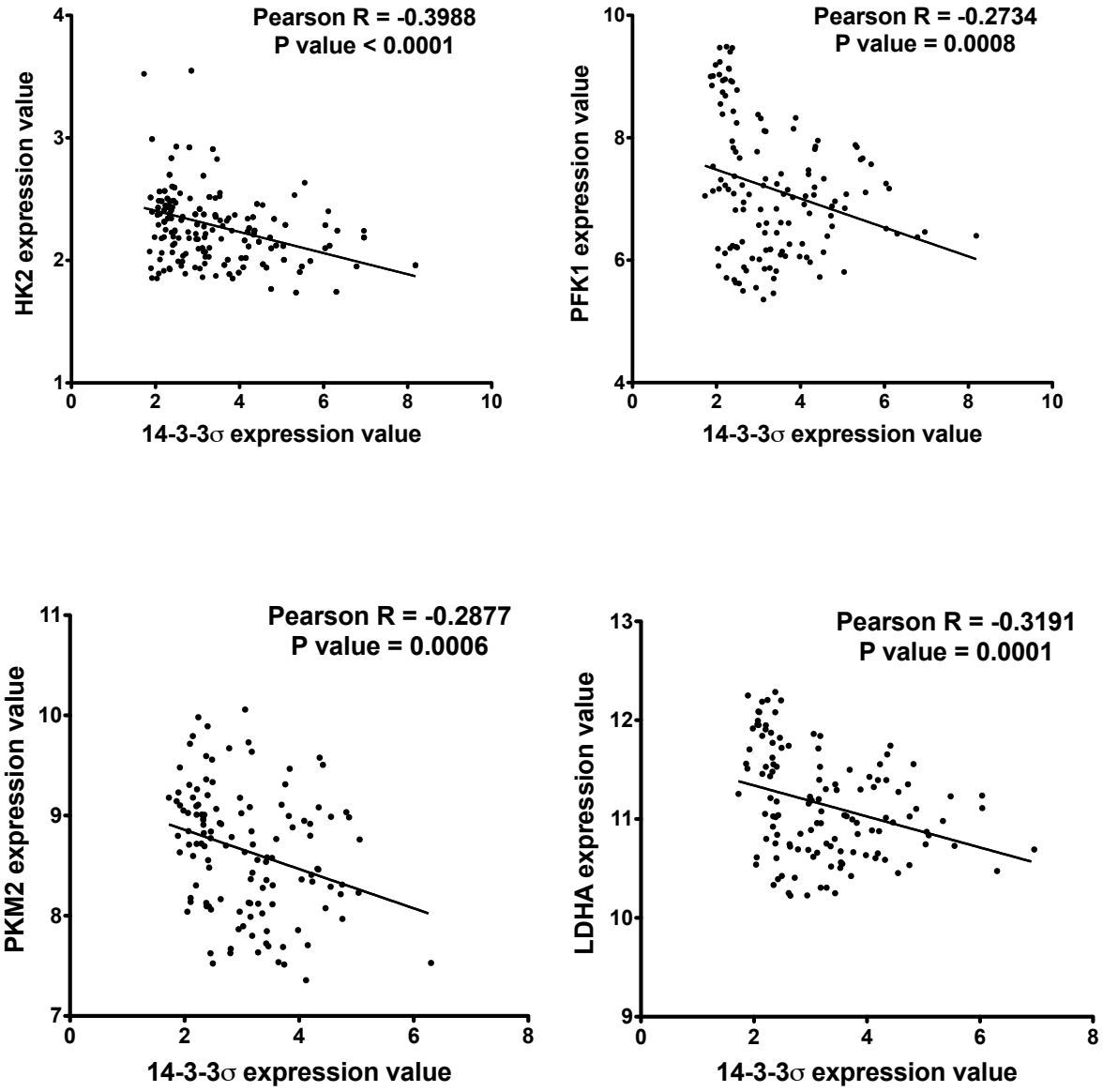
Pearson R = -0.3988
P value < 0.0001
HK2 expression value
14-3-3σ expression value
Pearson R = -0.2734
P value = 0.0008
PFK1 expression value
14-3-3σ expression value
Pearson R = -0.2877
P value = 0.0006
PKM2 expression value
14-3-3σ expression value
Pearson R = -0.3191
P value = 0.0001
LDHA expression value
14-3-3σ expression value

Figure 16

Figure 16. 14-3-3σ expression is inversely correlated with Myc-induced metabolic target genes levels. Pearson correlation analysis suggests an inverse correlation between 14-3-3σ presence and the expression of major Myc-induced glycolytic target genes.

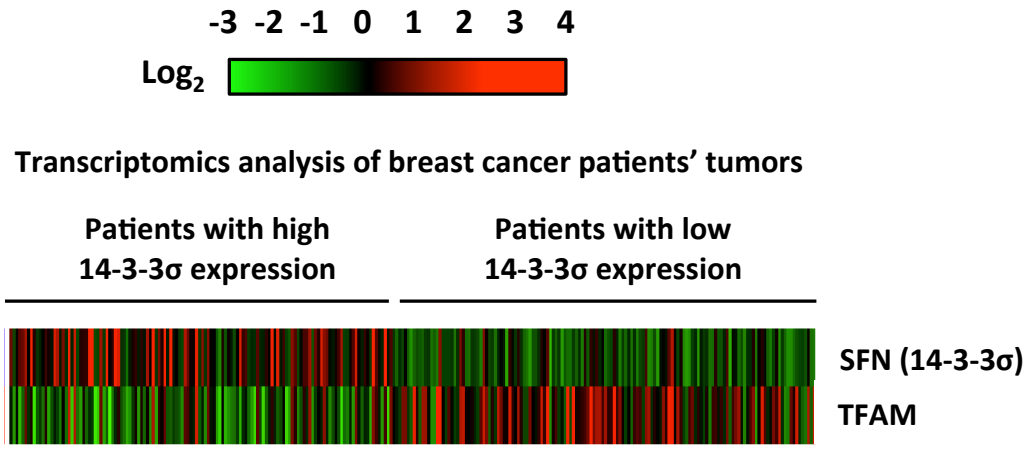
-3 -2 -1 0 1 2 3 4
Log2
Transcriptomics analysis of breast cancer patients' tumors
Patients with high 14-3-3σ expression
Patients with low 14-3-3σ expression
SFN (14-3-3σ)
TFAM

Figure 17

Figure 17. Transcriptomics analysis indicates a negative correlation between 14-3-3σ level and the expression of Transcription Factor A, Mitochondrial (*TFAM*), a Myc-induced gene that is crucial for mitochondrial gene transcription and mitochondrial DNA replication.

A

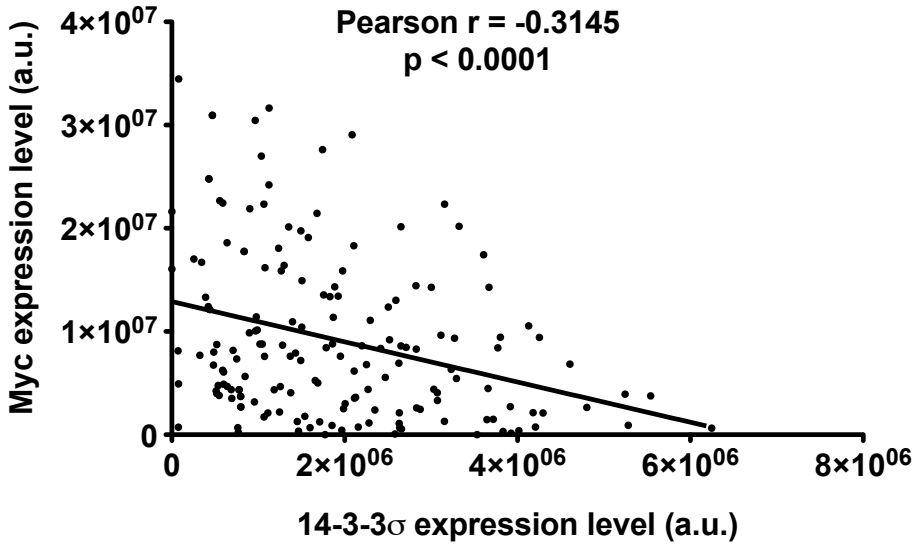
Pearson r = -0.3145
p < 0.0001
Myc expression level (a.u.)
4×10^07
3×10^07
2×10^07
1×10^07
0
0
2×10^06
4×10^06
6×10^06
8×10^06
14-3-3σ expression level (a.u.)

B

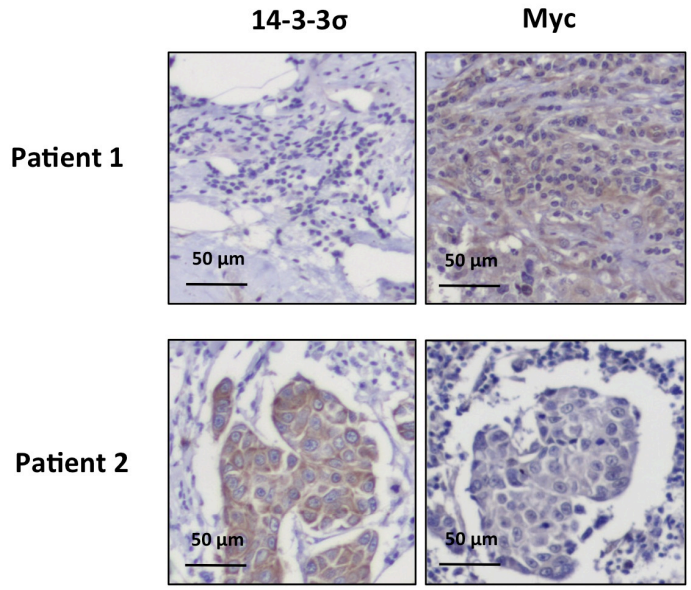
14-3-3σ
Myc
Patient 1
Patient 2
50 µm
50 µm
50 µm
50 µm

Figure 18

Figure 18. Negative correlation between 14-3-3σ and Myc protein expression in breast tumors.

(A) 14-3-3σ expression is inversely correlated with Myc protein level. 14-3-3σ and Myc protein expression were quantified from immunohistochemistry (IHC) staining of breast cancer patients tissue microarrays.

(B) Representative IHC pictures show the reverse relationship between 14-3-3σ and Myc expression in breast cancer patients' tumors.

3.2 Loss of 14-3-3σ leads to an increase in glucose consumption and glucose uptake in cancer cells

To study the impact of 14-3-3σ on cancer glycolysis, we first investigated the influence of 14-3-3σ on glucose consumption. We measured glucose consumption in two cell lines that are isogenic except their 14-3-3σ status. Strikingly, we found that 14-3-3σ null cells exhibit a significant elevation in glucose consumption when compared with 14-3-3σ wild-type (wt) cells (Figure 19A). 14-3-3σ knockdown leads to a similar observation (Figure 19B). Interestingly, when 14-3-3σ expression is restored in 14-3-3σ null cells, glucose consumption falls in a dose-dependent manner (Figure 20A). We also successfully established two tet-regulated (Tet-On) cell lines from 14-3-3σ null cells: HCT116 14-3-3$\sigma^{-/-}$, MDA-MB-231 (14-3-3σ expression is down-regulated due to hypermethylation of the promoter region), and again glucose consumption was reduced in these cells when 14-3-3σ was induced by Doxycycline treatment (Figure 20B). We then measured glucose uptake in cells using 2-(*N*-(7-Nitrobenz-2-oxa-1,3-diazol-4-yl)Amino)-2-Deoxyglucose (2-NBDG), a fluorescent glucose analog that can be imported into cells and detected by fluorescent microscopy and flow cytometry. The 14-3-3$\sigma^{-/-}$ cells had more green signals from 2-NBDG and a faster rate of glucose uptake (Figures 21A, 21B, 21C). More importantly, re-expression of 14-3-3σ in 14-3-3σ null cells reverses 2-NBDG incorporation in a dose-dependent manner (Figures 22A, 22B). We also observed, based on flow cytometry, that 14-3-3σ's induction led to a significant decline in the translocation of glucose transporter Glut1 to the cell membrane (Figures 23A, 23B).

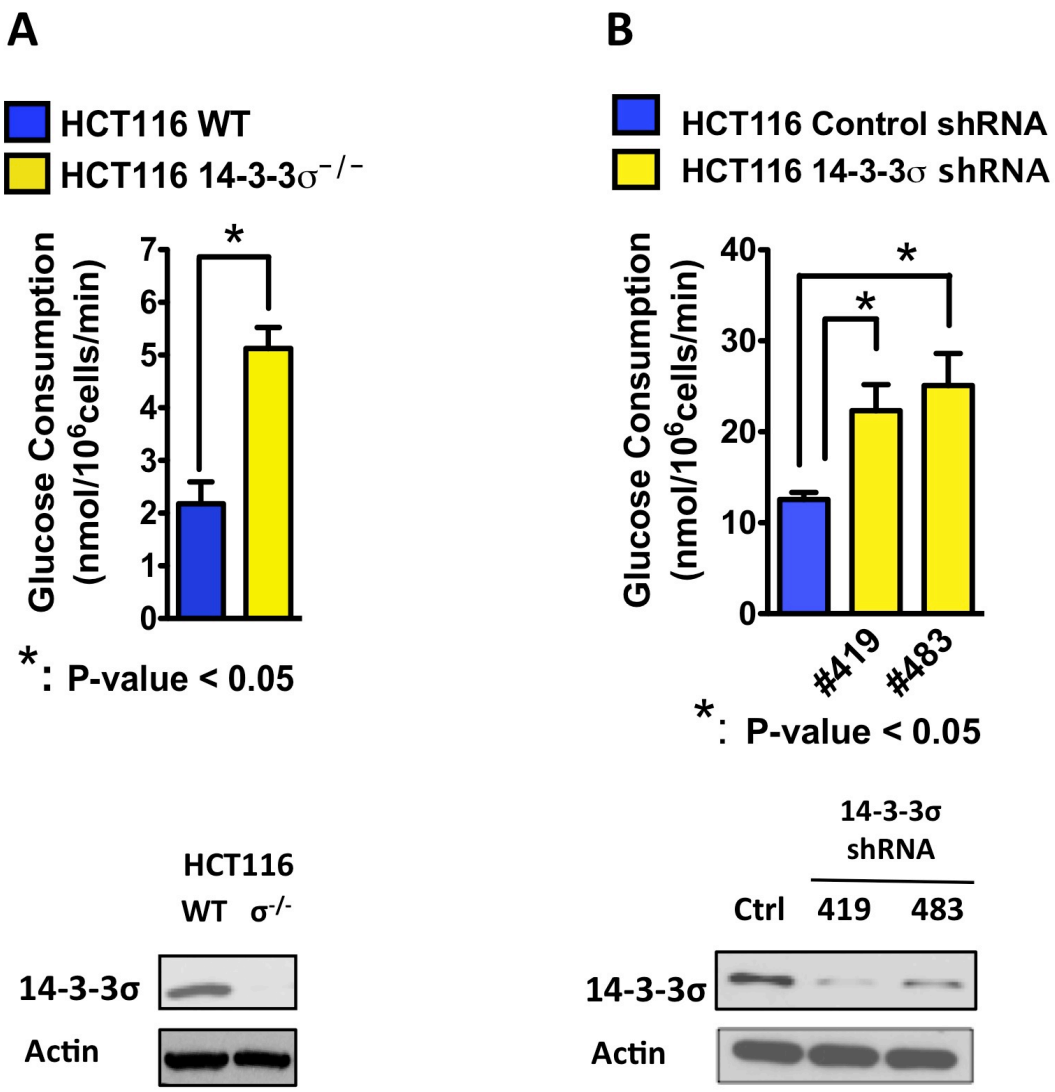
A
HCT116 WT
HCT116 14-3-3σ-/-
Glucose Consumption (nmol/10^6cells/min)
*
*: P-value < 0.05
HCT116
WT σ-/-
14-3-3σ
Actin
B
HCT116 Control shRNA
HCT116 14-3-3σ shRNA
Glucose Consumption (nmol/10^6cells/min)
*
*
#419
#483
*: P-value < 0.05
14-3-3σ shRNA
Ctrl 419 483
14-3-3σ
Actin

Figure 19

Figure 19. Loss and knockdown of 14-3-3σ leads to an increase in glucose consumption and uptake.
(A) Enhancement of glucose consumption in 14-3-3σ null cells. Glucose concentration of the medium was measured by Freestyle glucose meter. Glucose consumption is normalized to the final cell number and culture time.
(B) 14-3-3σ knockdown results in a significant increase in glucose consumption. 14-3-3σ expression was knocked down by lentiviral shRNA. Knockdown efficiency was verified by Western Blot with an anti-14-3-3σ antibody. Luciferase shRNA was used as a control. Glucose consumption was measured as described in (A).

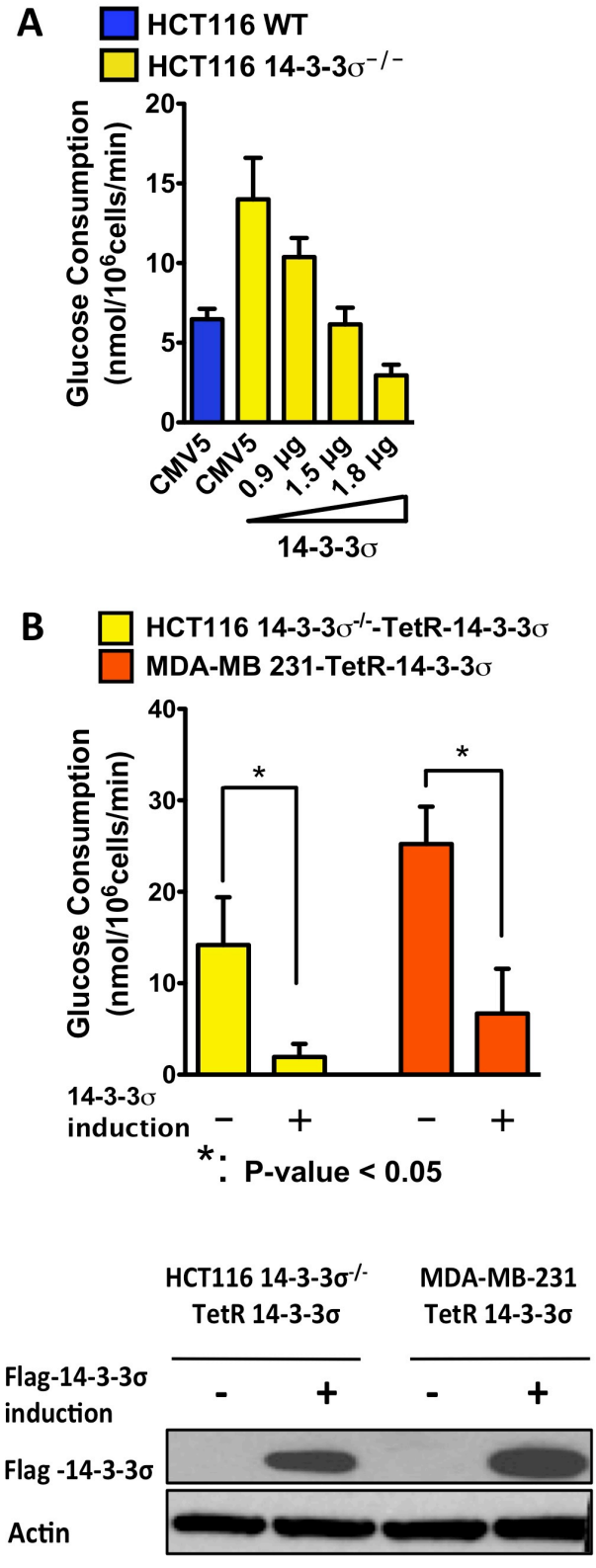
A
HCT116 WT
HCT116 14-3-3σ-/-
Glucose Consumption (nmol/10^6cells/min)
20
15
10
5
0
CMV5
CMV5
0.9 μg
1.5 μg
1.8 μg
14-3-3σ
B
HCT116 14-3-3σ-/--TetR-14-3-3σ
MDA-MB 231-TetR-14-3-3σ
Glucose Consumption (nmol/10^6cells/min)
40
30
20
10
0
*
*
14-3-3σ induction
–
+
–
+
*: P-value < 0.05
HCT116 14-3-3σ-/- TetR 14-3-3σ
MDA-MB-231 TetR 14-3-3σ
Flag-14-3-3σ induction
-
+
-
+
Flag -14-3-3σ
Actin

Figure 20

Figure 20. Restoration of 14-3-3σ expression in 14-3-3σ-deficient cancer cells leads to decreased glucose consumption.

(A) 14-3-3σ reduces glucose consumption in a dose dependent manner. HCT116 14-3-3σ$^{-/-}$ cells were transfected with increasing amounts of pCMV5-Flag-14-3-3σ plasmid, and glucose consumption was measured.

(B) Induced expression of 14-3-3σ significantly diminishes glucose consumption. Indicated cells were infected with retroviruses carrying a Tet On Flag-14-3-3σ system as described in Extended Experimental Procedures. Flag-14-3-3σ expression was induced (+) for 48 hours using 5 ng/ml Doxycycline. Non-induced (-) cells are used as the corresponding control. Flag-14-3-3σ induction was verified by Western Blot. Glucose consumption was measured.

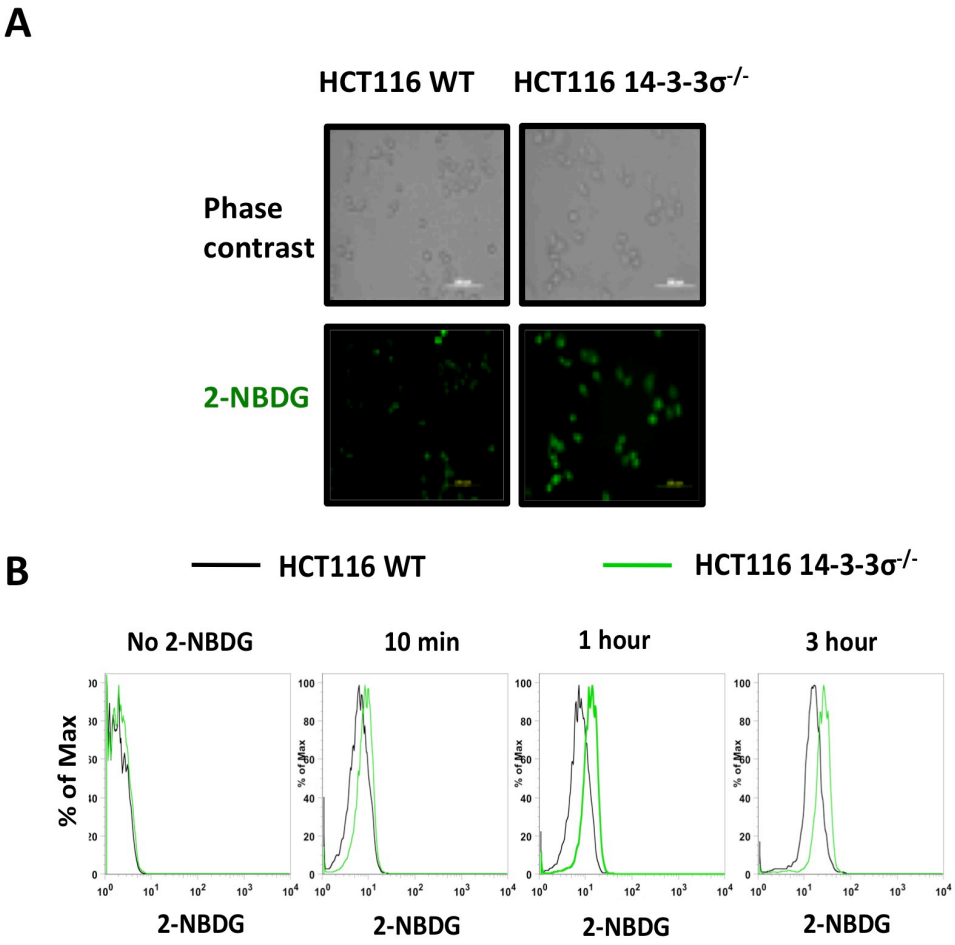
A
HCT116 WT
HCT116 14-3-3σ-/-
Phase contrast
2-NBDG
B
HCT116 WT
HCT116 14-3-3σ-/-
No 2-NBDG
10 min
1 hour
3 hour
% of Max
2-NBDG
C
HCT116 WT
HCT116 14-3-3σ-/-
2-NBDG signal integration (a.u.)
2000
1500
1000
500
0
1 min
10 min
30 min
1 hour
2 hour
3 hour

Figure 21

Figure 21. Loss of 14-3-3σ increases glucose uptake.
(A) Microscopic pictures demonstrate that loss of 14-3-3σ results in a remarkable enhancement of glucose uptake. Cells were incubated in a DMEM glucose-free medium containing 120 μM of 2-NBDG, for the indicated times. 2-NBDG signals were observed using fluorescent microscopy.
(B) Flow cytometry analysis shows a significant increase in 2-NBDG signals in HCT116 14-3-3$\sigma^{-/-}$ cells when compared with HCT116 wt cells.
(C) Bar graph and statistic analysis of Figure 21B. Data is represented as mean ± 95% confidence interval (CI)

A

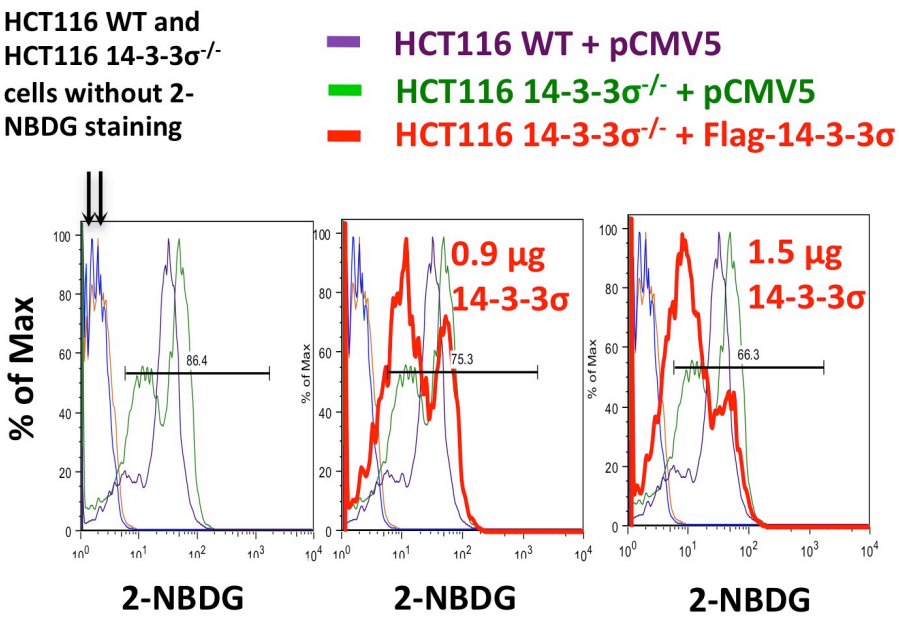
HCT116 WT and HCT116 14-3-3σ-/- cells without 2-NBDG staining
HCT116 WT + pCMV5
HCT116 14-3-3σ-/- + pCMV5
HCT116 14-3-3σ-/- + Flag-14-3-3σ
% of Max
86.4
0.9 µg 14-3-3σ
75.3
1.5 µg 14-3-3σ
66.3
2-NBDG
2-NBDG
2-NBDG

B

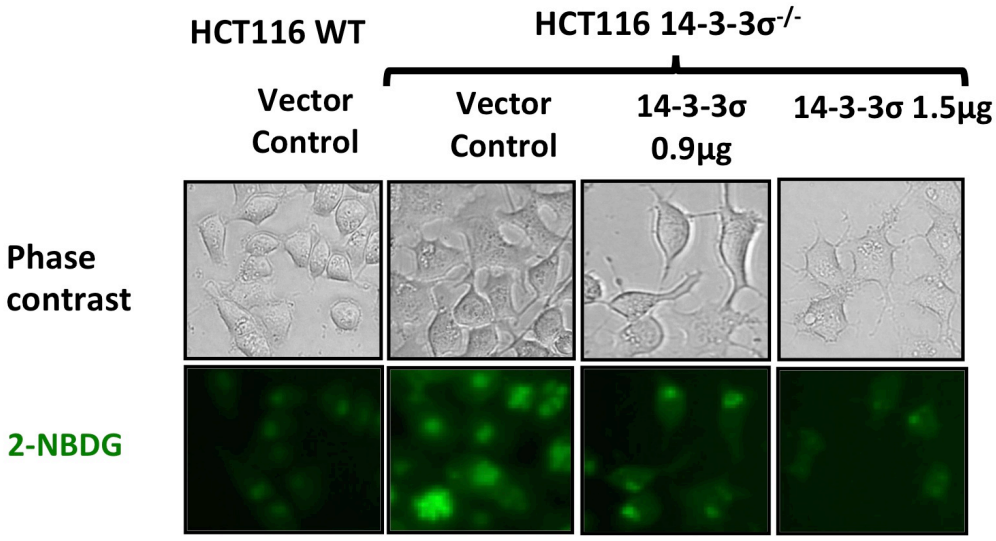
HCT116 WT
HCT116 14-3-3σ-/-
Vector Control
Vector Control
14-3-3σ 0.9µg
14-3-3σ 1.5µg
Phase contrast
2-NBDG

Figure 22

Figure 22. 14-3-3σ expression decreases glucose uptake in HCT116 14-3-3σ$^{-/-}$ cancer cells.
(A) 14-3-3σ transfection decreases 2-NBDG uptake in a dose-dependent manner. Indicated cells were transfected with indicated amounts of pCMV5-Flag-14-3-3σ. 2-NBDG signal was measured using a flow cytometer as in Figure 21.
(B) Representative pictures from a fluorescent microscope for the experiment in Figure 22A.

A

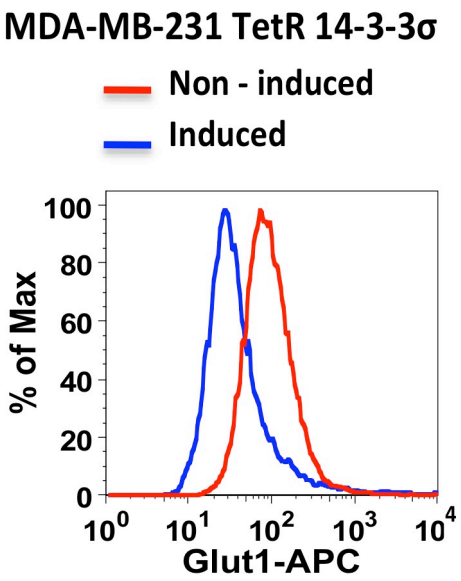
MDA-MB-231 TetR 14-3-3σ
Non - induced
Induced
% of Max
100
80
60
40
20
0
10^0
10^1
10^2
10^3
10^4
Glut1-APC

B

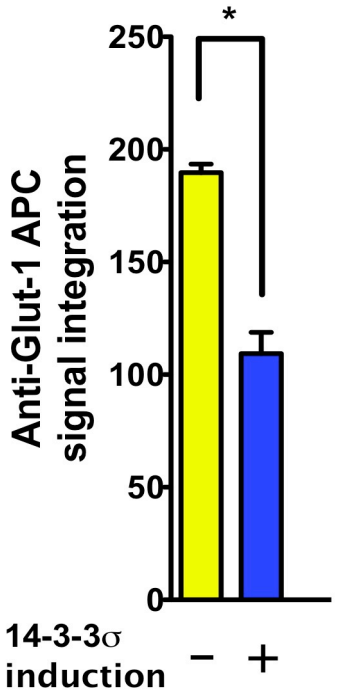
*
250
200
150
100
50
0
Anti-Glut-1 APC
signal integration
14-3-3σ
induction
–
+

Figure 23

Figure 23. 14-3-3σ decreases the expression of glucose transporter Glut1 on cellular membrane.
(A) Doxycycline-induced expression of Flag-14-3-3σ results in a sharp decline of Glut1 expression on cellular membrane surface. Flag-14-3-3σ was induced by Doxycycline in MDA-MB-231 as previously described. Cells were stained with specific anti-Glut1 antibodies conjugated with APC fluorophore and analyzed by flow cytometry.
(B) Bar graph and statistical analyses of Figure 23A were done using GraphPad Prism v5.0d and Sigma Plot 12.0. Data is represented as mean ± 95% CI.

3.3 14-3-3σ suppresses lactate production and decreases ATP concentration in cancer cells

Lactate is a final product of aerobic glycolysis. Therefore, we hypothesize that since 14-3-3σ null cells have increased glucose consumption and uptake, they may produce more lactate. As we expected, 14-3-3σ null cells produced significantly more lactate when compared with 14-3-3σ wt cells (Figures 24A and 24C). Accordingly, 14-3-3σ knockdown led to higher lactate production (Figure 24B). Significantly, re-expressing 14-3-3σ in 14-3-3σ null cells reduced lactate generation in a dose-dependent manner (Figure 25A). We also found that Doxycycline-induced restoration of 14-3-3σ expression in HCT116 14-3-3σ$^{-/-}$ and MDA-MB-231 cells led to the reduction of lactate accumulation in the culture medium (Figure 25B).

Since the production of lactate acidifies the extracellular environment, we next measured the extracellular acidification rate (ECAR) using a Seahorse Extracellular Flux Analyzer XF24 (Seahorse Bioscience). We found that HCT116 14-3-3σ$^{-/-}$ cells had a higher ECAR when compared with HCT116 wt cells (Figure 26A). The impact of 14-3-3σ was even more obvious when the cells were treated with oligomycin, a drug that inhibits mitochondrial ATP synthesis and drives the cells to utilize more glycolytic pathway (Figure 26A). ECAR also increased when 14-3-3σ expression was knocked down in MCF10A and T47D breast cancer cells (Figure 26B). We also analyzed ECAR in tet-regulated HCT116 14-3-3σ$^{-/-}$, MDA-MB-231 and MDA-MB-435 cells. Again, ECAR was reduced in these cells when 14-3-3σ expression was induced by the Doxycycline treatment (Figures 27A, 27B, 27C). In hypoxic condition, restoring 14-3-3σ expression also suppressed lactate production of HCT116 14-3-3σ$^{-/-}$ and MDA-MB-231 cells

(Figures 28A, 28B).

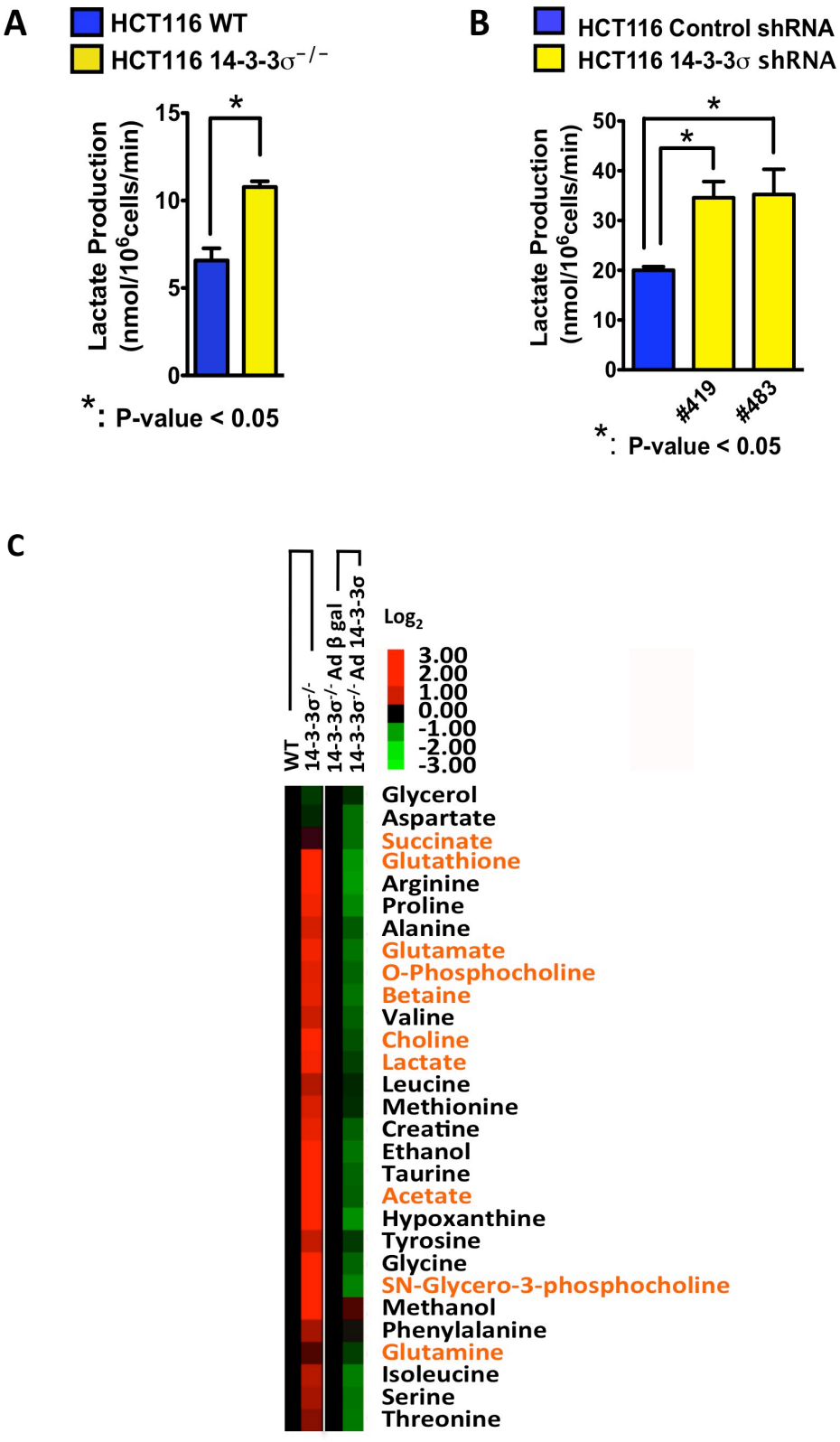
A
HCT116 WT
HCT116 14-3-3σ-/-
Lactate Production (nmol/10^6cells/min)
15
10
5
0
*
*: P-value < 0.05
B
HCT116 Control shRNA
HCT116 14-3-3σ shRNA
Lactate Production (nmol/10^6cells/min)
50
40
30
20
10
0
*
*
#419
#483
*: P-value < 0.05
C
WT
14-3-3σ-/-
14-3-3σ-/- Ad β gal
14-3-3σ-/- Ad 14-3-3σ
Log2
3.00
2.00
1.00
0.00
-1.00
-2.00
-3.00
Glycerol
Aspartate
Succinate
Glutathione
Arginine
Proline
Alanine
Glutamate
O-Phosphocholine
Betaine
Valine
Choline
Lactate
Leucine
Methionine
Creatine
Ethanol
Taurine
Acetate
Hypoxanthine
Tyrosine
Glycine
SN-Glycero-3-phosphocholine
Methanol
Phenylalanine
Glutamine
Isoleucine
Serine
Threonine

Figure 24

Figure 24. Loss of 14-3-3σ increases lactate production.

(A) Loss of 14-3-3σ increases lactate production. Lactate concentration was measured in the medium of the indicated cultured cells using the lactate analyzer Accutrend (Roche) and normalized to the final cell number and culture time.
(B) 14-3-3σ knockdown increases lactate production. 14-3-3σ expression was knocked down using lentiviral shRNA as mentioned above. Lactate production assay was measured as in (A).
(C) Loss of 14-3-3σ results in a significant increase in the concentrations of lactate and other important metabolites. Metabolites are extracted from HCT116 wt, 14-3-3$\sigma^{-/-}$ cells and HCT116 14-3-3$\sigma^{-/-}$ cells that are infected with Adenoviruses carrying β galactosidase or 14-3-3σ using freezing/thawing method. Metabolite concentrations are then measured using Nuclear Magnetic Resonance by Chenomx (Alberta, Canada). Metabolite names that are printed in orange color are related to glycolysis, glutaminolysis, phospholipid metabolism and the Tricarboxylic Acid cycle.

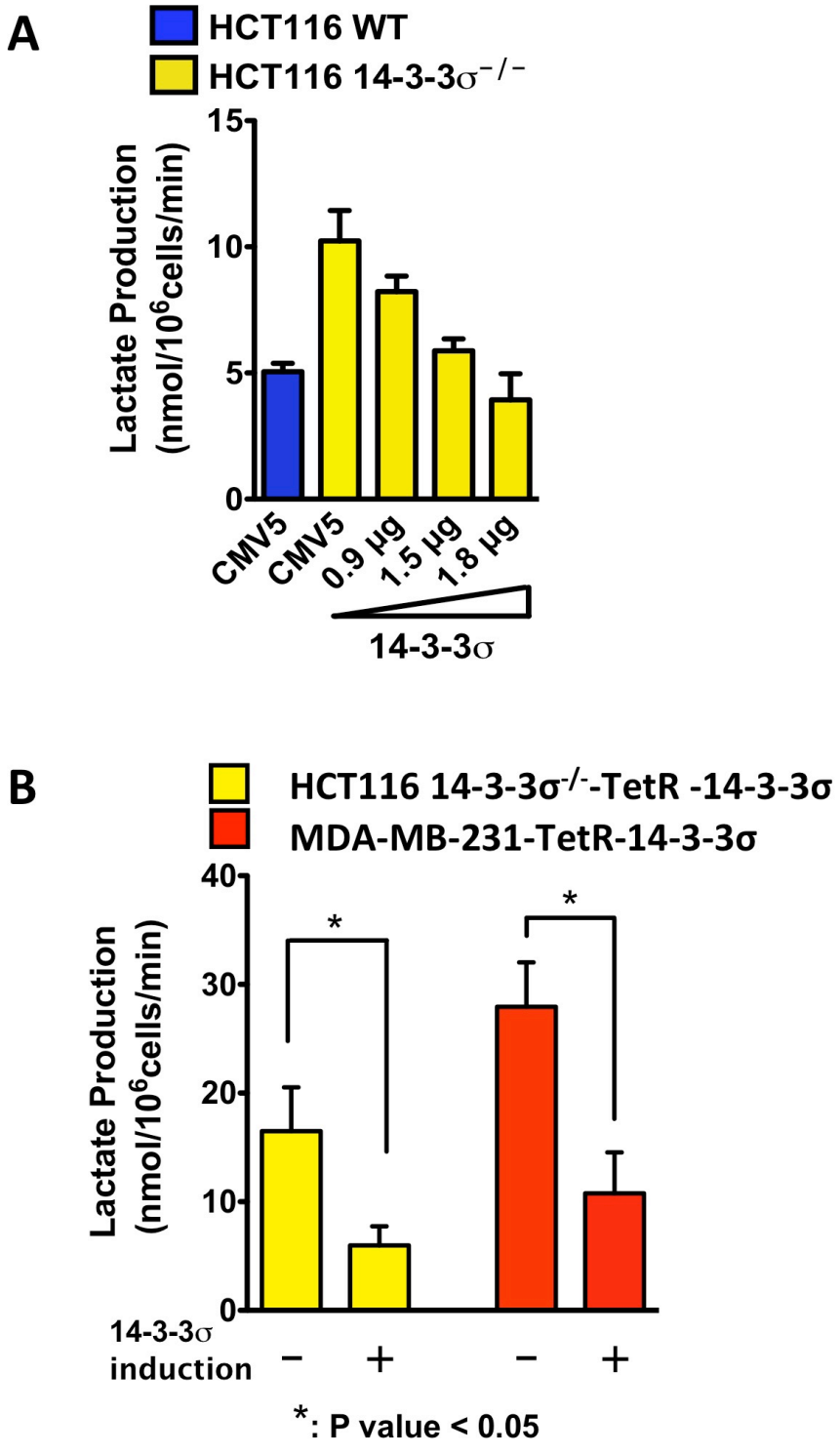
A
HCT116 WT
HCT116 14-3-3σ-/-
Lactate Production (nmol/10^6cells/min)
15
10
5
0
CMV5
CMV5
0.9 µg
1.5 µg
1.8 µg
14-3-3σ
B
HCT116 14-3-3σ-/--TetR -14-3-3σ
MDA-MB-231-TetR-14-3-3σ
Lactate Production (nmol/10^6cells/min)
40
30
20
10
0
*
*
14-3-3σ induction
−
+
−
+
*: P value < 0.05

Figure 25

Figure 25. 14-3-3σ expression decreases lactate production of cancer cells.
(A) 14-3-3σ transfection reduces lactate production in a dose-dependent manner. Indicated cells were transfected with increasing amounts of pCMV5-Flag-14-3-3σ plasmid. Lactate production was measured as previously described.
(B) Induced expression of 14-3-3σ results in a sharp decline of lactate production. Flag-14-3-3σ was induced by Doxycycline in the indicated cells. Lactate production was measured as previously described.

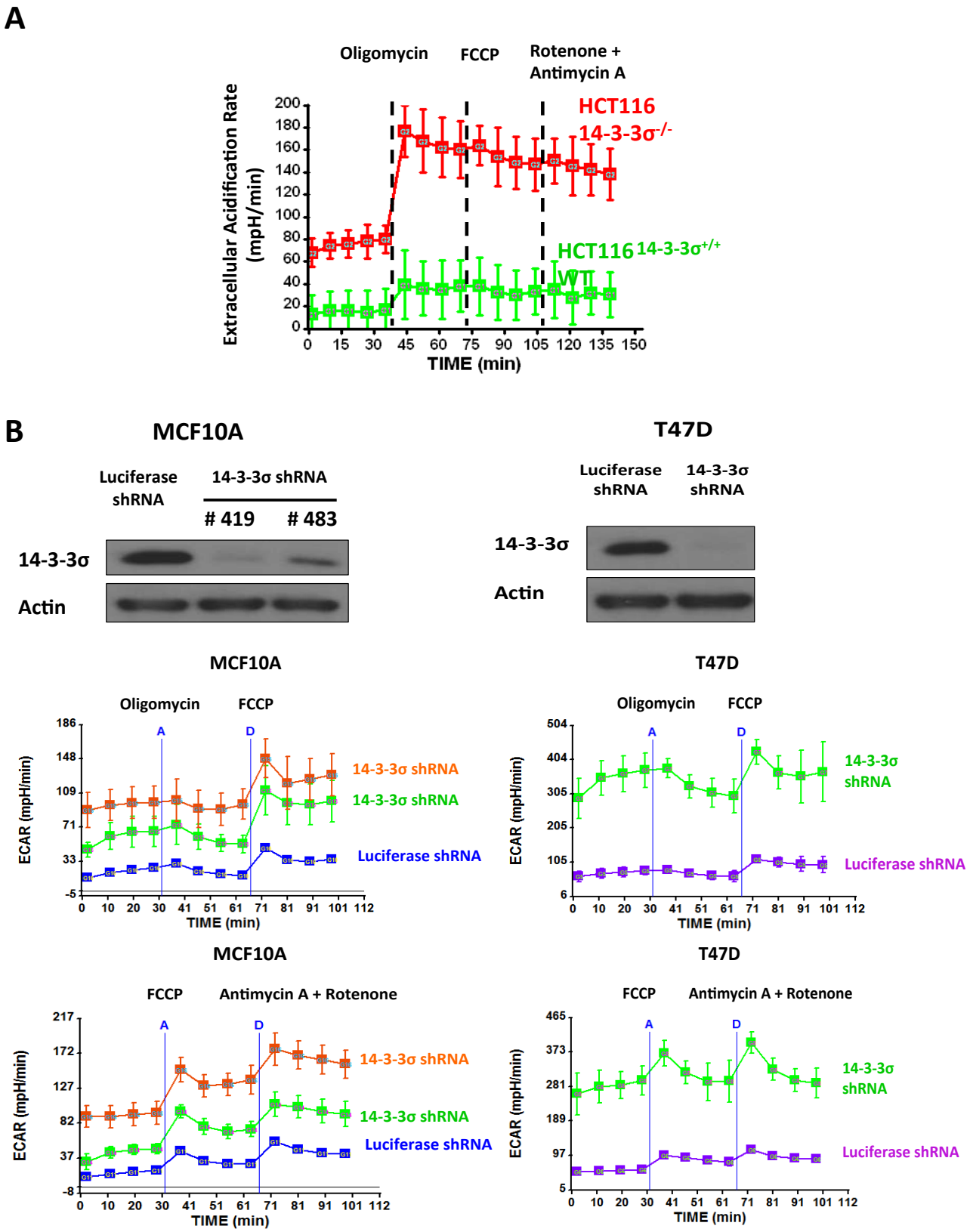
A
Oligomycin
FCCP
Rotenone +
Antimycin A
Extracellular Acidification Rate
(mpH/min)
HCT116
14-3-3σ-/-
HCT116 14-3-3σ+/+
WT
TIME (min)
B
MCF10A
T47D
Luciferase
shRNA
14-3-3σ shRNA
419
483
14-3-3σ
Actin
MCF10A
T47D
Oligomycin
FCCP
ECAR (mpH/min)
14-3-3σ shRNA
14-3-3σ shRNA
Luciferase shRNA
TIME (min)
MCF10A
T47D
FCCP
Antimycin A + Rotenone
ECAR (mpH/min)
14-3-3σ shRNA
14-3-3σ shRNA
Luciferase shRNA
TIME (min)

Figure 26

Figure 26. Loss and knockdown of 14-3-3σ elevates Extracellular Acidification Rate (ECAR).
(A) Loss of 14-3-3σ increases ECAR. Indicated cells were plated in a Seahorse Bioscience microplate for ECAR measurement using a Seahorse Extracellular Flux Analyzer XF24.
(B) Knockdown of 14-3-3σ in MCF10A and T47D breast cancer cells significant increases ECAR.

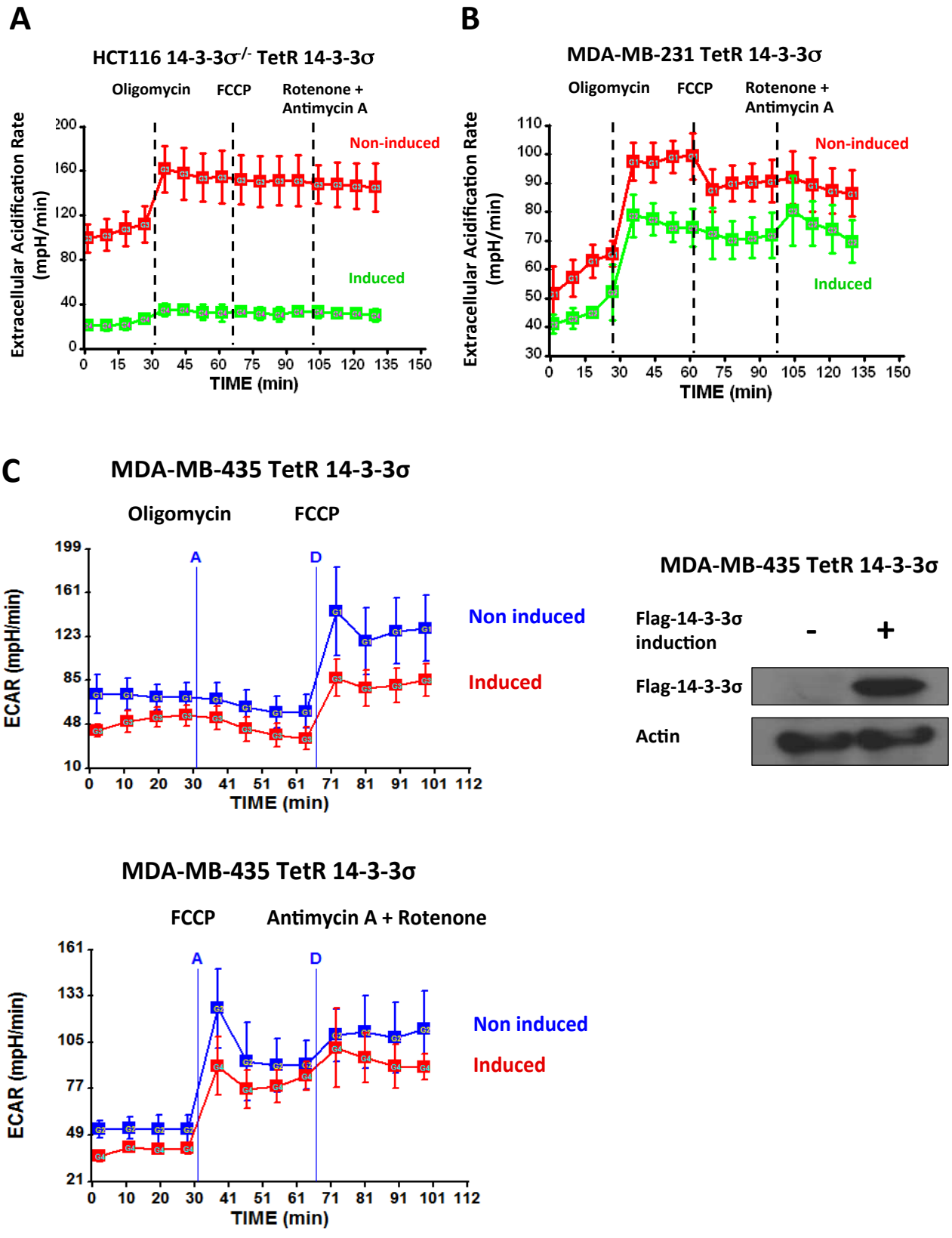
A
HCT116 14-3-3σ-/- TetR 14-3-3σ
Oligomycin
FCCP
Rotenone + Antimycin A
Non-induced
Induced
Extracellular Acidification Rate (mpH/min)
TIME (min)
B
MDA-MB-231 TetR 14-3-3σ
Oligomycin
FCCP
Rotenone + Antimycin A
Non-induced
Induced
Extracellular Acidification Rate (mpH/min)
TIME (min)
C
MDA-MB-435 TetR 14-3-3σ
Oligomycin
FCCP
A
D
ECAR (mpH/min)
TIME (min)
Non induced
Induced
MDA-MB-435 TetR 14-3-3σ
Flag-14-3-3σ induction
-
+
Flag-14-3-3σ
Actin
MDA-MB-435 TetR 14-3-3σ
FCCP
Antimycin A + Rotenone
A
D
ECAR (mpH/min)
TIME (min)
Non induced
Induced

Figure 27

Figure 27. 14-3-3σ decreases lactate production.
(A) Induced expression of Flag-14-3-3σ in HCT116 14-3-3σ$^{-/-}$ cells diminishes ECAR. Flag-14-3-3σ is induced by Doxycycline as described above.
(B) Flag-14-3-3σ expression decreases ECAR in MDA-MB-231 cells.
(C) 48-hour inducible expression of Flag-14-3-3σ in MDA-MB-435 breast cancer cells remarkably reduces ECAR.

A

Hypoxia

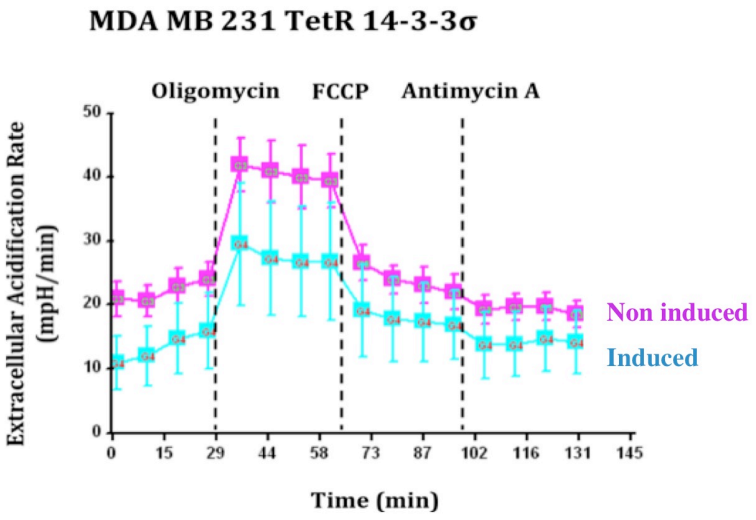

B

Hypoxia

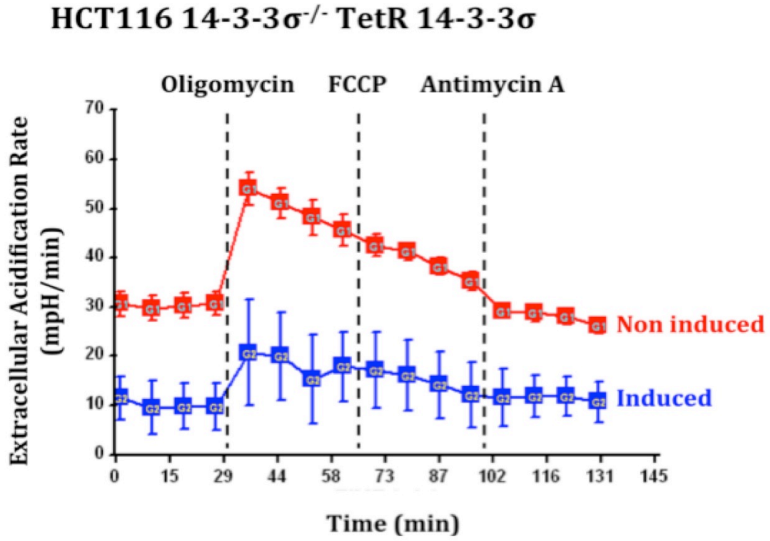

Figure 28

Figure 28. 14-3-3σ expression decreases lactate production in hypoxia.

Inducible expression of Flag-14-3-3σ in MDA-MB-231 (A) and HCT116 14-3-3σ$^{-/-}$ (B) cancer cells remarkably decreases ECAR in hypoxic condition. MDA-MB-231 and HCT116 14-3-3σ$^{-/-}$ cells that carry a Tet On 14-3-3σ system are cultured in hypoxic condition (1% oxygen) and treated with 5 ng/ml Doxycycline for 48 hours to induce Flag-14-3-3σ expression.

Since ATP production is tightly linked to metabolic activities, we also evaluated the impact of 14-3-3σ on ATP in cancer cells. Significantly, we found that HCT116 14-3-3σ null cell have a higher ATP concentration when compared with 14-3-3σ wt cells (Figure 29A). Accordingly, we found that HCT116 14-3-3σ knockdown cells also had significantly higher levels of ATP when compared with 14-3-3σ control cells (Figure 29B). Another line of evidence also showed that Doxycycline-induced Flag-14-3-3σ expression in HCT116 14-3-3$\sigma^{-/-}$ cells and MDA-MB-231 cells reduced ATP concentrations (Figure 29C). Our data suggests that 14-3-3σ loss not only enhances glycolysis but also potentiates cells to engage in a metabolic program that produces more ATP.

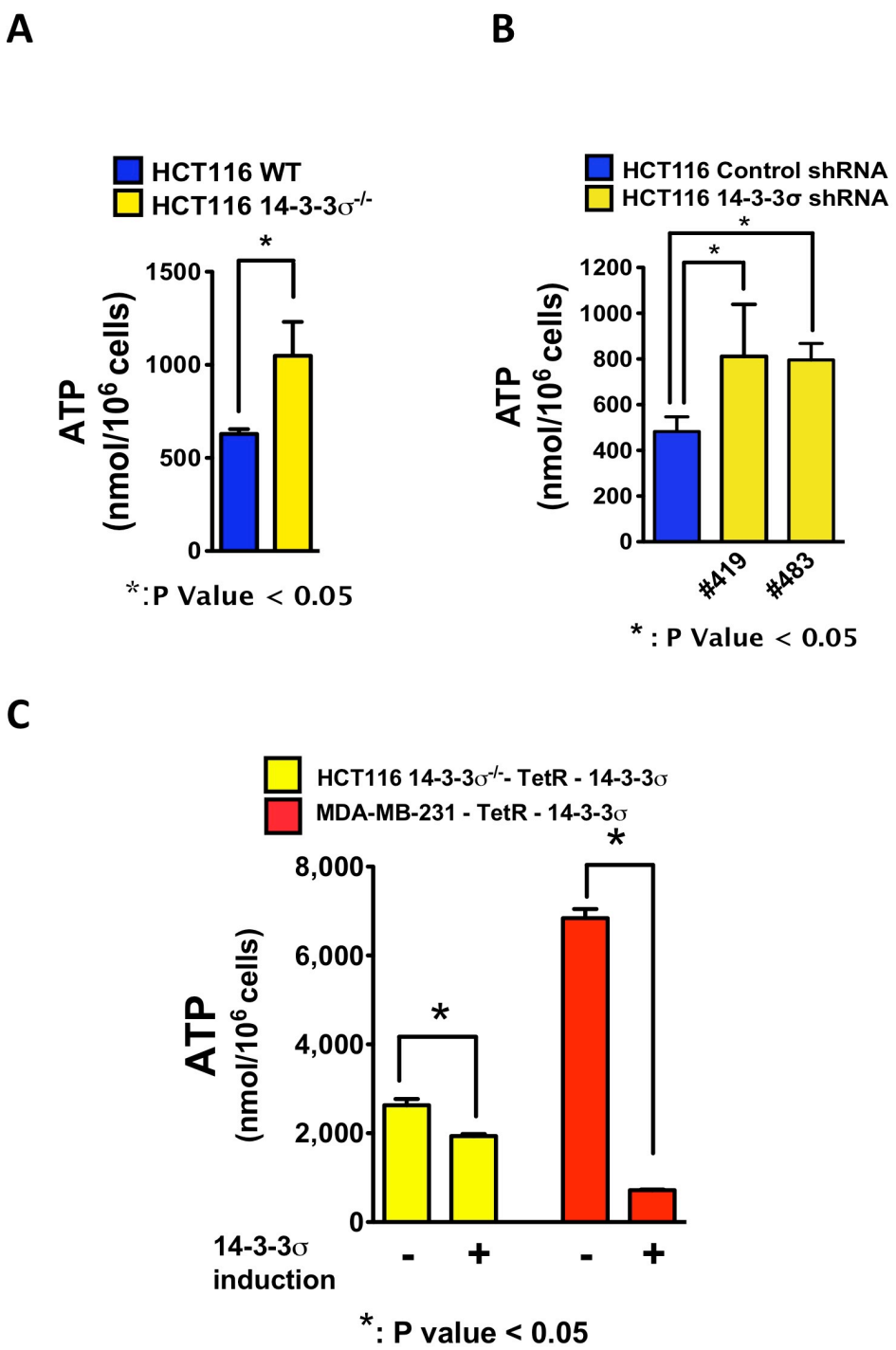
A
HCT116 WT
HCT116 14-3-3σ-/-
ATP (nmol/10^6 cells)
1500
1000
500
0
*
*:P Value < 0.05
B
HCT116 Control shRNA
HCT116 14-3-3σ shRNA
ATP (nmol/10^6 cells)
1200
1000
800
600
400
200
0
*
*
#419
#483
* : P Value < 0.05
C
HCT116 14-3-3σ-/- TetR - 14-3-3σ
MDA-MB-231 - TetR - 14-3-3σ
ATP (nmol/10^6 cells)
8,000
6,000
4,000
2,000
0
*
*
14-3-3σ induction
-
+
-
+
*: P value < 0.05

Figure 29

Figure 29. The negative impact of 14-3-3σ on ATP level in cancer cells
(A) Loss of 14-3-3σ increases ATP concentration.
(B) 14-3-3σ knockdown results in a significant rise of ATP concentration in HCT116 cells.
(C) Induced expression of 14-3-3σ causes a significant decline of ATP level. Flag-14-3-3σ was induced by Doxycycline in indicated cells as described above. All data is represented as mean ± 95% CI.

3.4 14-3-3σ promotes Myc ubiquitination, accelerates Myc turnover rate, suppresses its transcriptional activity, and decreases Myc-induced glycolytic target genes expression.

Since Myc has been identified as a major driver of cancer glycolysis and we observed a negative correlation between 14-3-3σ and Myc protein levels in breast cancer patients' tumors, we decided to further examine the impact of 14-3-3σ on Myc. Interestingly, we found that Doxycycline-induced Flag-14-3-3σ expression in HCT116 14-3-3σ$^{-/-}$ and MDA-MB-231 increased Myc poly-ubiquitination in these cells (Figure 30A). In addition, the induction of 14-3-3σ expression in HCT116 p53$^{-/-}$ cells and H1299 cells (both of which are p53 null cells) also enhanced Myc poly-ubiquitination, which suggests that 14-3-3σ's impact on Myc ubiquitination is p53-independent (Figure 30B). Furthermore, the protein turnover rate of Myc increased in HCT116 14-3-3σ$^{-/-}$ and MDA-MB-231 cells when Flag-14-3-3σ expression was induced by Doxycycline compared with the non-induced cells (Figures 31A, 31B, 31C).

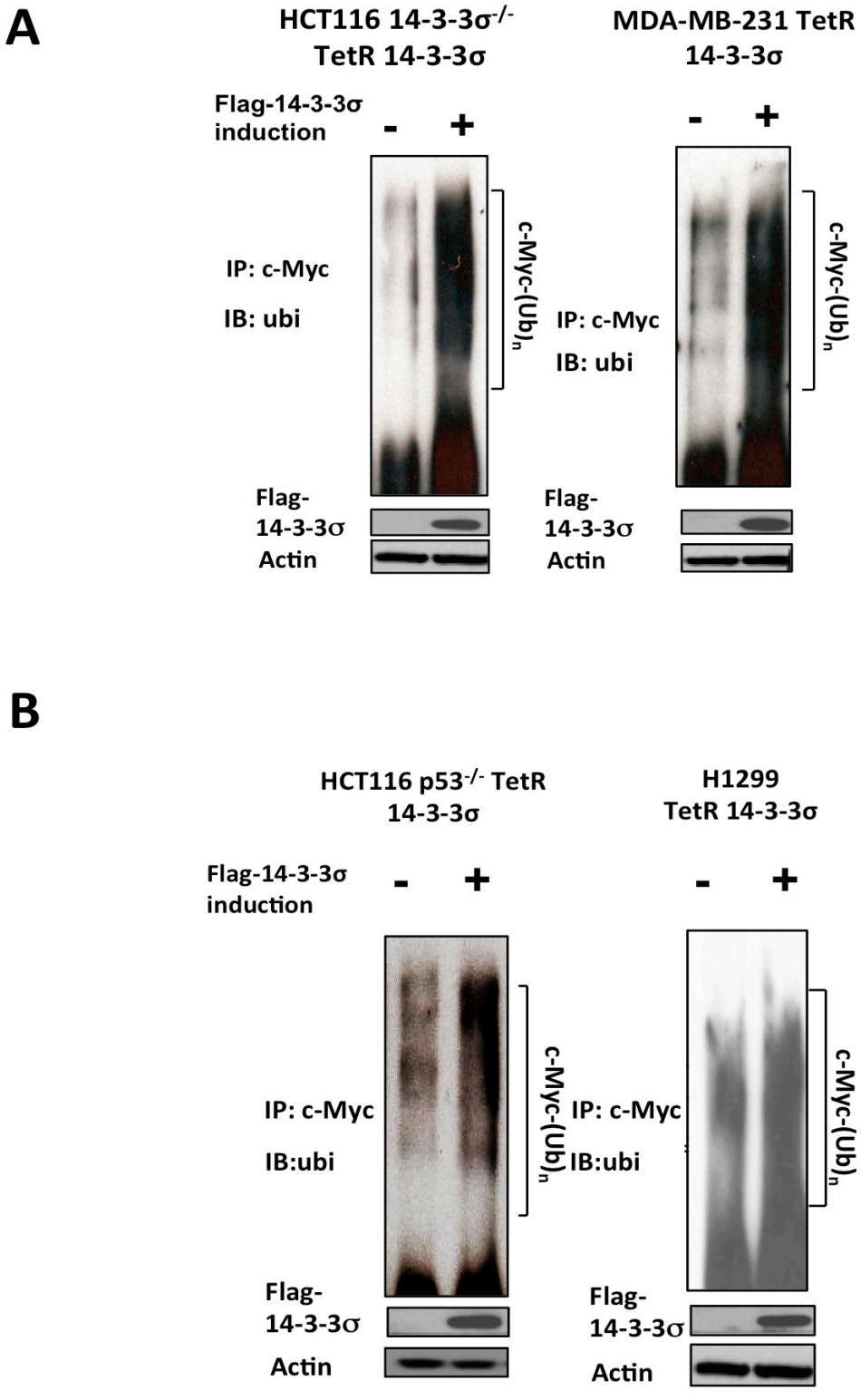
A
HCT116 14-3-3σ-/- TetR 14-3-3σ
MDA-MB-231 TetR 14-3-3σ
Flag-14-3-3σ induction
-
+
-
+
IP: c-Myc
IB: ubi
c-Myc-(Ub)n
IP: c-Myc
IB: ubi
c-Myc-(Ub)n
Flag-14-3-3σ
Actin
Flag-14-3-3σ
Actin
B
HCT116 p53-/- TetR 14-3-3σ
H1299 TetR 14-3-3σ
Flag-14-3-3σ induction
-
+
-
+
IP: c-Myc
IB:ubi
c-Myc-(Ub)n
IP: c-Myc
IB:ubi
c-Myc-(Ub)n
Flag-14-3-3σ
Actin
Flag-14-3-3σ
Actin

Figure 30

Figure 30. 14-3-3σ promotes c-Myc poly-ubiquitination.

(A) Doxycycline-induced Flag-14-3-3σ increases Myc ubiquitination. HCT116 14-3-3σ$^{-/-}$ TetR 14-3-3σ and MDA-MB-231 TetR 14-3-3σ cells are treated with Doxycycline to induce Flag-14-3-3σ expression (+). Non-induced cells were used as a control (-). Cell lysates were immunoprecipitated with anti-Myc antibodies and immunoblotted with anti-ubiquitin antibodies.
(B) 14-3-3σ enhances c-Myc ubiquitination in p53-deficient cancer cells. H1299 TetR 14-3-3σ and HCT116 p53$^{-/-}$ TetR 14-3-3σ cells are grown in the presence of 5 ng/ml Doxycycline for 48 hours to induce Flag-14-3-3σ expression. Non-induced cells are used as control for comparison. All cells are then treated with MG132, a potent proteasome inhibitor, for 5 hours. Cell lysates are collected and immunoprecipitated with anti-Myc antibodies (Sigma Aldrich) and immunoblotted with anti-ubiquitin antibodies (Santa Cruz).

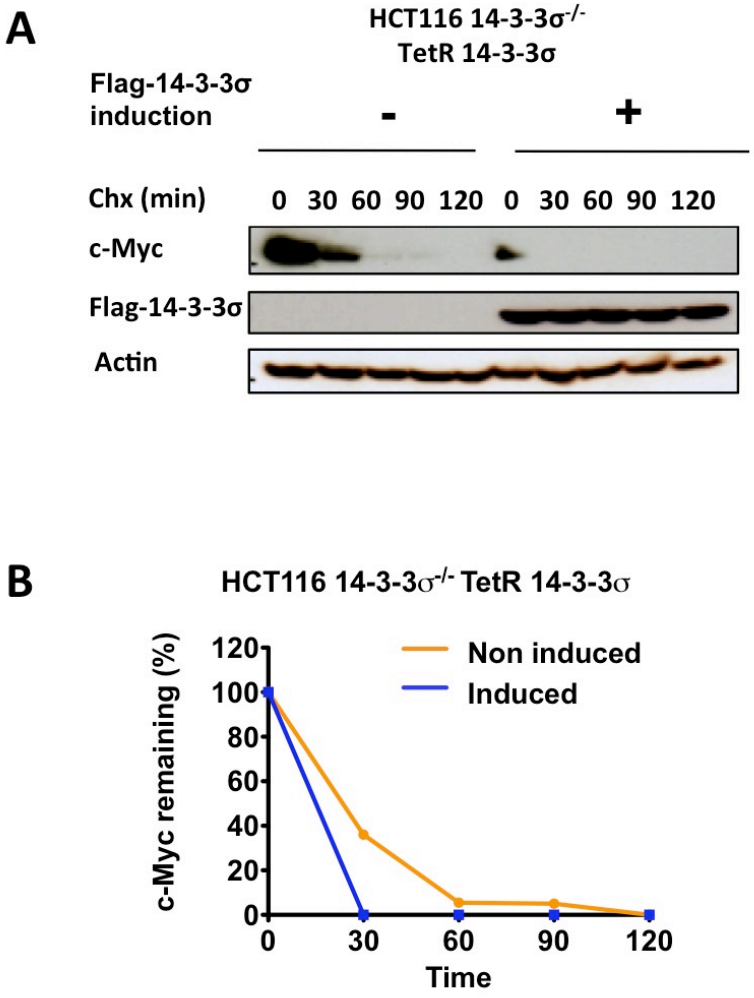
A
HCT116 14-3-3σ-/-
TetR 14-3-3σ
Flag-14-3-3σ induction
-
+
Chx (min)
0 30 60 90 120 0 30 60 90 120
c-Myc
Flag-14-3-3σ
Actin
B
HCT116 14-3-3σ-/- TetR 14-3-3σ
c-Myc remaining (%)
120
100
80
60
40
20
0
Non induced
Induced
0 30 60 90 120
Time
C
MDA-MB-231 TetR 14-3-3σ
Flag-14-3-3σ induction
-
+
CHX (min)
0 30 60 90 120 0 30 60 90 120
Myc
Flag-14-3-3σ
Actin

Figure 31

Figure 31. 14-3-3σ increases Myc turnover rate.
(A) Flag-14-3-3σ was induced by Doxycycline in HCT116 14-3-3σ$^{-/-}$ TetR 14-3-3σ cells as described above. Cells were treated with 200 μg/ml Cycloheximide (Chx) for the indicated times. Cell lysates are immunoblotted with indicated antibodies.
(B) Inducible expression of Flag-14-3-3σ accelerates Myc degradation in HCT116 14-3-3σ$^{-/-}$ cells. Line graph is built based on Western Blot data of Figure 32A.
(C) 14-3-3σ promotes Myc degradation in MDA-MB-231 TetR 14-3-3σ cells. This experiments was done in a similar way as Figure 31A.

To correlate the decrease in Myc stability with the regulation of Myc transcriptional activity, we did a luciferase reporter gene assay. We found that Flag-14-3-3σ induction by Doxycycline treatment diminished Myc transcriptional activity in both HCT116 14-3-3$\sigma^{-/-}$ and MDA-MB-231 cells (Figure 32). Significantly, our quantitative Real time PCR (qRT-PCR) data show that loss and knockdown of 14-3-3σ enhanced the expression of Myc glycolytic target genes, e.g., *HK2, GPI, PFK1, ALDOA, ENO1, TPI1, PGK1, PKM2, LDHA,* among others, both in normoxic and hypoxic conditions (Figures 33 & 34). Conversely, Flag-14-3-3σ induction by Doxycycline treatment resulted in strong suppression of Myc glycolytic target genes both in normoxia and hypoxia (Figure 35).

To further confirm the gene expression data, we performed Western Blot to determine the protein expression of glycolytic enzymes in these cells. We found that the protein levels of Myc glycolytic target genes were consistent with the mRNA expression pattern (Figures 36A, 36B, 37). It is important to point out that Phosphoglucose Mutase 1 (*PGM1*), the only glycolytic enzyme that is not a transcriptional target of Myc, was not affected by the loss, knockdown and re-expression of 14-3-3σ (Figures 33A, 33B, 35A, 36A, 36B, 37). This indicates that 14-3-3σ's negative impact on glycolytic gene expression is selective for Myc targets. Together, these data demonstrate that 14-3-3σ reduces the expression of Myc target genes involved in glycolysis by promoting Myc degradation and suppressing Myc transcriptional activity.

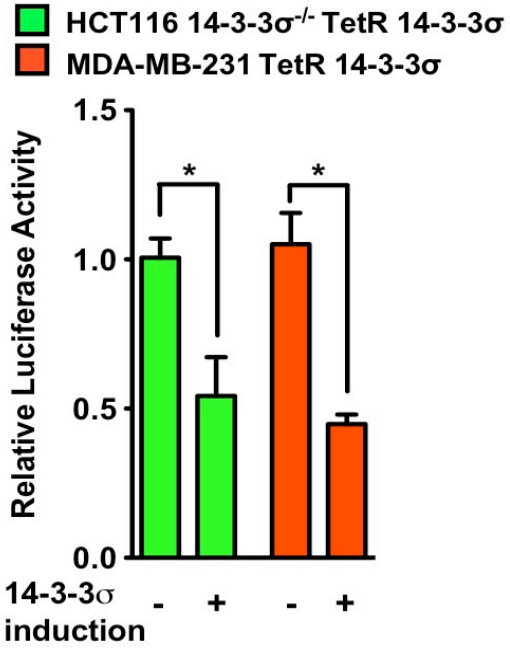
HCT116 14-3-3σ-/- TetR 14-3-3σ
MDA-MB-231 TetR 14-3-3σ
Relative Luciferase Activity
1.5
1.0
0.5
0.0
*
*
14-3-3σ induction
-
+
-
+
* P value < 0.05

Figure 32

Figure 32. 14-3-3σ decreases Myc transactivational activity. Indicated cells were transfected with Tert luciferase reporter plasmid containing a c-Myc response element (Ebox). Relative Luciferase Activity was measured.

A

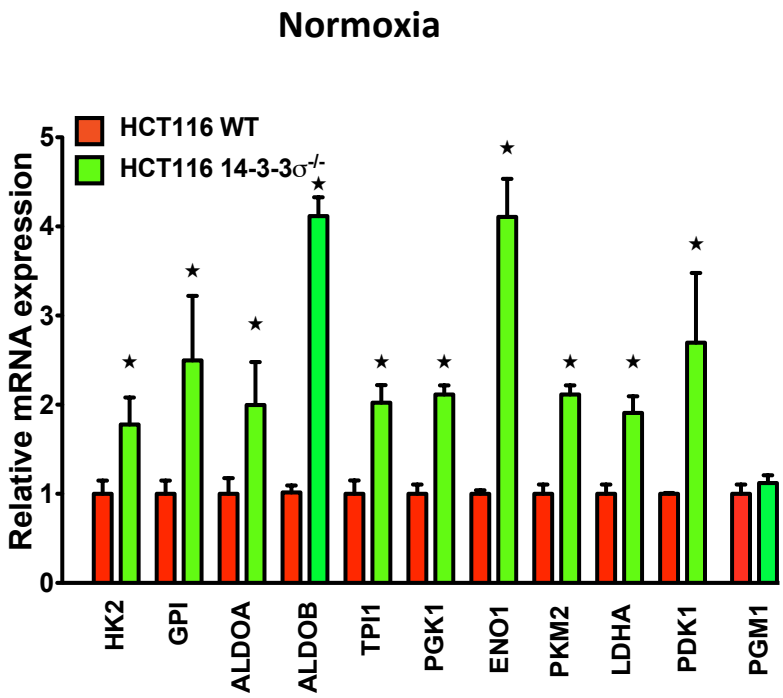
Normoxia
HCT116 WT
HCT116 14-3-3σ-/-
Relative mRNA expression
0
1
2
3
4
5
HK2
GPI
ALDOA
ALDOB
TPI1
PGK1
ENO1
PKM2
LDHA
PDK1
PGM1

B

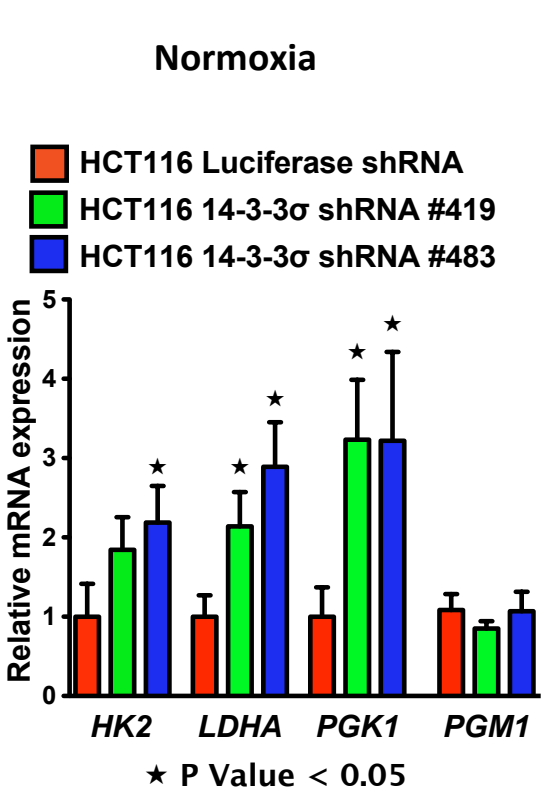
Normoxia
HCT116 Luciferase shRNA
HCT116 14-3-3σ shRNA #419
HCT116 14-3-3σ shRNA #483
Relative mRNA expression
0
1
2
3
4
5
HK2
LDHA
PGK1
PGM1
★ P Value < 0.05

Figure 33

Figure 33. Loss and knockdown of 14-3-3σ increases the expression of Myc-induced glycolytic target genes.
(A) Loss of 14-3-3σ leads to mRNA upregulation of Myc-targeted glycolytic genes. Total RNA is extracted from HCT116 wt and 14-3-3σ$^{-/-}$ cells for qRT-PCR using specific primers for the indicated genes.
(B) Knockdown of 14-3-3σ elevates Myc-targeted glycolytic genes mRNA levels. 14-3-3σ expression was knocked down using lentiviral shRNAs. Luciferase shRNA-infected cells were used as a control.

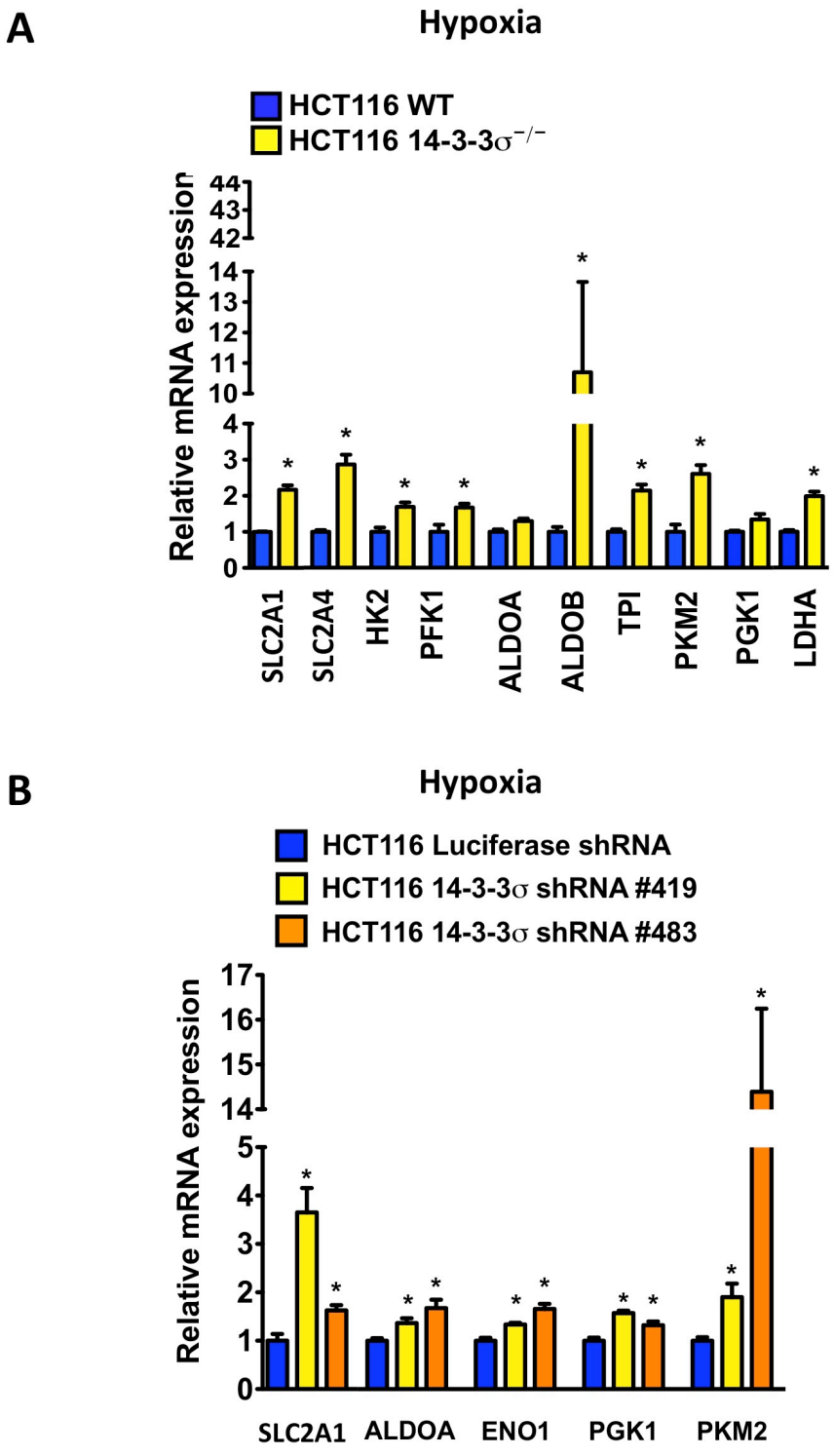
A
Hypoxia
HCT116 WT
HCT116 14-3-3σ−/−
Relative mRNA expression
SLC2A1
SLC2A4
HK2
PFK1
ALDOA
ALDOB
TPI
PKM2
PGK1
LDHA
B
Hypoxia
HCT116 Luciferase shRNA
HCT116 14-3-3σ shRNA #419
HCT116 14-3-3σ shRNA #483
Relative mRNA expression
SLC2A1
ALDOA
ENO1
PGK1
PKM2

Figure 34

Figure 34. Loss and knockdown of 14-3-3σ increase the expression of Myc-induced glycolytic target genes in hypoxic condition.
(A) Loss of 14-3-3σ increases Myc-induced glycolytic target genes expression in hypoxia. HCT116 WT and HCT116 14-3-3σ$^{-/-}$ cells are cultured in hypoxia (1% oxygen) for 48 hours. Total RNA is collected, converted to cDNA and used for qRT-PCR.
(B) Knockdown of 14-3-3σ elevates Myc-induced glycolytic target genes expression in hypoxia. 14-3-3σ expression is knockdown in HCT116 WT using lentiviral shRNA. Luciferase shRNA is used as a control. All cells are cultured in hypoxia (1% oxygen) for 48 hours. Total RNA is collected, converted to cDNA and used for qRT-PCR.

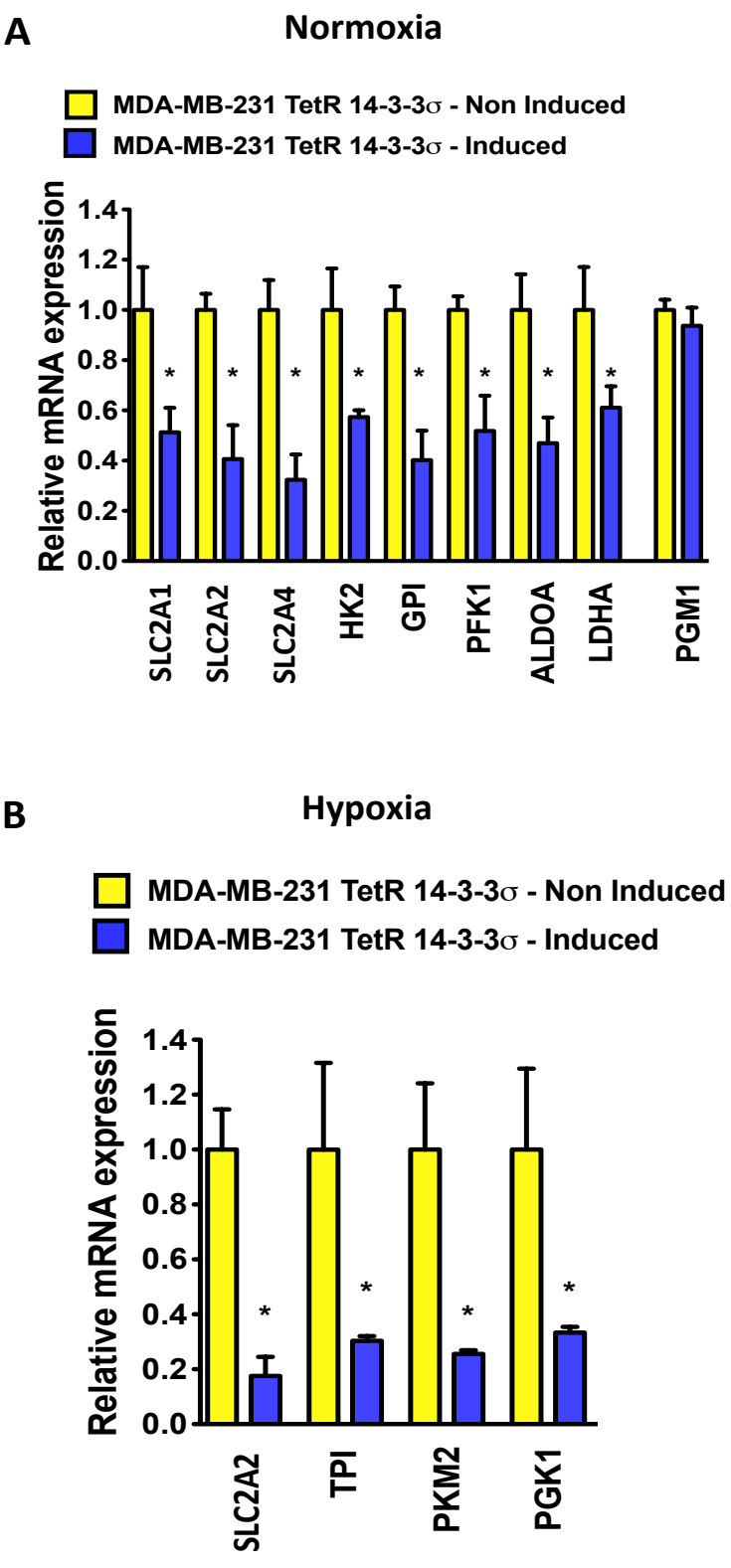
A
Normoxia
MDA-MB-231 TetR 14-3-3σ - Non Induced
MDA-MB-231 TetR 14-3-3σ - Induced
Relative mRNA expression
1.4
1.2
1.0
0.8
0.6
0.4
0.2
0.0
SLC2A1
SLC2A2
SLC2A4
HK2
GPI
PFK1
ALDOA
LDHA
PGM1
B
Hypoxia
MDA-MB-231 TetR 14-3-3σ - Non Induced
MDA-MB-231 TetR 14-3-3σ - Induced
Relative mRNA expression
SLC2A2
TPI
PKM2
PGK1

Figure 35

Figure 35. 14-3-3σ down-regulates Myc-induced glycolytic target genes expression both in normoxic and hypoxic conditions.
(A) Doxycycline-induced Flag-14-3-3σ decreases mRNA expression of Myc-induced glycolytic target genes in normoxic condition. Flag-14-3-3σ was induced by Doxycycline as described above. qRT-PCR is performed using specific primers for the indicated genes.
(B) Inducible expression of Flag-14-3-3σ decreases Myc-induced glycolytic target genes level in MDA-MB-231 cells in hypoxic condition. MDA-MB-231 cells that carries a Tet On 14-3-3σ system are cultured in hypoxia (1% oxygen) and treated with 5 ng/ml Doxycycline for 48 hours. Non-induced cells are used as a control. Total RNA is collected, converted to cDNA and used for qRT-PCR.

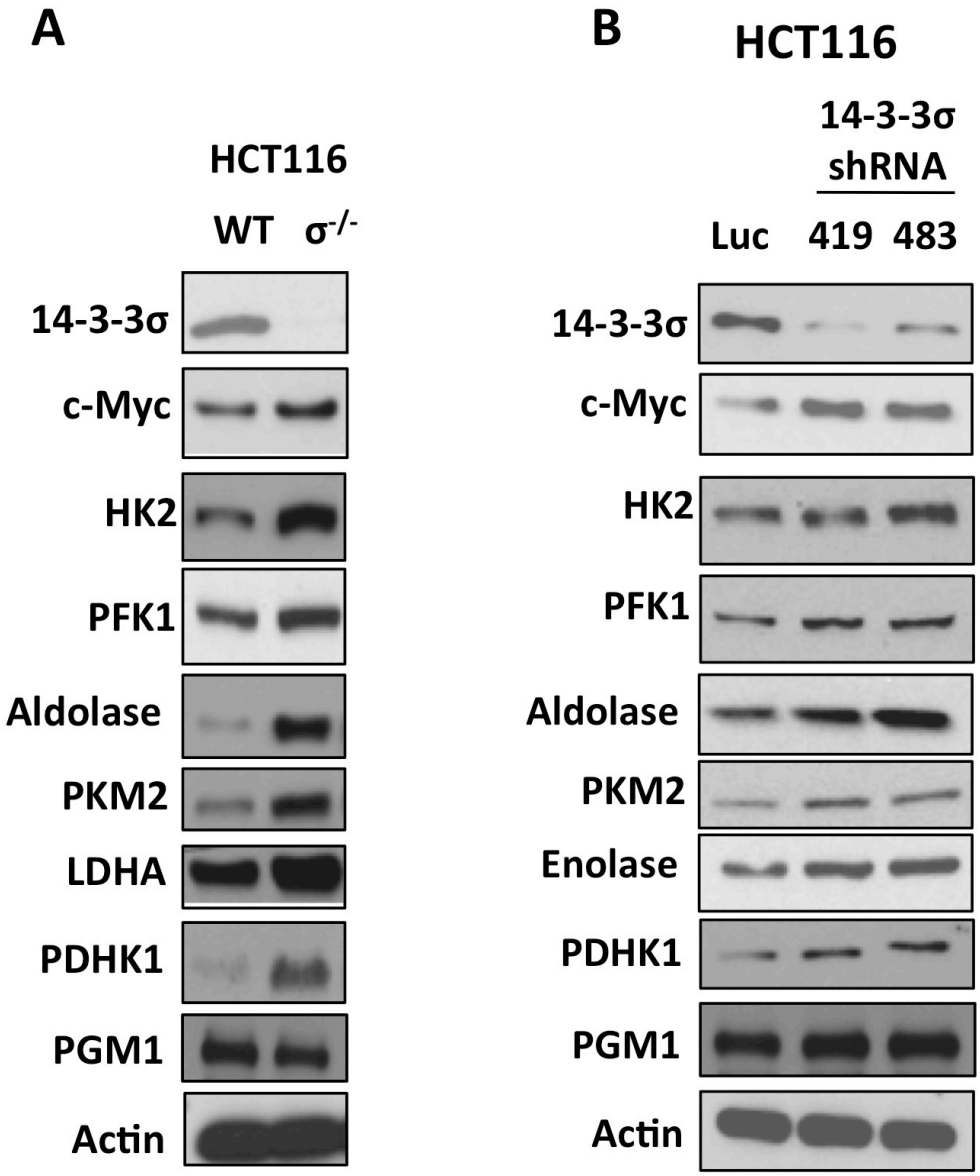
A
HCT116
WT
σ-/-
14-3-3σ
c-Myc
HK2
PFK1
Aldolase
PKM2
LDHA
PDHK1
PGM1
Actin
B
HCT116
14-3-3σ shRNA
Luc
419
483
14-3-3σ
c-Myc
HK2
PFK1
Aldolase
PKM2
Enolase
PDHK1
PGM1
Actin

Figure 36

Figure 36. Loss and knockdown of 14-3-3σ increase Myc-induced glycolytic target genes expression at protein level.
(A) Loss of 14-3-3σ increases the protein level of Myc-induced glycolytic target genes. Indicated cell lysates were immunoblotted with indicated antibodies.
(B) Knockdown of 14-3-3σ upregulates protein level of Myc-induced glycolytic target genes. Indicated cell lysates from cells infected with Luciferase shRNA or 14-3-3σ shRNA #419 and #483 were immunoblotted with indicated antibodies.

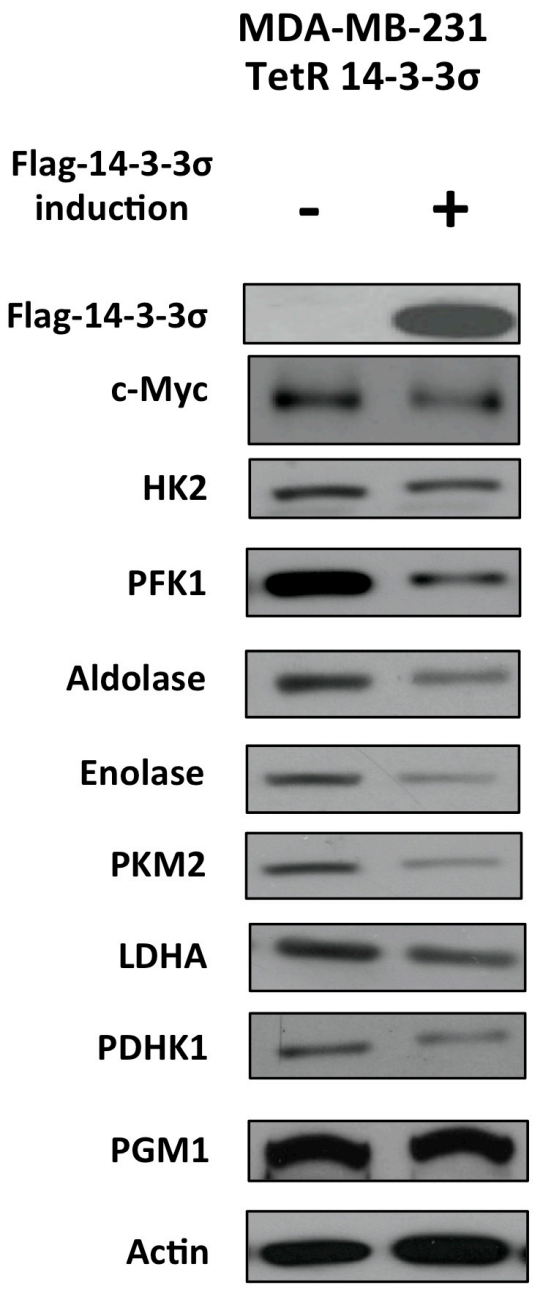
MDA-MB-231
TetR 14-3-3σ
Flag-14-3-3σ induction
-
+
Flag-14-3-3σ
c-Myc
HK2
PFK1
Aldolase
Enolase
PKM2
LDHA
PDHK1
PGM1
Actin

Figure 37

Figure 37. Doxycycline-induced Flag-14-3-3σ decreases protein level of Myc-targeted glycolytic genes. Flag-14-3-3σ was induced by Doxycycline as described above. Cell lysates were immunoblotted with indicated antibodies.

3.5 14-3-3σ regulates glutaminolysis and mitochondrial biogenesis by controlling Myc transcriptional activity

Since Myc induces glutaminolysis and mitochondrial biogenesis, both of which enhance cellular oxygen usage, we employed the Seahorse Bioscience Extracellular Flux Analyzer XF24 (Wu et al., 2007) to measure the influence of 14-3-3σ on oxygen consumption rate (OCR). We found that loss of 14-3-3σ increased oxygen consumption in HCT116 cells (Figure 38A). Similar results were found using another oxygen consumption measurement method (Figure 38B). Likewise, knockdown of 14-3-3σ elevated OCR. On the contrary, we observed that inducing Flag-14-3-3σ expression in HCT116 14-3-3σ$^{-/-}$, MDA-MB-231 and MDA-MB-435 cells led to a reduction in OCR in comparison to the control cells (Figure 39).

In the OCR assay, oligomycin, a mitochondrial ATP synthase inhibitor, is added to measure the respiratory capacity used for ATP synthesis. Then, oxygen consumption can be stimulated again when oxidative phosphorylation is uncoupled by addition of FCCP (Carbonyl cyanide 4-(trifluoromethoxy)phenylhydrazone), which destroys the mitochondrial membrane potential and causes a short-circuit in the respiratory chain. Thus, using FCCP allows us to determine the reserved maximal respiratory capacity of mitochondria. Following this, oxygen consumption can be completely stopped when rotenone (inhibitor of mitochondrial complex I) and antimycin A (inhibitor of mitochondrial complex III) are injected to stop mitochondrial electron transport. Hence, rotenone and antimycin A usage enables us to quantify the non-mitochondrial

respiration.

Our measurements show that induced 14-3-3σ re-expression in HCT116 14-3-3σ$^{-/-}$, MDA-MB-231 and MDA-MB-435 cells resulted in a remarkable reduction of basal oxygen consumption level, respiration-mediated ATP production, maximal respiration capacity as well as non-mitochondrial respiration (Figure 39). Reversely, loss and knockdown of 14-3-3σ expression increased all recently described respiratory parameters (Figure 38). Thus, 14-3-3σ has a strong negative impact on oxygen consumption in cancer cells.

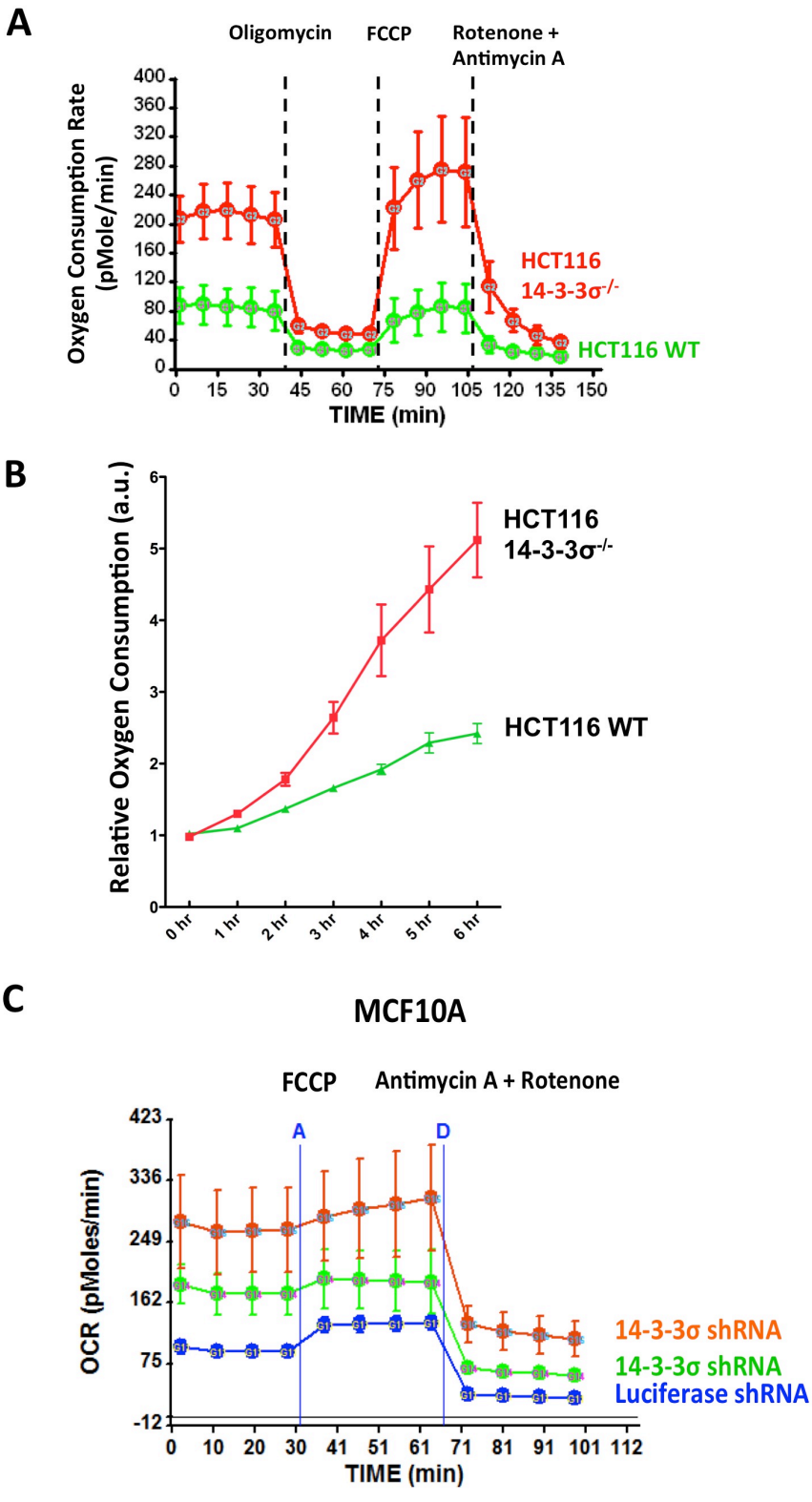
A
Oligomycin
FCCP
Rotenone +
Antimycin A
Oxygen Consumption Rate
(pMole/min)
400
360
320
280
240
200
160
120
80
40
0
0 15 30 45 60 75 90 105 120 135 150
TIME (min)
HCT116
14-3-3σ-/-
HCT116 WT
B
Relative Oxygen Consumption (a.u.)
6
5
4
3
2
1
0
0 hr
1 hr
2 hr
3 hr
4 hr
5 hr
6 hr
HCT116
14-3-3σ-/-
HCT116 WT
C
MCF10A
FCCP
Antimycin A + Rotenone
A
D
OCR (pMoles/min)
423
336
249
162
75
-12
0 10 20 30 41 51 61 71 81 91 101 112
TIME (min)
14-3-3σ shRNA
14-3-3σ shRNA
Luciferase shRNA

Figure 38

Figure 38. 14-3-3σ suppresses oxygen consumption.
(A) Loss of 14-3-3σ enhances oxygen consumption. Oxygen Consumption Rate (OCR) of HCT116 wt and 14-3-3$\sigma^{-/-}$ cells was measured using a Seahorse Bioscience Extracellular Flux Analyzer XF96 as described in Chapter 2 (Materials and Methods).
(B) Loss of 14-3-3σ increases oxygen consumption. HCT116 wt and HCT116 14-3-3$\sigma^{--/-}$ cells are cultured in BD Biosciences Oxygen Biosensor System microplates that have been previously coated with fibronectin to enhance cell attachment. The bottom of each well is embedded with an oxygen sensitive fluorescent compound (tris 1,7-diphenyl-1,10 phenanthroline ruthenium (II) chloride) that emits fluorescence when oxygen is consumed. To prevent oxygen exchange with environment, prior to measurement, mineral oil is applied to the surface of each well. Fluorescent signals, the indicators of oxygen consumption, are quantified by a Biotek luminometer that excites the oxygen sensitive fluorescent compound at 485 nm wavelength and capture the emitted 630 nm fluorescence.
(C) Knockdown of 14-3-3σ expression increases OCR in MCF10A cells. 14-3-3σ expression is knockdown in MCF10A cells using lentiviral shRNA. Luciferase shRNA is used as a control.

A

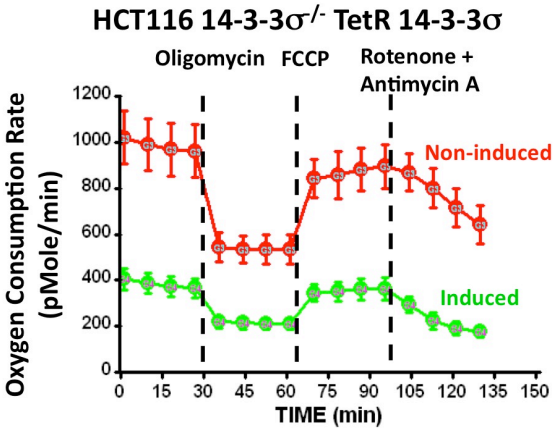

B

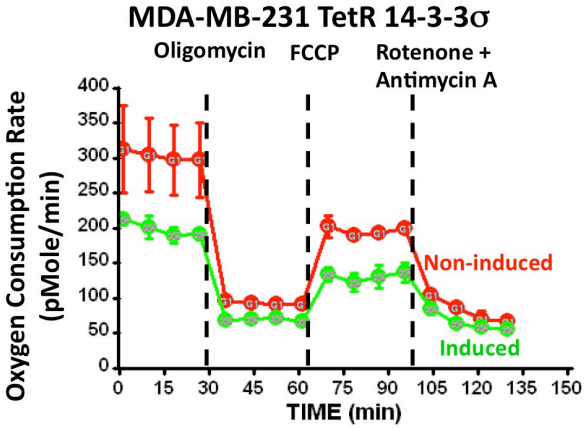

C

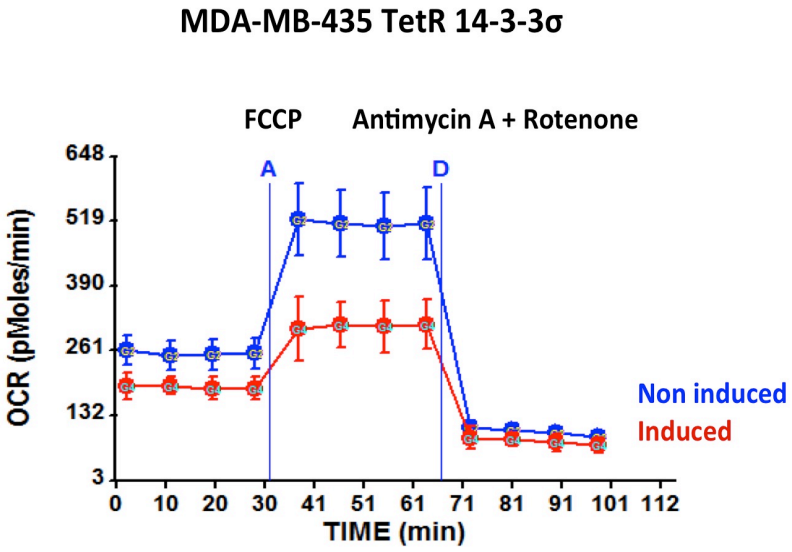

Figure 39

Figure 39. Induction of Flag-14-3-3σ decreases Oxygen Consumption Rate (OCR). Flag-14-3-3σ expression is induced in HCT116 14-3-3σ$^{-/-}$ TetR 14-3-3σ (A), MDA-MB-231 TetR 14-3-3σ (B) and MDA-MB-435 TetR 14-3-3σ (C) cancer cells with 5 ng/ml Doxycycline for 48 hours. Non-induced cells are used as a control. OCR is measured using Seahorse Extracellular Flux Analyzer XF96 as previously described.

Myc is known to promote glutaminolysis by elevating the gene expression of glutamine transporters (*SN2* and *ASCT2*) and Glutaminase 1 (*GLS1*) (Dang, 2010a; Gao et al., 2009; Wise et al., 2008; Yeung et al., 2008). Glutamine is transported into cells by transporters and is converted to α- ketoglutarate (α-KG) through the anaplerotic metabolism of glutamate to enter TCA cycle. Glutaminase is involved in the conversion of glutamine to glutamate. We showed that induced Flag-14-3-3σ expression down-regulates *SN2, ASCT2,* and *GLS1* (Figures 40A, 40B). Also, induced Flag-14-3-3σ expression leads to a reduction in ammonia production (Figure 41A), an important by-product of glutaminolysis (Eng et al., 2010), indicating the suppression of cancer glutaminolysis by 14-3-3σ. Additionally, glutamate concentration increased upon 14-3-3σ loss and decreased upon 14-3-3σ re-expression (Figure 24C). Also, 14-3-3σ induction by doxycycline treatment suppressed *GLS1* protein level in three different cell lines (Figure 41B), whereas loss and knockdown of 14-3-3σ led to increased *GLS1* protein expression (Figure 41C). Thus, these findings show that 14-3-3σ has a negative impact on glutaminolysis in cancer.

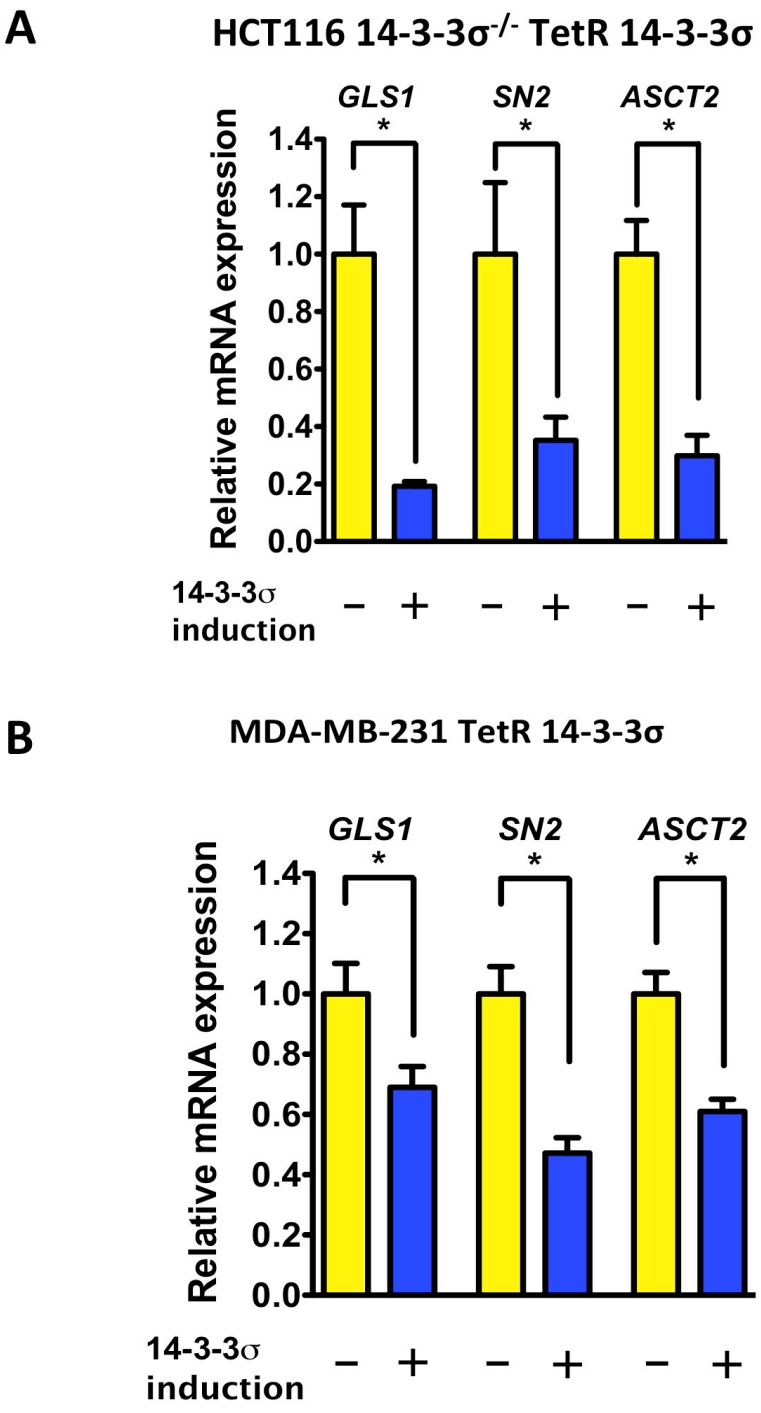
A
HCT116 14-3-3σ-/- TetR 14-3-3σ
GLS1
SN2
ASCT2
*
*
*
Relative mRNA expression
1.4
1.2
1.0
0.8
0.6
0.4
0.2
0.0
14-3-3σ induction
– + – + – +
B
MDA-MB-231 TetR 14-3-3σ
GLS1
SN2
ASCT2
*
*
*
Relative mRNA expression
1.4
1.2
1.0
0.8
0.6
0.4
0.2
0.0
14-3-3σ induction
– + – + – +

Figure 40

Figure 40. 14-3-3σ expression down-regulates Myc target genes involved in glutaminolysis.
(A) HCT116 14-3-3σ$^{-/-}$ TetR 14-3-3σ cells are grown in the presence of 5 ng/ml Doxycycline for 48 hours to induce Flag-14-3-3σ expression. Non-induced cells are used as a control. Total RNA is then extracted and converted to cDNA for qRT-PCR reactions with specific primers for *GLS1, SN2* and *ASCT2*, the three Myc target genes involved in glutaminolysis.
(B) Doxycycline-induced Flag-14-3-3σ decreases *GLS1, SN2* and *ASCT2* mRNA expression. Flag-14-3-3σ was induced by Doxycycline in MDA-MB-231 TetR 14-3-3σ cells as described above. qRT-PCR was performed using specific primers for the indicated genes.

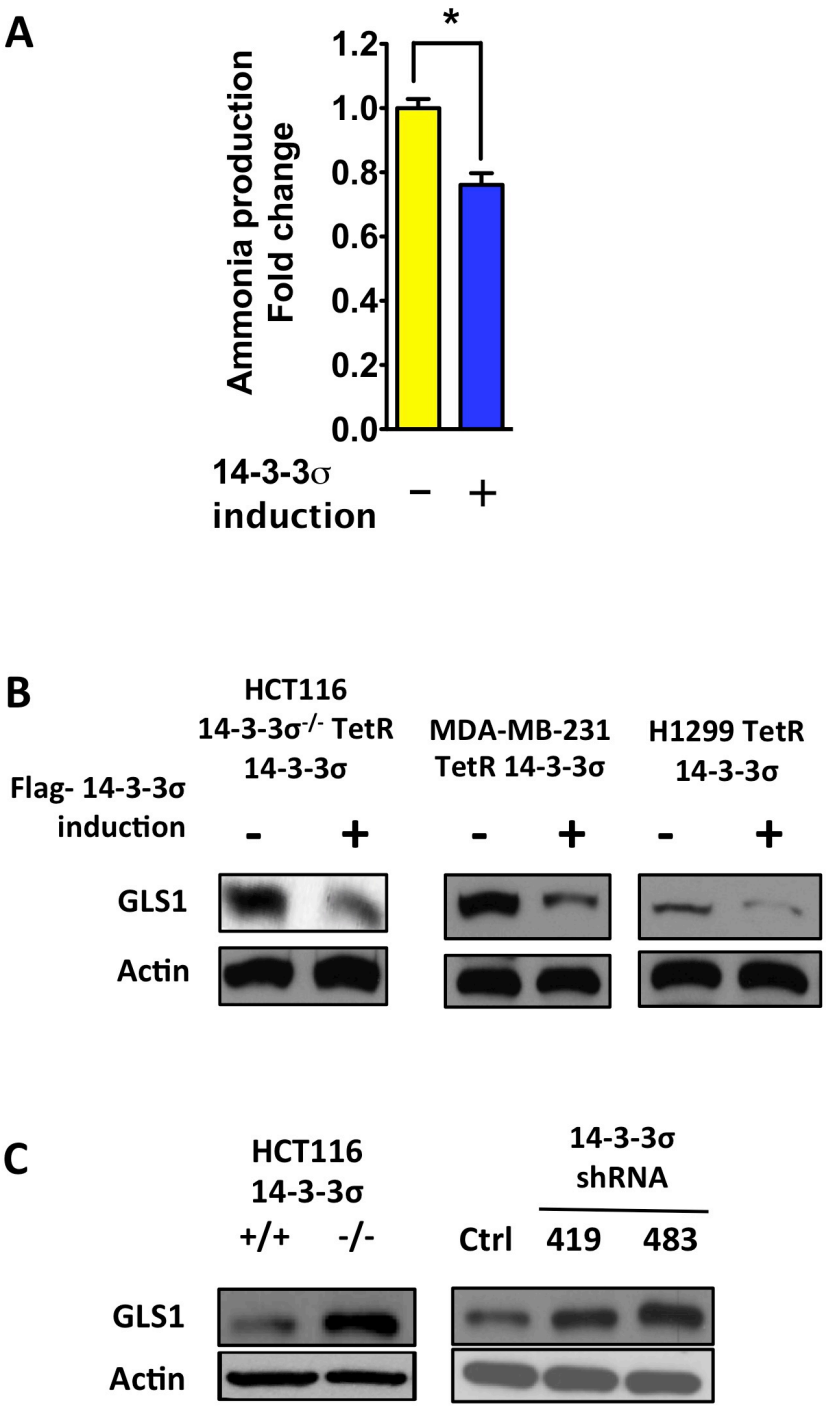
A
*
1.2
1.0
0.8
0.6
0.4
0.2
0.0
Ammonia production
Fold change
14-3-3σ
induction
–
+
B
HCT116
14-3-3σ-/- TetR
14-3-3σ
MDA-MB-231
TetR 14-3-3σ
H1299 TetR
14-3-3σ
Flag- 14-3-3σ
induction
-
+
-
+
-
+
GLS1
Actin
C
HCT116
14-3-3σ
+/+
-/-
14-3-3σ
shRNA
Ctrl
419
483
GLS1
Actin

Figure 41

Figure 41. 14-3-3σ decreases ammonia production (an important by-product of glutaminolysis) and down-regulates Glutaminase 1 protein expression.

(A) Doxycycline-induced Flag-14-3-3σ decreases ammonia production. Flag-14-3-3σ was induced by Doxycycline in cells as described above. Cell lysates are used for ammonia production measurement.
(B) Doxycycline-induced 14-3-3σ reduces Glutaminase 1 (*GLS1*) protein expression. Flag-14-3-3σ was induced by Doxycycline in cells as described above. Cell lysates were immunoblotted with anti-GLS1 antibodies.
(C) Loss and knockdown of 14-3-3σ increase GLS1 protein level. Cell lysates of HCT116 wt, HCT116 14-3-3σ$^{-/-}$, HCT116 Luciferase shRNA, HCT116 14-3-3σ shRNA #419 and #483 cells are collected and immunoblotted with anti-GLS1 antibodies.

Myc is a strong inducer of mitochondrial biogenesis by upregulating multiple genes that are mitochondrial components and increasing mitochondrial DNA replication (Li et al., 2005). As 14-3-3σ down-regulates Myc, we hypothesize that 14-3-3σ will also have a suppressive impact on Myc-mediated mitochondrial biogenesis. Therefore, we stained the cells with 10-Nonyl Acridine Orange *(*NAO), which associates with mitochondrial Cardiolipin and allows us to measure mitochondrial mass (Li et al., 2005). We found that loss of 14-3-3σ leads to an increase in mitochondrial mass (Figures 42A, 42B). Also, using MitoTracker Green FM, a dye that binds to the thiol group of mitochondria and only stains functional mitochondria, we observed that induced Flag-14-3-3σ expression has a negative impact on mitochondrial mass in HCT116 14-3-3σ$^{-/-}$, MDA-MB-231, HCT116 p53$^{-/-}$, and H1299 cancer cells (Figures 43A, 43B).

Moreover, induced Flag14-3-3σ expression in cancer cells leads to the reduction of gene expression of mitochondrial cytochrome c oxidase I (*MT-CO1*), NADH dehydrogenase 1 (*MT-ND1*) and *TFAM* (Li et al., 2005) (Figure 44), which is a Myc-transactivated target gene. *TFAM* is very important for mitochondrial gene transcription and mitochondrial DNA (mtDNA) replication (Li et al., 2005). Therefore, we then measured the ratio of mtDNA to nuclear DNA using qRT-PCR (Bogacka et al., 2005; Li et al., 2005). Both the ratio of *MT-CO1* to nuclear peroxisome proliferator-activated receptor gamma (*PPRC1*) and the ratio of *MT-ND1* to nuclear lipoprotein lipase (*LPL*) were reduced when Flag-14-3-3σ was induced, which suggests a reduction of mtDNA copy number due to Flag-14-3-3σ induction (Figure 44). Thus, by promoting Myc degradation, 14-3-3σ decreases the expression of many Myc target genes that are important for glutaminolysis, and mitochondrial biogenesis.

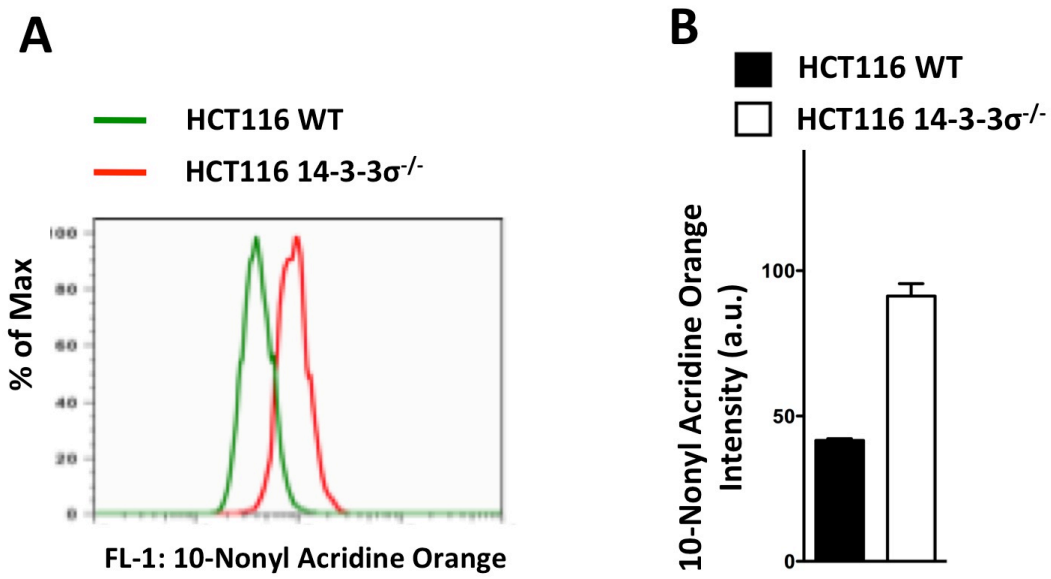
A
HCT116 WT
HCT116 14-3-3σ-/-
% of Max
100
80
60
40
20
0
FL-1: 10-Nonyl Acridine Orange
B
HCT116 WT
HCT116 14-3-3σ-/-
10-Nonyl Acridine Orange Intensity (a.u.)
100
50
0

Figure 42

Figure 42. Loss of 14-3-3σ significantly increases mitochondrial mass. Indicated cells were stained with 10-Nonyl Acridine Orange (10-NAO). The 10-NAO signal was quantified by flow cytometry (A). The 10-NAO signal intensity is presented as a bar graph (B).

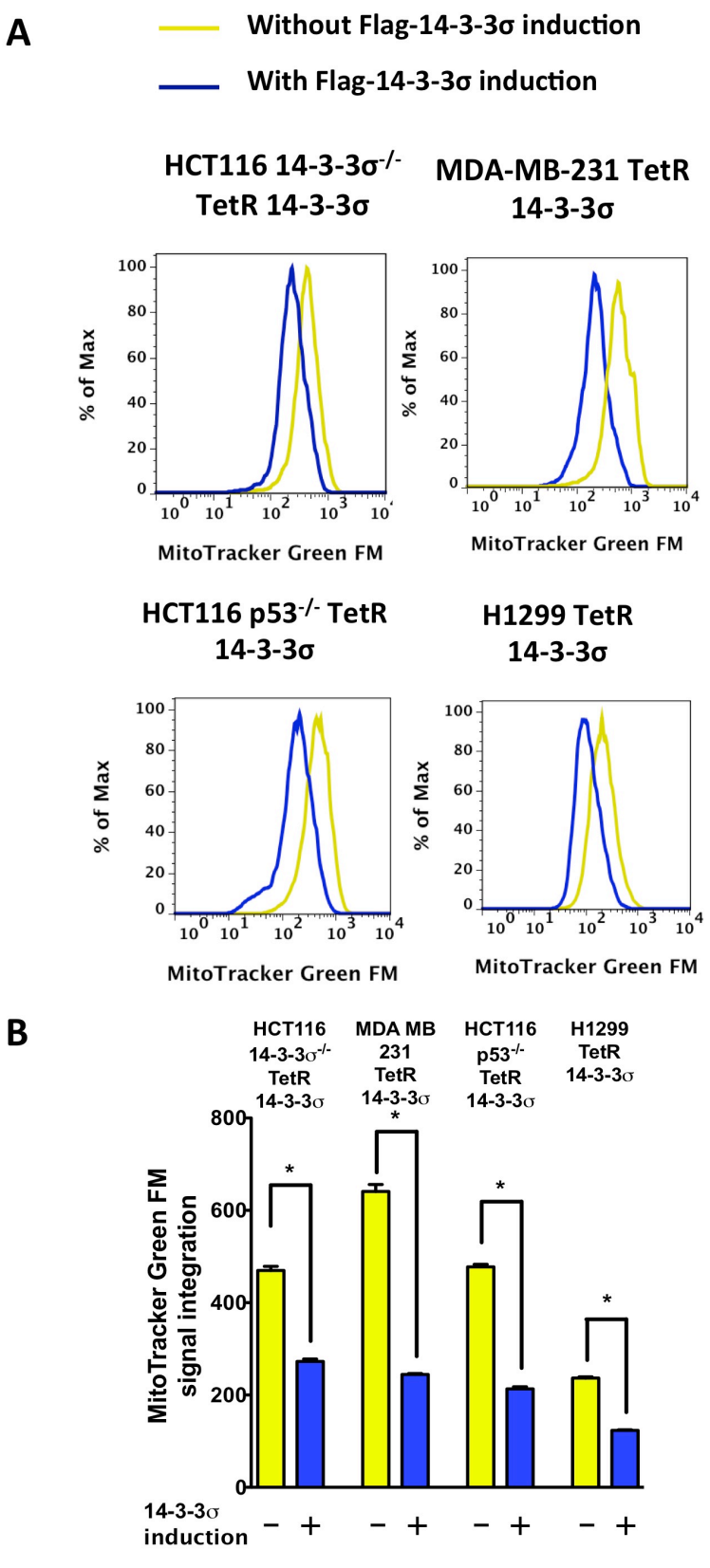
A
Without Flag-14-3-3σ induction
With Flag-14-3-3σ induction
HCT116 14-3-3σ-/- TetR 14-3-3σ
MDA-MB-231 TetR 14-3-3σ
HCT116 p53-/- TetR 14-3-3σ
H1299 TetR 14-3-3σ
% of Max
MitoTracker Green FM
B
HCT116 14-3-3σ-/- TetR 14-3-3σ
MDA MB 231 TetR 14-3-3σ
HCT116 p53-/- TetR 14-3-3σ
H1299 TetR 14-3-3σ
MitoTracker Green FM signal integration
14-3-3σ induction
− + − + − + − +

Figure 43

Figure 43. 14-3-3σ expression decreases mitochondrial mass.
(A) Doxycycline-induced Flag-14-3-3σ leads to a significant decline in mitochondrial mass in multiple cancer cell lines. Cell were stained with MitoTracker Green FM and then analyzed by flow cytometry.
(B) Bar graphs of Figure 43A showing the negative impact of 14-3-3σ on mitochondrial mass of cancer cells. All data is represented as mean ± 95% CI.

HCT116 14-3-3σ$^{-/-}$ TetR 14-3-3σ

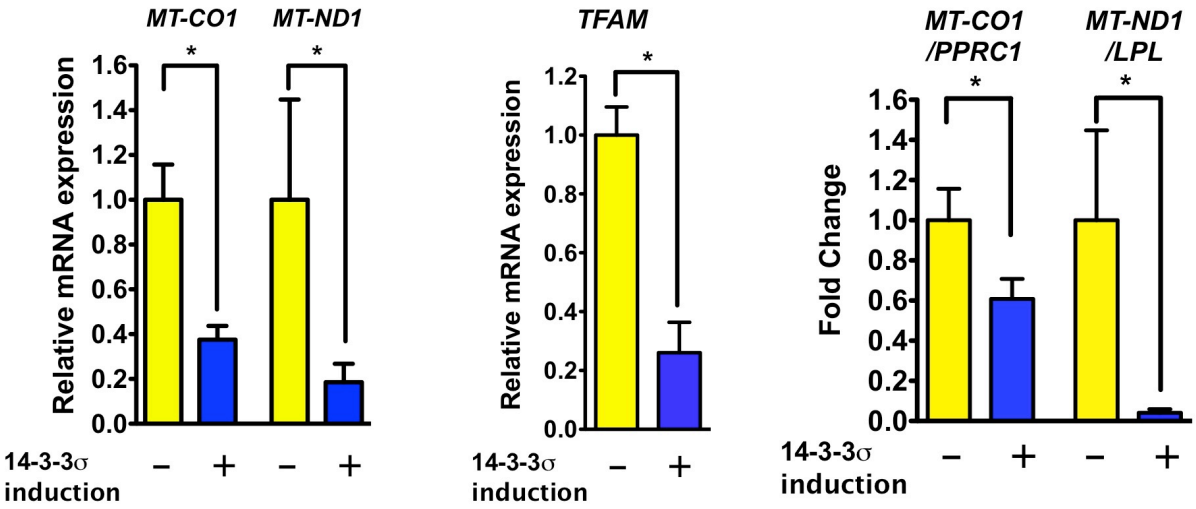

MDA-MB-231 TetR 14-3-3σ

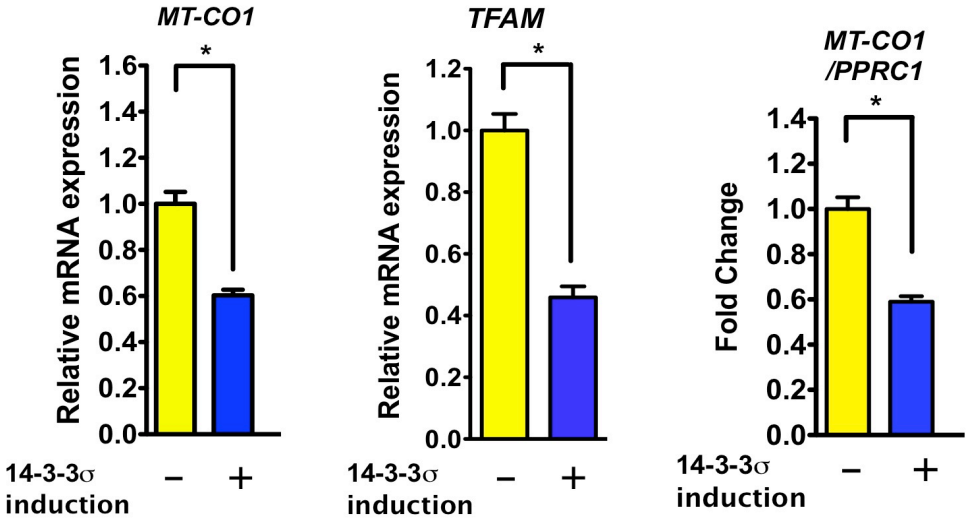

Figure 44

Figure 44. Flag-14-3-3σ induction decreases mitochondrial gene expression and biogenesis. Flag-14-3-3σ was induced by Doxycycline in HCT116 14-3-3σ$^{-/-}$ TetR 14-3-3σ and MDA-MB-231 TetR 14-3-3σ cells as described above. qRT-PCR was performed using specific primers for the indicated genes. The expression ratios of *MT-CO1/ PPRC1* and *MT-ND1/LPL* were also quantitated using qRT-PCR. All data is represented as mean ± 95% CI.

3.6 The regulation of cancer metabolism by 14-3-3σ is via targeting Myc and does not require p53 impact.

To study whether Myc is a critical mediator in cancer metabolism suppression by 14-3-3σ, we used lentiviral shRNA to knockdown Myc (Figure 45). We observed that in the presence of Myc knockdown, neither ECAR nor OCR decreased any further when 14-3-3σ was induced, suggesting that Myc down-regulation is a major mechanism for 14-3-3σ-mediated inhibition of cancer cell metabolism (Figure 45).

On the other hand, as 14-3-3σ is a p53-induced target gene that exerts a positive feedback to stabilize p53 (Yang et al., 2003; Yang et al., 2007) and p53 is also a major metabolic regulator (Bensaad et al., 2006; Ide et al., 2009; Matoba et al., 2006), it is important to determine whether 14-3-3σ-mediated regulation of cancer energy metabolism depends on p53 impact. Interestingly, ECAR and OCR were also reduced upon Flag-14-3-3σ induction in these p53 null cells (Figure 46). Furthermore, induced expression of Flag-14-3-3σ in p53 null cell lines (H1299 and HCT116 $p53^{-/-}$) still diminished glucose consumption, ATP level and Myc transcriptional activity (Figure 47A, 47B, 47C).

Additionally, we found that induced expression of 14-3-3σ in H1299 cells led to the down-regulation of Myc, HK2, PFK1 and PKM2 (Figure 47D). Furthermore, mitochondrial mass decreased when 14-3-3σ was re-expressed in MDA-MB-231 (p53 mutated), HCT116 $p53^{-/-}$ and H1299 cancer cells (Figures 43A, 43B, 44). The negative

influence of 14-3-3σ on Myc stability, Myc transactivational ability, and Myc-induced glycolytic target gene expression was also observed in p53 mutated cell line MDA-MB-231 (Figures 30A, 32, 35A, 37). Thus, these data suggest that 14-3-3σ controls cancer energy metabolism through the regulation of Myc in a manner that doesn't require p53 impact.

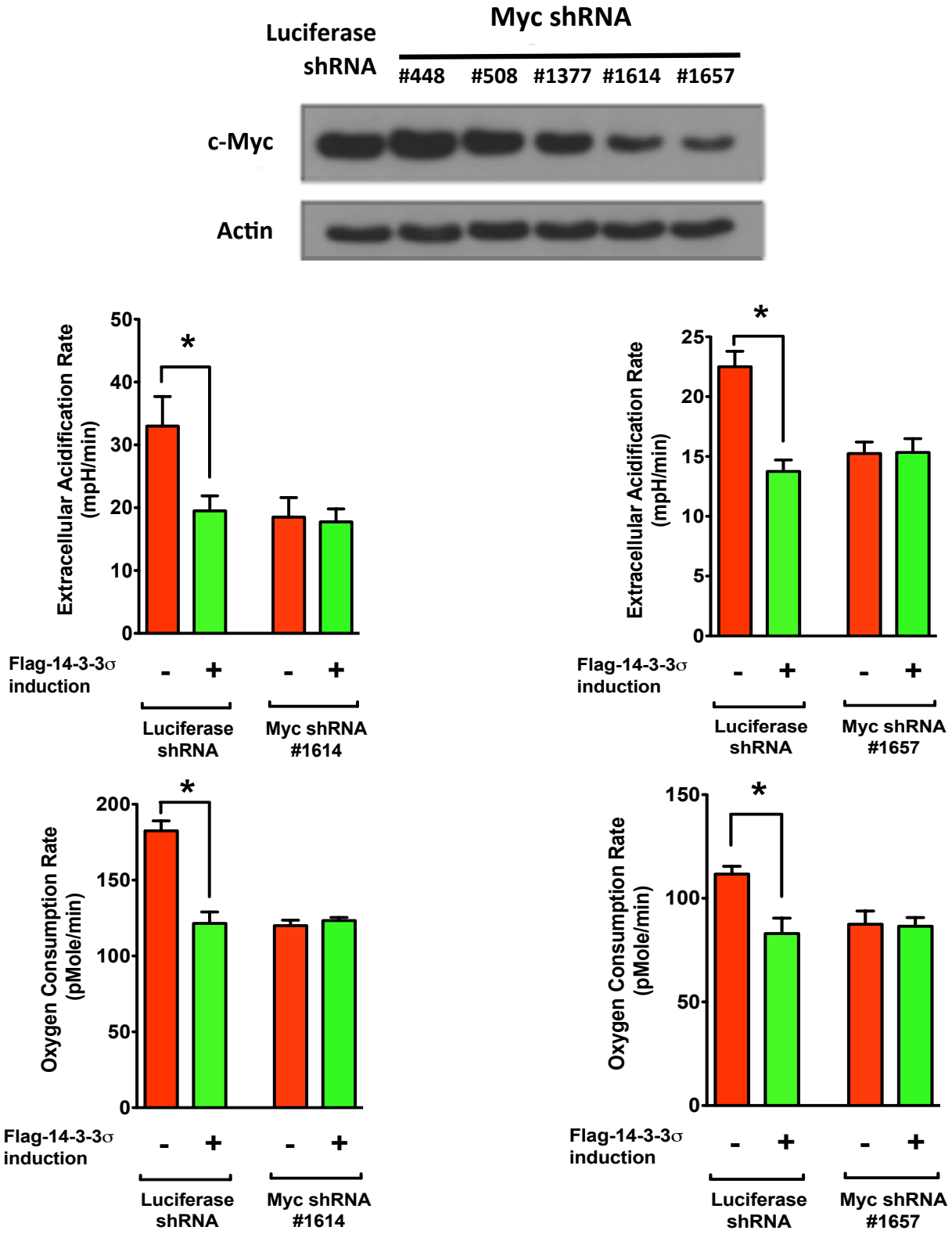
Luciferase shRNA
Myc shRNA
#448
#508
#1377
#1614
#1657
c-Myc
Actin
Extracellular Acidification Rate (mpH/min)
Oxygen Consumption Rate (pMole/min)
Flag-14-3-3σ induction
Luciferase shRNA
Myc shRNA #1614
Myc shRNA #1657

Figure 45

Figure 45. c-Myc knockdown compromises 14-3-3σ-mediated down-regulation of ECAR and OCR. MDA-MB-231 TetR 14-3-3σ cells were infected with lentiviruses carrying c-Myc shRNA. Cell lysates were immunoblotted with anti-Myc antibodies. Cells infected with Luciferase shRNA, Myc shRNA #1614 and Myc shRNA #1657 were then treated with Doxycycline to induce Flag-14-3-3σ expression (+). Non-induced cells were used as a control (-). ECAR and OCR were measured as previously described.

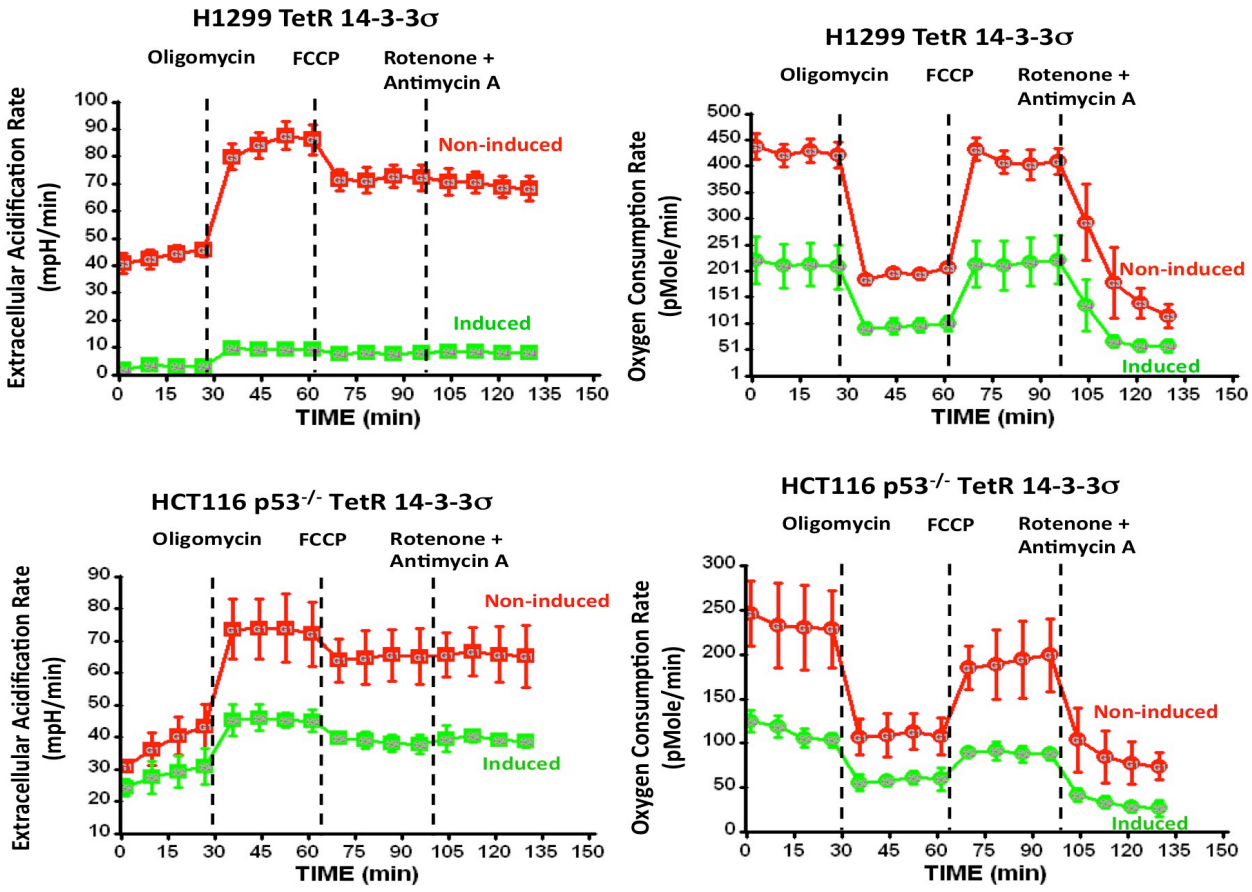
H1299 TetR 14-3-3σ
Oligomycin
FCCP
Rotenone + Antimycin A
Extracellular Acidification Rate (mpH/min)
Non-induced
Induced
TIME (min)
H1299 TetR 14-3-3σ
Oligomycin
FCCP
Rotenone + Antimycin A
Oxygen Consumption Rate (pMole/min)
Non-induced
Induced
TIME (min)
HCT116 p53-/- TetR 14-3-3σ
Oligomycin
FCCP
Rotenone + Antimycin A
Extracellular Acidification Rate (mpH/min)
Non-induced
Induced
TIME (min)
HCT116 p53-/- TetR 14-3-3σ
Oligomycin
FCCP
Rotenone + Antimycin A
Oxygen Consumption Rate (pMole/min)
Non-induced
Induced
TIME (min)

Figure 46

Figure 46. Lack of p53 does not hinder 14-3-3σ's ability to suppress ECAR and OCR. H1299 TetR 14-3-3σ and HCT116 $p53^{-/-}$ TetR 14-3-3σ cells were treated with Doxycycline to induce Flag-14-3-3σ expression (+). Non-induced cells were used as a control (-). ECAR and OCR were measured. All data is represented as mean ± standard deviation.

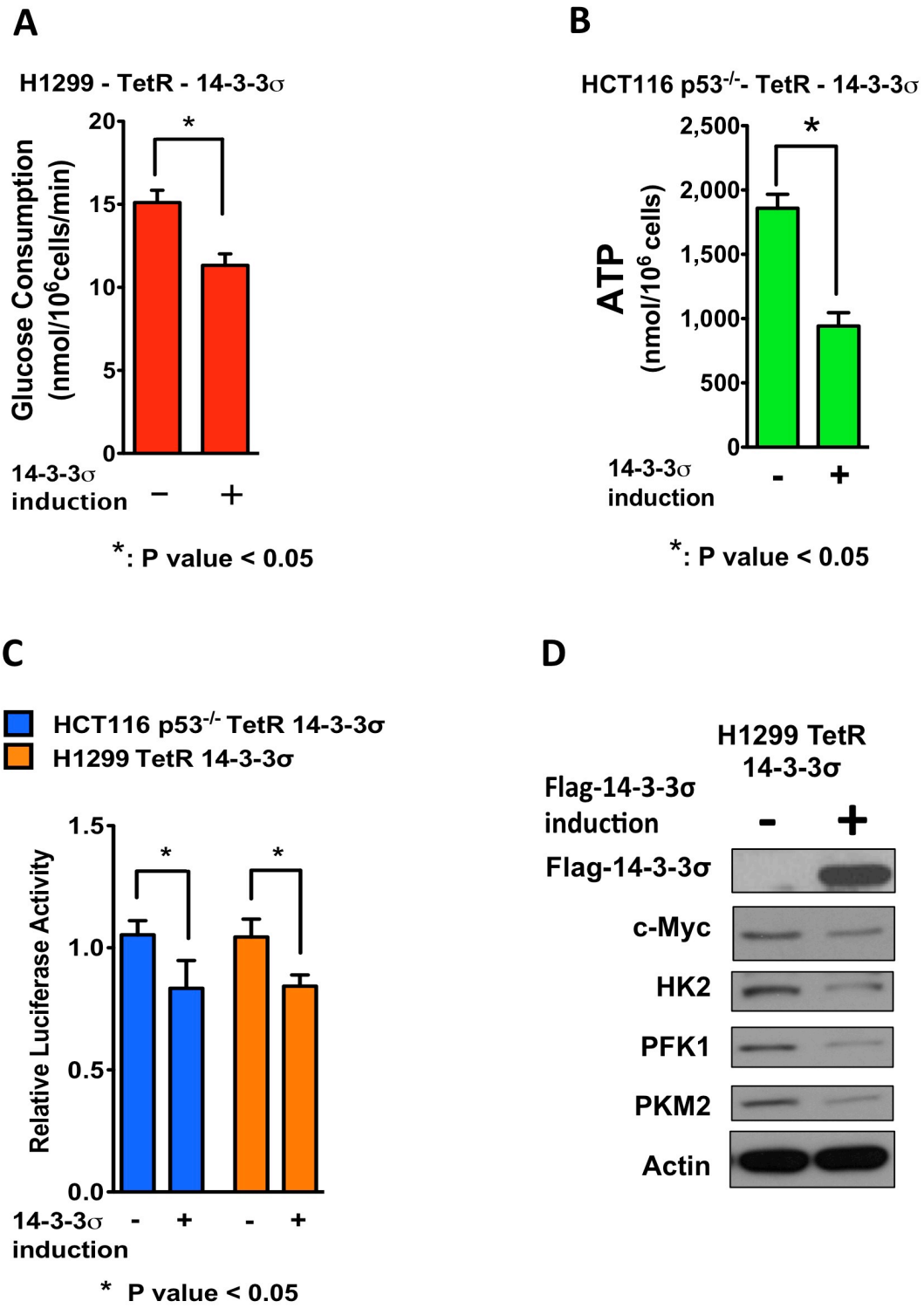
A
H1299 - TetR - 14-3-3σ
Glucose Consumption (nmol/10^6cells/min)
20
15
10
5
0
*
14-3-3σ induction
−
+
*: P value < 0.05
B
HCT116 p53-/- TetR - 14-3-3σ
ATP (nmol/10^6 cells)
2,500
2,000
1,500
1,000
500
0
*
14-3-3σ induction
-
+
*: P value < 0.05
C
HCT116 p53-/- TetR 14-3-3σ
H1299 TetR 14-3-3σ
Relative Luciferase Activity
1.5
1.0
0.5
0.0
*
*
14-3-3σ induction
- + - +
* P value < 0.05
D
H1299 TetR 14-3-3σ
Flag-14-3-3σ induction
- +
Flag-14-3-3σ
c-Myc
HK2
PFK1
PKM2
Actin

Figure 47

Figure 47. Lack of p53 doesn't prevent the negative impact of 14-3-3σ on cancer metabolism and Myc-induced glycolytic target gene expression.
(A) Induction of Flag-14-3-3σ decreases glucose consumption in H1299 cancer cells. H1299 is a lung cancer cell line that lost p53 expression. H1299 cells that carry a Tet On 14-3-3σ system are cultured with 5 ng/ml Doxycycline to induce Flag-14-3-3σ expression for 48 hours. Glucose consumption is measured as previously described.
(B) Induction of Flag-14-3-3σ diminishes ATP level in HCT116 $p53^{-/-}$ cancer cells. HCT116 $p53^{-/-}$ cancer cells lost p53 expression due to homologous recombination. HCT116 $p53^{-/-}$ cells that carry a Tet On 14-3-3σ system are cultured with 5 ng/ml Doxycycline to induce Flag-14-3-3σ expression for 48 hours. ATP concentration is measured as previously described.
(C) 14-3-3σ reduces Myc transactivational activity in p53 null cells. H1299 TetR 14-3-3σ and HCT116 $p53^{-/-}$ TetR 14-3-3σ cells are transfected with Luciferase reporter plasmid that contains Myc binding sites (Ebox), and Renilla Luciferase plasmid. 24 hours after transfection, Flag-14-3-3σ expression is then induced with 5 ng/ml Doxycycline for 48 hours. Non-induced cells are used as control. Cell lysates are then collected and used in Dual Luciferase Assay (Promega).
(D) 14-3-3σ diminishes the expression of Myc and Myc glycolytic target genes in p53-deficient H1299 cells. H1299 TetR 14-3-3σ cells are cultured in the presence of 5 ng/ml Doxycycline for 48 hours to induce Flag-14-3-3σ expression. Non-induced cells are used as control. Cell lysates are collected and immunoblotted with the indicated antibodies.

3.7 14-3-3σ suppresses cancer glycolysis, glutaminolysis and mitochondrial biogenesis *in vivo*

We have found that 14-3-3σ functioned as an important regulator of cancer metabolism *in vitro*. To validate the impact of 14-3-3σ on cancer bioenergetics *in vivo*, we established an orthotopic xenograft mouse model using MDA-MB-231 breast cancer cells that carry an inducible tet-On 14-3-3σ expression system (please see Materials and Methods #2.5, page 29). The experimental group received Doxycycline in their drinking water for 2 weeks to induce 14-3-3σ expression while the control group was not treated with Doxycycline. We then used ^{18}FDG microPET scan to assess the impact of 14-3-3σ on glucose uptake *in vivo*.

Our data showed that Flag-14-3-3σ induction caused a 50% reduction in glucose uptake of the xenograft tumors (Figure 48A). To further confirm that 14-3-3σ expression suppresses cancer glycolysis, we extracted and analyzed the xenograft tumors using qRT-PCR and Western Blot. We found that induction of Flag-14-3-3σ by Doxycycline led to the suppression of all Myc-induced glycolytic target genes (Figures 48B, 49A). Again, expression of *PGM1, (*a glycolytic gene that is not controlled by Myc), was not suppressed by the induction of 14-3-3σ, indicating the selective impact of 14-3-3σ on Myc-induced glycolytic target genes (Figures 48B, 49A).

Immunohistochemistry studies on cancer samples from this mouse model also indicated that the expression of key glycolytic enzymes such as PKM2 and PFK1 was

suppressed during tumorigenesis by Flag-14-3-3σ induction (Figure 49B). Flag-14-3-3σ induction also resulted in higher cleaved Caspase 3 level, suggesting an increase in apoptosis (Figure 49B). More importantly, induction of Flag-14-3-3σ in the xenograft tumors additionally led to the reduced expression of Myc-regulated genes involved in glutaminolysis, e.g, *GLS1, SN2* and *ASCT2* (Figures 49A and 50A). Similarly, induction of Flag-14-3-3σ in tumors diminishes the expression of *MT-CO1, MT-ND1,* and *MT-CO1/PPRC1* ratio, which reflects a reduction of the mtDNA copy number due to 14-3-3σ (Figure 50B).

We also used this Doxycycline-induced mouse cancer model for Magnetic Resonance Spectroscopy Imaging with a hyperpolarized ^{13}C pyruvate tracer (Figure 51). We found that after 2 weeks of Flag-14-3-3σ induction (day 14), ^{13}C pyruvate-to-^{13}C lactate flux markedly diminished in MDA-MB-231 xenograft tumors compared with non-induced control tumors at day 0 (Figure 51A). A snapshot of Magnetic Resonance spectra additionally indicates that 14-3-3σ hinders the ^{13}C pyruvate-to-^{13}C lactate conversion (Figure 51B). The rate constant of ^{13}C pyruvate-to-^{13}C lactate reaction (k_{PL}) in MDA-MB-231 xenograft tumors was calculated (Harris et al., 2009) and shown to be reduced by 45% after induction of Flag-14-3-3σ when compared with the non-induced group (Figure 51C).

In summary, our data indicates that the role of 14-3-3σ in suppressing Myc-promoted glycolysis, glutaminolysis, and mitochondrial biogenesis can be recapitulated *in vivo.*

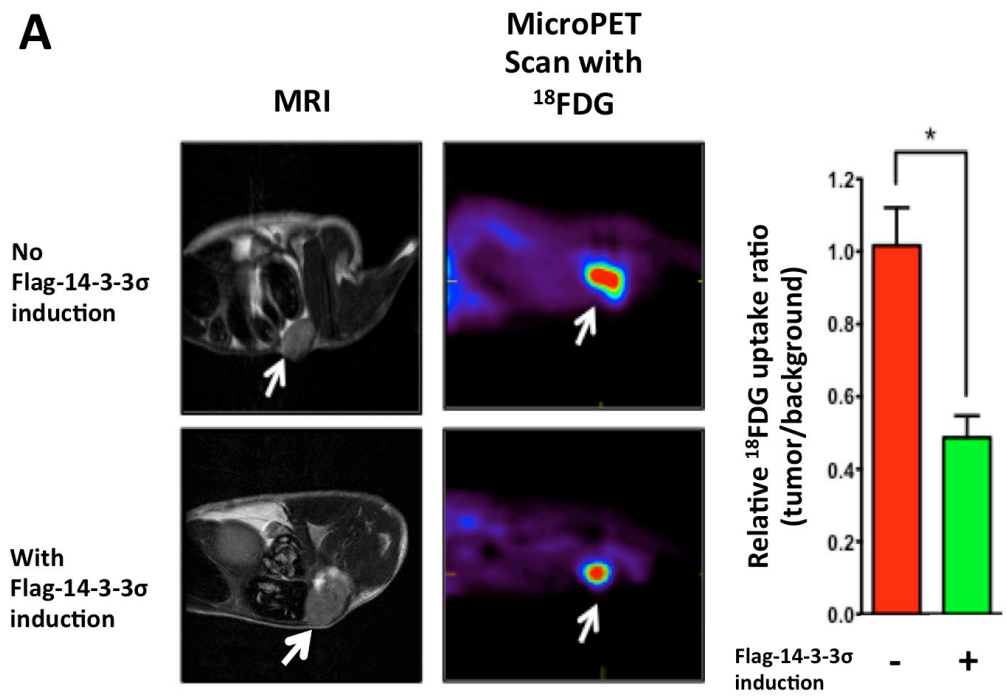
A
MRI
MicroPET Scan with 18FDG
No Flag-14-3-3σ induction
With Flag-14-3-3σ induction
Relative 18FDG uptake ratio (tumor/background)
1.2
1.0
0.8
0.6
0.4
0.2
0.0
*
Flag-14-3-3σ induction
-
+

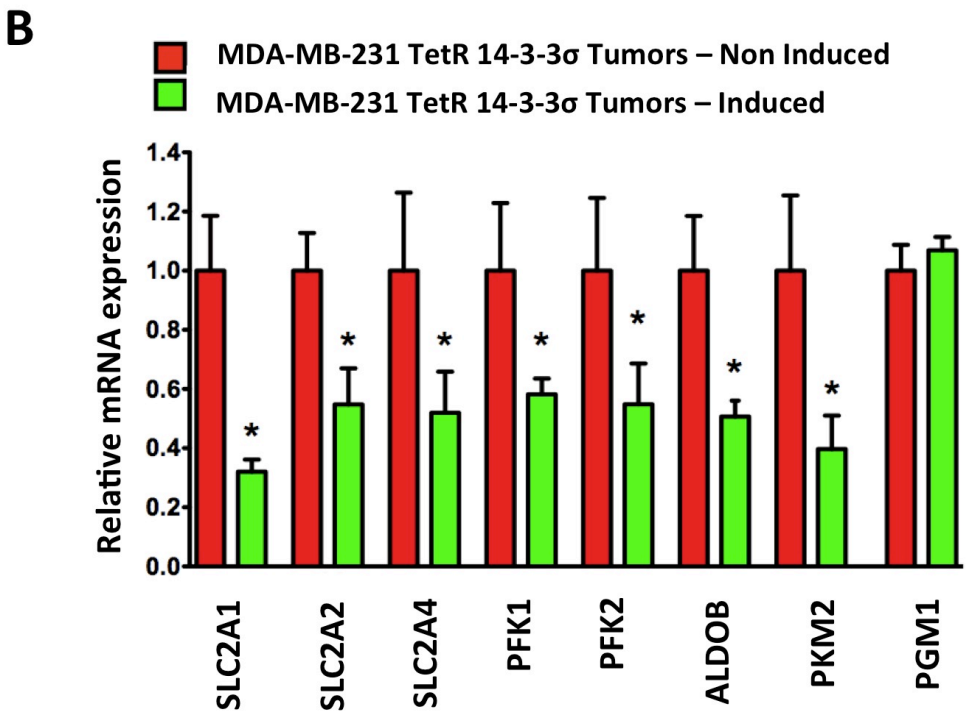
B
MDA-MB-231 TetR 14-3-3σ Tumors – Non Induced
MDA-MB-231 TetR 14-3-3σ Tumors – Induced
Relative mRNA expression
1.4
1.2
1.0
0.8
0.6
0.4
0.2
0.0
*
SLC2A1
SLC2A2
SLC2A4
PFK1
PFK2
ALDOB
PKM2
PGM1

Figure 48

Figure 48. 14-3-3σ suppresses cancer glycolysis *in vivo.*
(A) Doxycycline-induced Flag-14-3-3σ expression results in a remarkable decrease in ^{18}FDG uptake in MDA-MB-231 xenograft breast tumors. MDA-MB-231 TetR 14-3-3σ breast cancer cells were injected into the mammary fat pad of a female nude mouse. Tumor growth was monitored for 4 weeks. After that, mice were divided into 2 groups. The experimental group received 200 μg/ml doxycycline in their drinking water for 2 weeks to induce Flag-14-3-3σ expression (+). The control group only received normal drinking water (-). All mice were then imaged with Magnetic Resonance Imaging and microPET Scan. The white arrows indicate tumor location. The relative ^{18}FDG uptake ratio was calculated and is presented as a bar graph.
(B) Down-regulation of Myc-targeted glycolytic gene expression in xenograft breast tumors with Flag-14-3-3σ induction. After microPET and MRI imaging, tumors were extracted from the mice. Total RNA was collected for qRT-PCR using specific primers for the indicated genes.

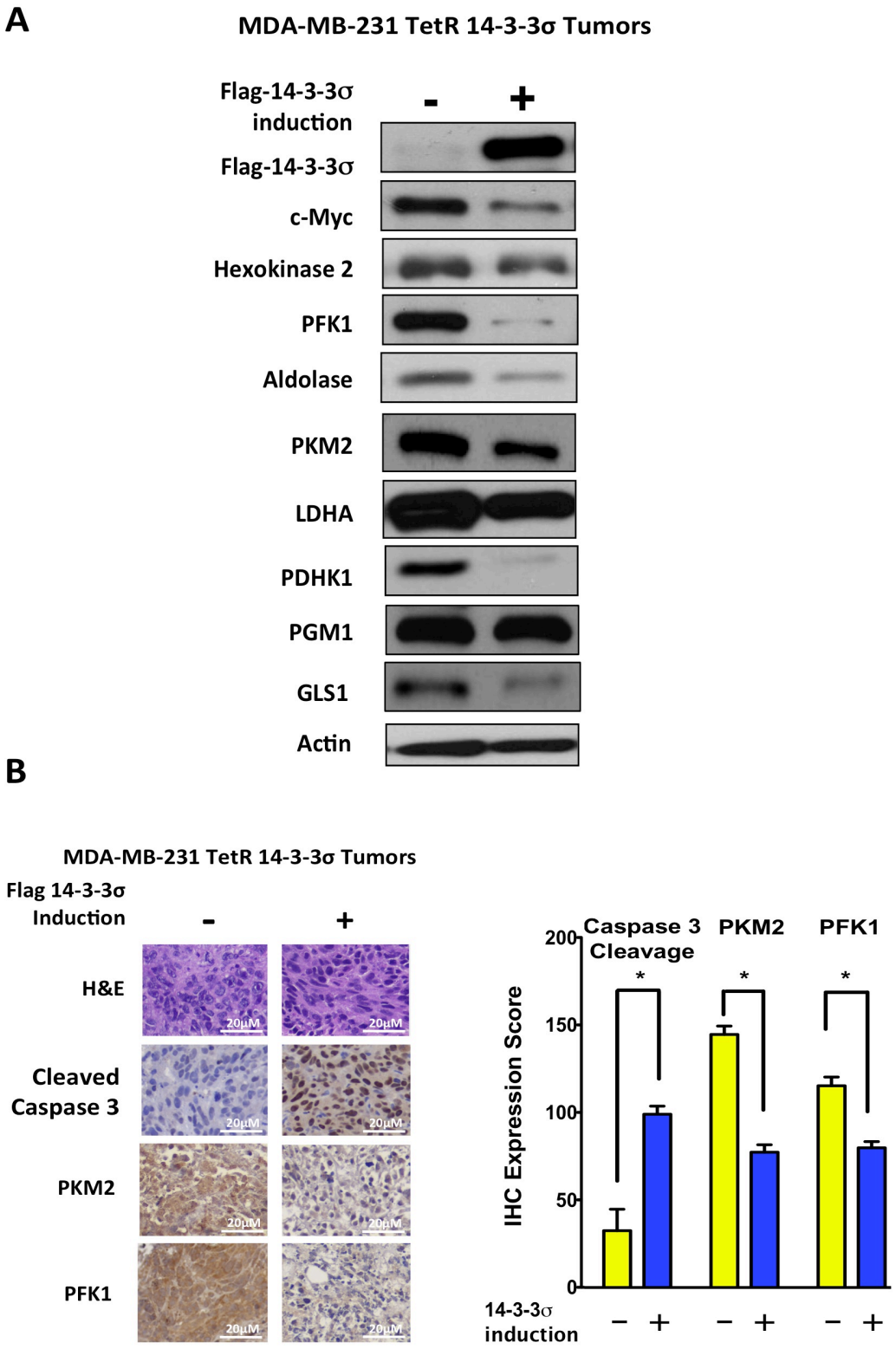
A
MDA-MB-231 TetR 14-3-3σ Tumors
Flag-14-3-3σ induction
-
+
Flag-14-3-3σ
c-Myc
Hexokinase 2
PFK1
Aldolase
PKM2
LDHA
PDHK1
PGM1
GLS1
Actin
B
MDA-MB-231 TetR 14-3-3σ Tumors
Flag 14-3-3σ Induction
-
+
H&E
Cleaved Caspase 3
PKM2
PFK1
20μM
Caspase 3 Cleavage
PKM2
PFK1
IHC Expression Score
200
150
100
50
0
*
14-3-3σ induction
− + − + − +

Figure 49

Figure 49. The negative impact of 14-3-3σ on Myc-targeted glycolytic genes expression *in vivo.*

(A) Flag-14-3-3σ induction down-regulates protein level of Myc-targeted glycolytic genes in xenograft tumors. Cell lysates from MDA-MB-231 TetR 14-3-3σ xenograft tumors were immunoblotted with the indicated antibodies.

(B) Flag-14-3-3σ induction reduces PKM2 and PFK1 expression in xenograft tumors. Immunohistochemistry (IHC) staining of indicated xenograft tumors was performed with the indicated antibodies. Representative pictures are shown. IHC signals on all slides were then quantified using a Dako ChromaVision ACIS III system and are displayed in bar graphs.

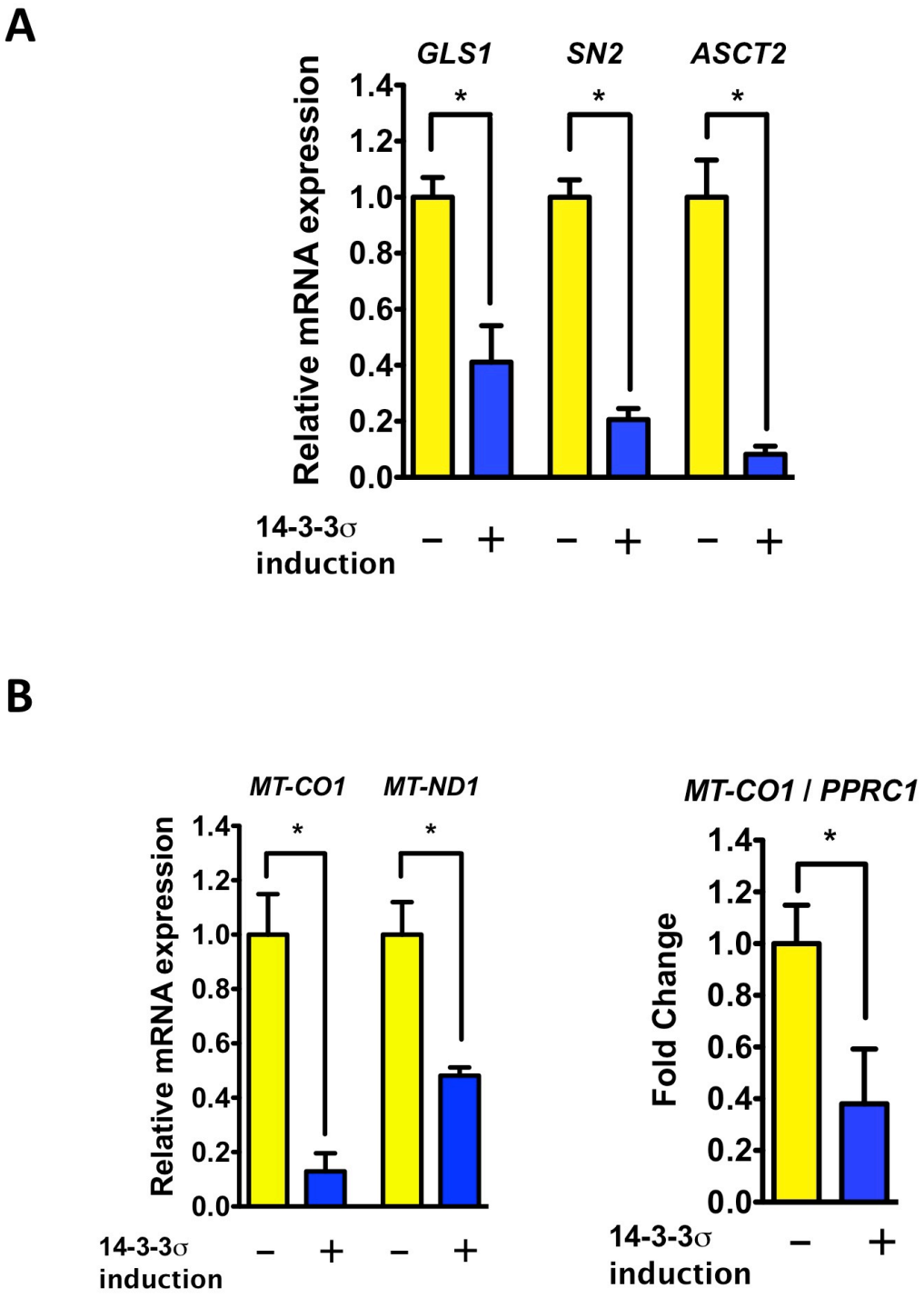
A
GLS1
SN2
ASCT2
Relative mRNA expression
1.4
1.2
1.0
0.8
0.6
0.4
0.2
0.0
*
*
*
14-3-3σ induction
– + – + – +
B
MT-CO1
MT-ND1
Relative mRNA expression
1.4
1.2
1.0
0.8
0.6
0.4
0.2
0.0
*
*
14-3-3σ induction
– + – +
MT-CO1 / PPRC1
Fold Change
1.4
1.2
1.0
0.8
0.6
0.4
0.2
0.0
*
14-3-3σ induction
– +

Figure 50

Figure 50. 14-3-3σ decreases glutaminolysis and mitochondrial biogenesis *in vivo*.
(A) Flag-14-3-3σ induction reduces expression of genes involved in glutaminolysis in xenograft breast tumors. Indicated mRNA levels were measured by qRT-PCR as previously described.
(B) Reduction of mitochondrial biogenesis in xenograft breast tumor upon Flag-14-3-3σ induction. Mitochondrial gene expression and *TFAM* level was quantified by qRT-PCR using the cDNA from xenograft tumor RNA. The expression ratio of *MT-CO1/ PPRC1* was also quantitated using qRT-PCR.

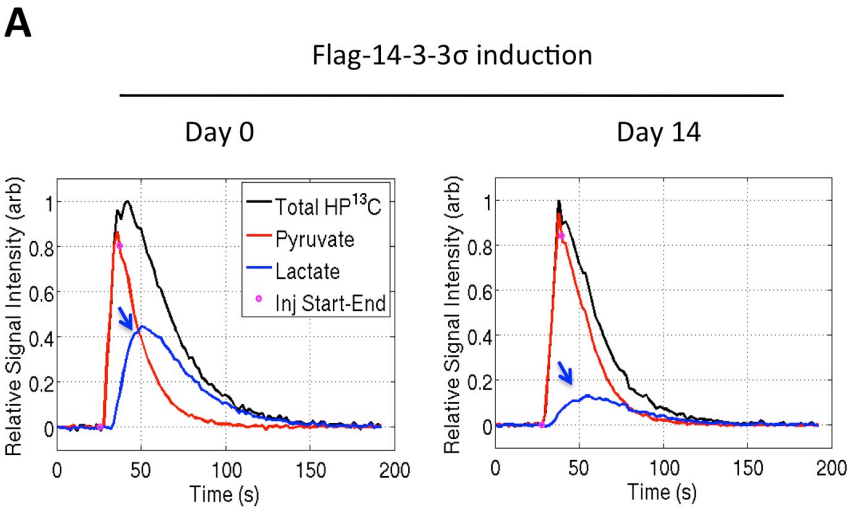
A
Flag-14-3-3σ induction
Day 0
Day 14
Total HP13C
Pyruvate
Lactate
Inj Start-End
Relative Signal Intensity (arb)
Time (s)

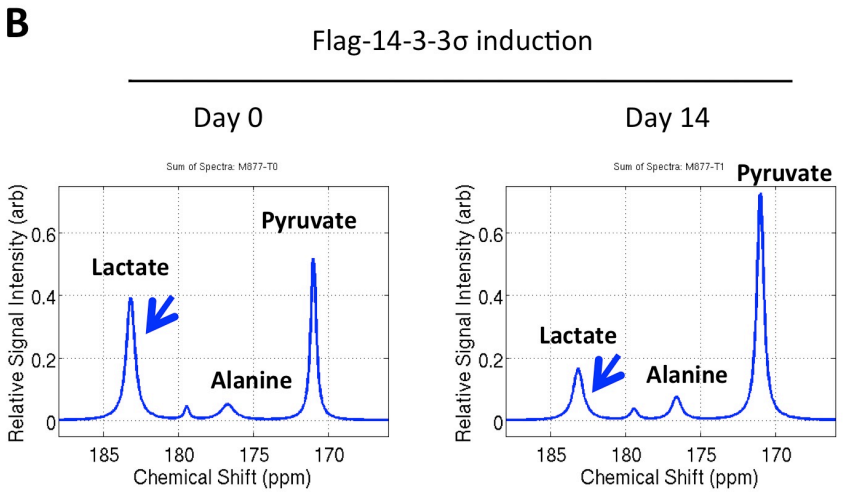
B
Flag-14-3-3σ induction
Day 0
Day 14
Sum of Spectra: M877-T0
Sum of Spectra: M877-T1
Pyruvate
Lactate
Alanine
Relative Signal Intensity (arb)
Chemical Shift (ppm)

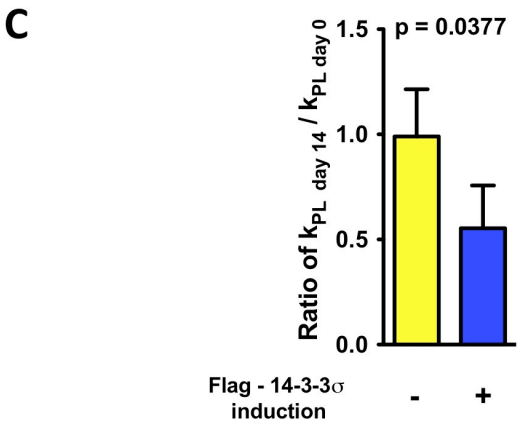
C
p = 0.0377
Ratio of kPL day 14 / kPL day 0
Flag - 14-3-3σ induction
-
+

Figure 51

Figure 51. 14-3-3σ suppresses pyruvate-to-lactate conversion in xenografted breast tumors.
(A) Flag-14-3-3σ induction remarkably diminishes ^{13}C pyruvate-to-^{13}C lactate flux in xenograft tumors. Pyruvate-to-lactate flux was measured by employing hyperpolarized ^{13}C-pyruvate tracer, following the time course at day 0 and day 14 (after Flag-14-3-3σ induction) (left panels).
(B) Magnetic Resonance spectra show Flag-14-3-3σ induction decreased of ^{13}C lactate concentration in tumors.
(C) Flag-14-3-3σ expression decelerates the rate constant of ^{13}C pyruvate-to- ^{13}C lactate reaction. k_{PL} represents the rate constant of ^{13}C pyruvate-to- ^{13}C lactate reaction. The ratio of $k_{PL\ day\ 14}$ / $k_{PL\ day\ 0}$ was calculated with (+) or without (-) induction of Flag-14-3-3σ. All data is represented as mean ± 95% CI.

Chapter 4. Discussions

Metabolic reprogramming has emerged as a new hallmark of cancers. Many oncogenes or tumor suppressor genes are deregulated, which leads to abnormal cellular bioenergetics that give cancer cells significant advantages either by providing fuel for cancer cell growth and proliferation or creating microenvironments that facilitate cancer invasion. Among alterations in cancer metabolism, increase in glycolysis and glutaminolysis are two of the most prominent metabolic reprogramming events in tumor (Dang, 2010a; Hanahan and Weinberg, 2011; Yeung et al., 2008). Furthermore, mitochondrial biogenesis is also essential for cancer cells because mitochondria provide not only energy but also important metabolites for rapid cell growth, proliferation and biosynthesis (Wallace, 2012). Therefore, blocking these metabolic processes could severely affect tumor cells.

Interestingly, our data indicate that 14-3-3σ could suppress all these three essential metabolic pathways by promoting the degradation of their main driver, c-Myc. Thus, our study reveals 14-3-3σ – Myc as a new axis of cancer metabolism regulation. In addition, our findings also suggest that the tumor suppressor 14-3-3σ could be considered as a potential target in anti-cancer metabolism therapy development.

4.1 Lack of 14-3-3σ enhances glucose uptake in cancer cells

Enhanced glucose uptake and increased glycolysis are common and important for most of cancer cells. Significantly, our clinical data analysis found an inverse correlation between 14-3-3σ expression and PET SUVs of breast tumors (Figures 13A, 13B, Table 3). This could be because 14-3-3σ deficiency leads to upregulation of glycolytic genes expression, especially glucose transporter genes, which are known targets of Myc (Figures 15A, 15B, 16). Moreover, our experiments on human cancer cell lines and mouse models confirm that 14-3-3σ can strongly inhibit the glucose uptake of cancer cells both *in vitro* and *in vivo* (Figures 19-23; 48-51), providing a new insight into our clinical observations.

The relationship between 14-3-3σ and PET SUVs could be further explained by the fact that 14-3-3σ promotes Myc degradation via ubiquitination (Figures 30, 31), thereby reducing the expression of important Myc-induced glucose transporters (Figures 15, 35). In addition to the regulation at the transcriptional level, we also observed that 14-3-3σ decreased Glut1 expression on cellular membrane surface (Figure 23). Thus, it is conceivable that 14-3-3σ suppresses glucose uptake by down-regulating the transcription and expression of important glucose transporters on cellular membrane surface.

4.2 14-3-3σ increases Myc degradation and suppresses Myc transcriptional activity

Myc is a major transcription factor that regulates multiple important cellular

processes, including metabolism. Therefore, a complete understanding about Myc stability regulation is essential. Our recent findings suggest that 14-3-3σ forms a homo-dimer to mediate the interaction between Myc and Pin1 (peptidylprolyl cis/trans isomerase, NIMA-interacting 1) (Wen et al., 2012). Through this interaction, Pin1 induces a conformational change in the c-Myc protein, which facilitates Protein Phosphatase 2A's dephosphorylation of c-Myc at Serine 62 (Amati, 2004; Yeh et al., 2004). Without a phosphate group at S62, c-Myc is degraded through an ubiquitin-mediated pathway (Welcker et al., 2004; Yada et al., 2004) (Figure 52).

Similarly, in this study, we found a negative correlation between 14-3-3σ and Myc protein levels in breast cancer patients' tumors (Figure 18) and xenograft breast tumor (Figure 49). In addition, 14-3-3σ induced Myc poly-ubiquitination, degradation and accelerated Myc turnover rate in several cancer cell lines (Figures 30, 31). This 14-3-3σ-mediated down-regulation of Myc protein stability translated into effects that negatively affect Myc target gene expression both *in vitro* and *in vivo*. Some of these genes are involved in glycolysis (Figures 33-37, 49), glutaminolysis (Figures 40, 41, 49, 50A), and mitochondrial biogenesis (Figures 42, 43, 44, 50B). This important functional link between Myc and 14-3-3σ provides an important insight into the relationship between metabolic dysregulation and the frequent loss of 14-3-3σ during tumorigenesis.

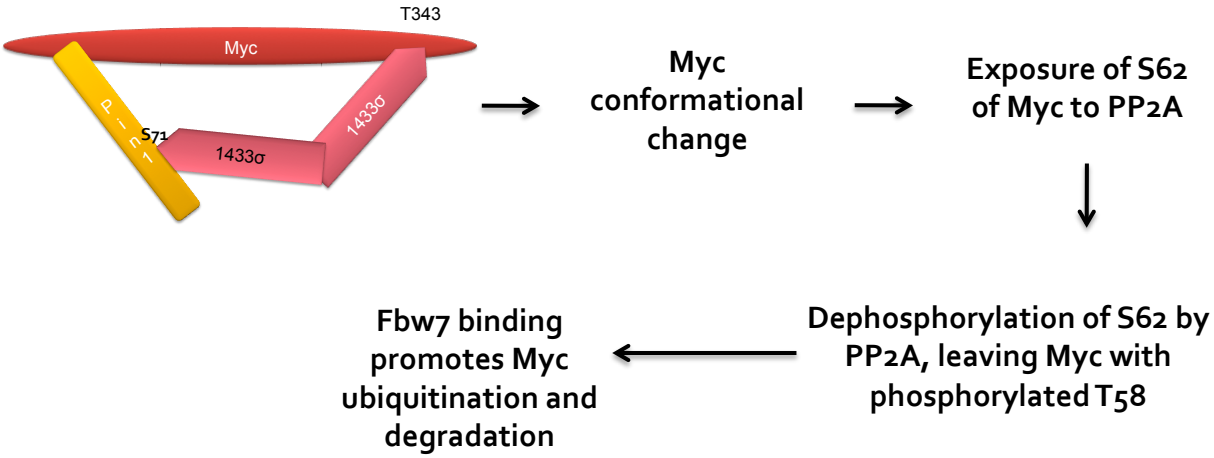
T343
Myc
S71
1433σ
1433σ
Myc conformational change
Exposure of S62 of Myc to PP2A
Dephosphorylation of S62 by PP2A, leaving Myc with phosphorylated T58
Fbw7 binding promotes Myc ubiquitination and degradation

Figure 52

Figure 52. The mechanism of 14-3-3σ-enhanced Myc poly-ubiquitination and degradation (adapted from Wen et al., 2012)**.** 14-3-3σ forms a homo-dimer to mediate the interaction between Myc and Pin1 (peptidylprolyl cis/trans isomerase, NIMA-interacting 1) by binding to phosphorylated T343 on Myc and phosphorylated S71 on Pin1 (Wen et al., 2012). Through this interaction, Pin1 induces a conformational change in the c-Myc protein, which facilitates Protein Phosphatase 2A's dephosphorylation of c-Myc at Serine 62 (Amati, 2004; Yeh et al., 2004). Without a phosphate group at S62, c-Myc with T58 phosphorylation is rapidly degraded through an ubiquitin-mediated pathway (Welcker et al., 2004; Yada et al., 2004).

4.3 14-3-3σ deficiency may facilitate tumor energy metabolism, cancer metastasis and progression

14-3-3σ expression is frequently down-regulated during tumorigenesis process (Ferguson et al., 2000; Lee and Lozano, 2006; Urano et al., 2002; Yang et al., 2006) as well as in many aggressive metastatic breast cancer cell lines (Figure 11). In this study, we showed that a high expression of 14-3-3σ in breast cancer patients' tumors is associated with increased breast cancer patients' overall survival and metastasis-free survival, while inversely correlated with tumor grade and glucose uptake of cancer cells (Figures 12, 13, Tables 2 and 3). The positive impact of 14-3-3σ in improving cancer patients' clinical outcomes could be in part attributed to its ability in suppressing three major Myc-induced cancer metabolic processes, i.e., glycolysis, glutaminolysis and mitochondrial biogenesis. In fact, it has been well documented that these cancer metabolic pathways are essential for tumor growth, proliferation, metastasis, survival and drug resistance (Dang, 2010a; Hanahan and Weinberg, 2011; Wallace, 2012; Yeung et al., 2008).

For instance, lactate, an important product of cancer aerobic glycolysis, has been shown to induce cancer cell invasion and metastasis. Lactate can significantly enhance cancer cell motility and facilitate the breaking down of extracellular matrix (Gatenby and Gillies, 2004). Lactate also stimulates the migration of epithelial cancer cells and promotes cancer metastasis to distant organs. For example, lactate administration increases lung metastasis in a breast cancer mouse model (Bonuccelli et al., 2011). In most of cancer cells, the increase in lactate production is primarily caused by the

elevation of Lactate Dehydrogenase A (*LDHA*) and glycolytic genes, which are induced by Myc and Hypoxia-Inducible Factor 1α (HIF1α) (Hanahan and Weinberg, 2011; Yeung et al., 2008). Data from our study demonstrate the significant suppressive impact of 14-3-3σ on lactate production. Our measurements indicate that the loss or knockdown of 14-3-3σ leads to elevated lactate production while re-expression of 14-3-3σ reduces lactate generation (Figures 24-28, 51). This elevation of lactate production upon 14-3-3σ deficiency is caused by the increase in glycolytic activity, glycolytic gene expression (including *LDHA*) and *PDHK1* upregulation (Figures 15, 16, 19-23, 30-37). Therefore loss of 14-3-3σ enhances lactate production and may facilitate cancer cells metastasis.

In addition, the fact that 14-3-3σ null cells have a high concentration of ATP means that cancer cells have an edge when it comes to cell growth and drug resistance (Figure 29). This is because ATP is both a major DNA precursor often used for repairing genetic damage and a key energy source for multidrug resistance efflux pumps that discard toxic chemotherapy agents (Yeung et al., 2008). Furthermore, ATP and NAD^+ from glycolysis can also be used by poly(ADP-ribose) polymerase (PARP-1) and ADP-ribosyl transferase to repair DNA damage caused by radiation and chemotherapy. Glycolysis also fuels pentose phosphate pathway (PPP) by providing glucose-6-phosphate. PPP generates nucleotides that are important for DNA damage repair. Moreover, PPP also supplies cancer cells with NADPH, a potent reductant that can be utilized by cytochrome P450 to detoxify toxic chemotherapy agents (Yeung et al., 2008). Thus, by blocking glycolysis, 14-3-3σ also contributes to reducing the resistance of tumors to anti-cancer therapies.

It has also been reported that glycolytic enzymes play important roles in cancer cell survival. For example, Hexokinase 2 (HK2) blocks cytochrome c release from mitochondria (Majewski et al., 2004; Pastorino et al., 2002), thereby protecting cancer cells from apoptosis. Indeed, our results show that 14-3-3σ expression reduces HK2 level while increasing caspase 3 cleavage in xenograft tumors (Figure 49). Additionally, Glucose-6-phosphate isomerase (*GPI*) has been shown to stimulate cell motility, an important step in the metastatic process (Funasaka et al., 2007) (Funasaka and Raz, 2007). In fact, our data showed that 14-3-3σ expression reduced GPI level (Figure 35). Therefore, the fact that loss of 14-3-3σ expression elevates the levels of these glycolytic enzymes has a broad impact not only on tumor bioenergetics but also other hallmarks of cancers.

4.4 14-3-3σ suppresses cancer glutaminolysis, mitochondria biogenesis and may affect amino acids, phospholipids and nucleotides biosynthesis

Glutaminolysis is both a major source of precursors for large-scale biosynthesis and a vital energy source for cancer cells (Dang, 2010a). In this process, glutamine is transported by glutamine transporters and is converted to α-ketoglutarate (α-KG) to replenish biosynthetic intermediates of the TCA cycle. It is important to point out that 14-3-3σ re-expression in 14-3-3σ null cells leads to the reduction of glutamate concentration levels, indicating that 14-3-3σ may suppress glutaminolysis (Figure 24C). Indeed, our biochemical data shows that re-expression of 14-3-3σ in 14-3-3σ null cells can down-regulate the Myc-activated genes involved in glutaminolysis (Figures 15, 40,

41, 49A, 50A). Given the important role of glutaminolysis in cancer metabolism, by suppressing this major metabolic pathway, 14-3-3σ may also negatively affect other metabolic processes in tumor cells.

Similarly, mitochondria are crucial for cancer cells because mitochondria are not only the cellular power stations but also factories that produce many important precursors for amino acid (oxaloacetate, α-ketoglutarate), lipid (citrate), heme group (succinyl CoA), and nucleotide (oxaloacetate transaminated to aspartate) biosyntheses. As a result, a strong decline in mitochondrial mass could have a deleterious impact on cancer cell growth (Wallace, 2012). Therefore, the fact that 14-3-3σ expression markedly reduced Myc-induced mitochondrial biogenesis, TFAM level and the expression of mitochondrial genes (Figures 42-44, 50B) suggests a widespread negative impact of 14-3-3σ on cancer metabolism. Indeed, our Nuclear Magnetic Resonance analysis demonstrated that 14-3-3σ expression correlates with a strong diminishment of many key amino acids (e.g., methionine, glutamate, glutamine, and arginine), phospholipid metabolites and precursors for nucleotide synthesis (Figure 24C). However, it is still unclear whether the reduction in amino acid and phospholipid levels is a direct effect of 14-3-3σ, a consequence of 14-3-3σ-mediated suppression of glycolysis, glutaminolysis and mitochondrial biogenesis, or both.

On the other hand, since Myc can induce multiple metabolic pathways, Myc helps cancer cells effectively adapt to microenvironments with fluctuating oxygen levels (both normoxia and hypoxia), and consume different sources of nutrients (e.g., glucose,

glutamine, among others) to fuel their metabolism and support their rapid proliferation. Therefore, by promoting Myc degradation, 14-3-3σ may severely affect the adaptability of cancer cells and the versatility of their metabolism.

4.5 Conclusions

In conclusion, this study identifies a new function of 14-3-3σ in controlling cancer metabolism, especially glycolysis, glutaminolysis and mitochondrial biogenesis. 14-3-3σ also has a negative and broad impact on cancer bioenergetics. In addition, 14-3-3σ exerts its suppressive influence on major cancer metabolic pathways by promoting c-Myc polyubiquitination and degradation.

Moreover, since 14-3-3σ is a direct p53 target gene, our findings may provide an additional insight into the regulation of cancer metabolism by p53. Furthermore, given the significantly positive impact of 14-3-3σ on patients' clinical outcomes and 14-3-3σ remarkable suppressive influence on cancer bioenergetics, we think that restoration of 14-3-3σ expression in cancer cells could be considered as a potential anti-cancer metabolism therapy.

4.6 Future research directions

Despite the new findings about the impact of 14-3-3σ on cancer metabolism from this study, there are still a couple of unanswered questions that could be considered as potential research directions in future. First of all, it is also important to determine whether 14-3-3σ can directly regulate the function, localization and stability of glycolytic enzymes. Our preliminary data suggest that 14-3-3σ may associate with Hexokinase 2

and suppress the function of this kinase, which implies a direct effect of 14-3-3σ on cancer glycolysis. Secondly, whether 14-3-3σ can regulate HIF1α is an interesting research direction. Our results show that 14-3-3σ can significantly inhibit glycolysis in hypoxia and down-regulates the expression of glycolytic enzymes (Figures 34 and 35). Since HIF1α is crucial for cancer cell survival and HIF1α is the major driver of glycolysis under hypoxic condition, it is intriguing to determine whether 14-3-3σ may block the activity or down-regulate this transcription factor. In addition, as 14-3-3σ can suppress tumorigenesis in multiple ways, for instance by suppressing cancer energy metabolism, decreasing cell proliferation, promoting c-Myc degradation, and stabilizing p53, restoration of 14-3-3σ expression in cancer cells using gene therapy or nanoparticles is a promising anti-cancer therapy.

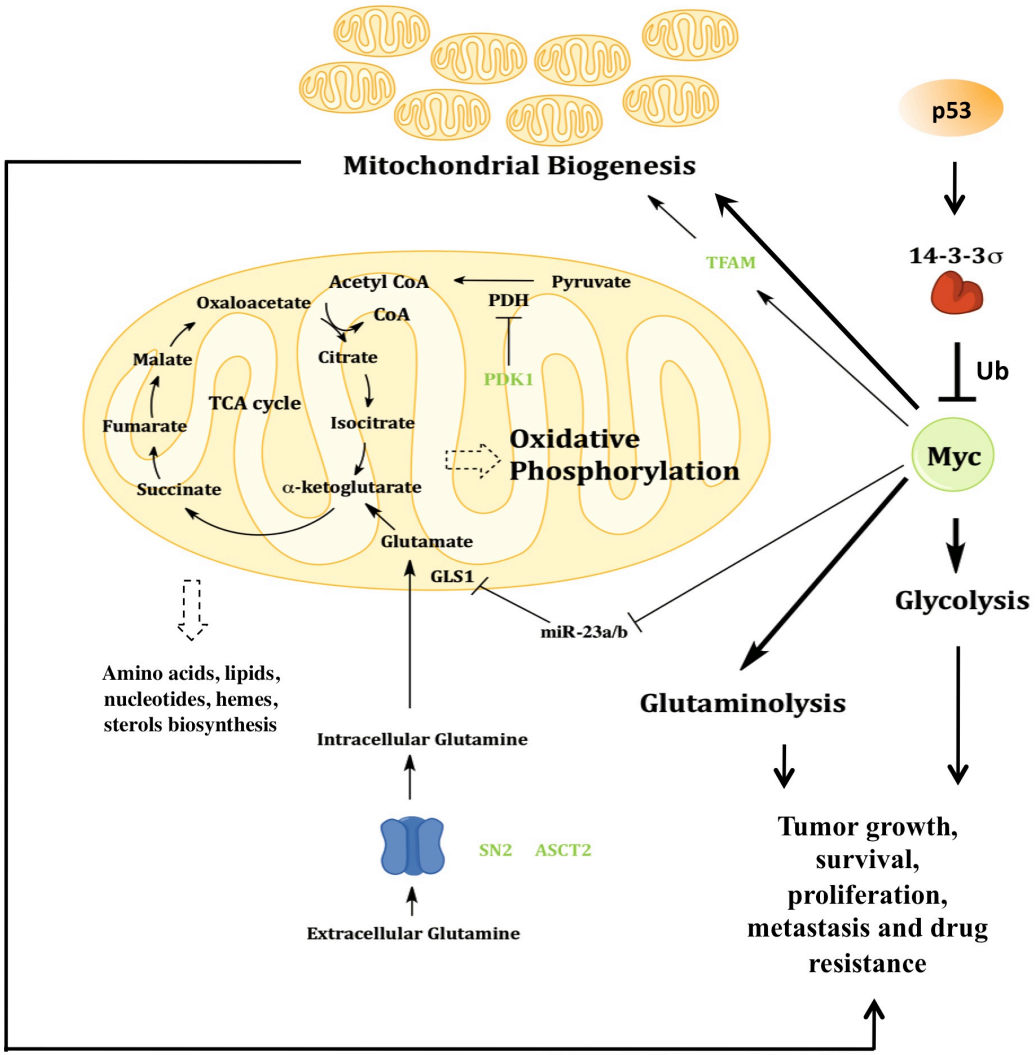
Mitochondrial Biogenesis
TFAM
p53
14-3-3σ
Ub
Myc
Acetyl CoA
Pyruvate
PDH
CoA
Oxaloacetate
Citrate
Malate
PDK1
TCA cycle
Isocitrate
Fumarate
Oxidative Phosphorylation
Succinate
α-ketoglutarate
Glutamate
GLS1
miR-23a/b
Glycolysis
Amino acids, lipids, nucleotides, hemes, sterols biosynthesis
Glutaminolysis
Intracellular Glutamine
SN2
ASCT2
Extracellular Glutamine
Tumor growth, survival, proliferation, metastasis and drug resistance

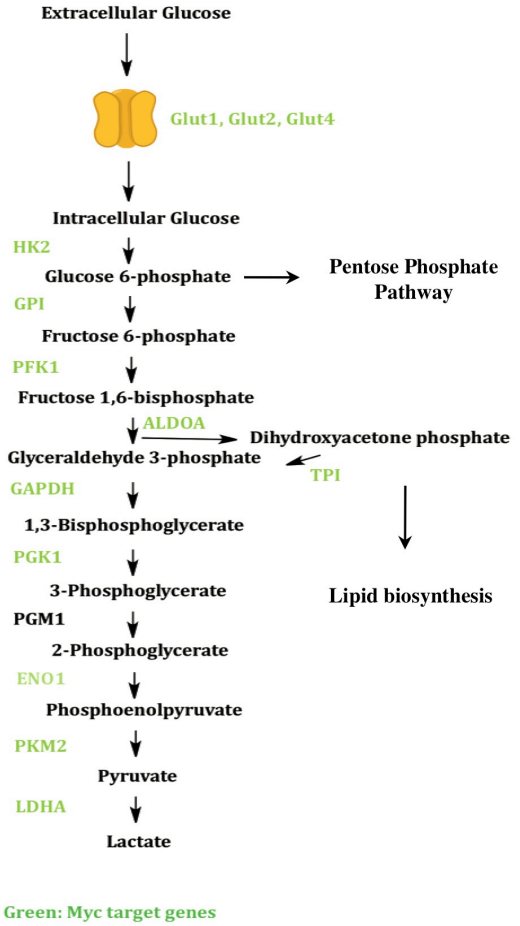
Extracellular Glucose
Glut1, Glut2, Glut4
Intracellular Glucose
HK2
Glucose 6-phosphate
Pentose Phosphate Pathway
GPI
Fructose 6-phosphate
PFK1
Fructose 1,6-bisphosphate
ALDOA
Dihydroxyacetone phosphate
Glyceraldehyde 3-phosphate
TPI
GAPDH
1,3-Bisphosphoglycerate
PGK1
3-Phosphoglycerate
Lipid biosynthesis
PGM1
2-Phosphoglycerate
ENO1
Phosphoenolpyruvate
PKM2
Pyruvate
LDHA
Lactate
Green: Myc target genes

Figure 53

Figure 53. 14-3-3σ has a broad negative impact on cancer metabolic network. Glycolysis and glutaminolysis provide important precursors and energy to support the rapid proliferation and large-scale biosynthesis in cancer cells. For instance, glucose-6-phosphate from glycolysis can be used in pentose phosphate pathway to synthesize nucleotides and NADPH. Dihydroxyacetone phosphate may be mobilized to produce lipids. Furthermore, the intermediates of TCA cycle that originate from glutaminolysis are important to generate amino acids, lipids, nucleotides, sterols, among other crucial macromolecules. The energy and metabolites derived from glycolysis and glutaminolysis are crucial for tumor growth, survival, proliferation, metastasis and resistance to anti-cancer therapies. On the other hand, mitochondrial biogenesis is also essential for tumorigenesis because mitochondria are the nexus of many energy production and metabolic pathways. Hence, mitochondria are vital for tumor cells to meet their constant demands for energy and materials to support their fast growth and division. Myc is a main driver of all these crucial cellular processes as well as other major metabolic pathways, enabling tumor cells to consume different nutrient sources for their survival and proliferation as well as to effectively adapt to various conditions. Therefore, the negative impact of 14-3-3σ on Myc stability results in a broad inhibitory effect on cancer bioenergetics and the versatility of their metabolism. Consequently, 14-3-3σ expression decreases metabolic activities in cancer cells and may ultimately suppress tumor growth, division, metastasis, survival and resistance to therapies. Thus, this study identifies a new function of 14-3-3σ in controlling cancer glycolysis, glutaminolysis and mitochondrial biogenesis by promoting Myc degradation, suggesting 14-3-3σ-Myc as a new regulatory axis of cancer metabolism. Moreover, since 14-3-3σ is a direct p53 target gene, these findings may provide an additional insight into the regulation of cancer metabolism by p53. Furthermore, based on the vital role of cancer metabolism in tumorigenesis and the remarkable inhibitory influence of 14-3-3σ on major cancer metabolic pathways, we think that restoration of 14-3-3σ expression in cancer cells could be considered as a anti-cancer metabolism therapy.

Chapter 5. References

Adhikary, S., and Eilers, M. (2005). Transcriptional regulation and transformation by Myc proteins. Nat Rev Mol Cell Biol 6, 635-645.

Amati, B. (2004). Myc degradation: dancing with ubiquitin ligases. Proc Natl Acad Sci U S A 101, 8843-8844.

Ardenkjaer-Larsen, J.H., Fridlund, B., Gram, A., Hansson, G., Hansson, L., Lerche, M.H., Servin, R., Thaning, M., and Golman, K. (2003). Increase in signal-to-noise ratio of > 10,000 times in liquid-state NMR. Proc Natl Acad Sci U S A 100, 10158-10163.

Bensaad, K., Tsuruta, A., Selak, M.A., Vidal, M.N., Nakano, K., Bartrons, R., Gottlieb, E., and Vousden, K.H. (2006). TIGAR, a p53-inducible regulator of glycolysis and apoptosis. Cell 126, 107-120.

Benzinger, A., Muster, N., Koch, H.B., Yates, J.R., 3rd, and Hermeking, H. (2005a). Targeted proteomic analysis of 14-3-3 sigma, a p53 effector commonly silenced in cancer. Mol Cell Proteomics 4, 785-795.

Benzinger, A., Popowicz, G.M., Joy, J.K., Majumdar, S., Holak, T.A., and Hermeking, H. (2005b). The crystal structure of the non-liganded 14-3-3sigma protein: insights into determinants of isoform specific ligand binding and dimerization. Cell Res 15, 219-227.

Bishop, J.M. (1982). Retroviruses and cancer genes. Advances in cancer research 37, 1-32.

Bishop, J.M. (1985). Viruses, genes, and cancer. II. Retroviruses and cancer genes. Cancer 55, 2329-2333.

Bishop, J.M., Baker, B., Fujita, D., McCombe, P., Sheiness, D., Smith, K., Spector, D.H., Stehelin, D., and Varmus, H.E. (1978). Genesis of a virus-transforming gene. National Cancer Institute monograph, 219-223.

Bister, K., and Jansen, H.W. (1986). Oncogenes in retroviruses and cells: biochemistry and molecular genetics. Advances in cancer research 47, 99-188.

Blackwell, T.K., Huang, J., Ma, A., Kretzner, L., Alt, F.W., Eisenman, R.N., and Weintraub, H. (1993). Binding of myc proteins to canonical and noncanonical DNA sequences. Mol Cell Biol 13, 5216-5224.

Blackwell, T.K., Kretzner, L., Blackwood, E.M., Eisenman, R.N., and Weintraub, H. (1990). Sequence-specific DNA binding by the c-Myc protein. Science 250, 1149-1151.

Blommaart, E.F., Luiken, J.J., Blommaart, P.J., van Woerkom, G.M., and Meijer, A.J. (1995). Phosphorylation of ribosomal protein S6 is inhibitory for autophagy in isolated rat hepatocytes. J Biol Chem 270, 2320-2326.

Bogacka, I., Xie, H., Bray, G.A., and Smith, S.R. (2005). Pioglitazone induces mitochondrial biogenesis in human subcutaneous adipose tissue in vivo. Diabetes 54, 1392-1399.

Bonnet, S., Archer, S.L., Allalunis-Turner, J., Haromy, A., Beaulieu, C., Thompson, R., Lee, C.T., Lopaschuk, G.D., Puttagunta, L., Harry, G., Hashimoto, K., Porter, C.J., Andrade, M.A., Thebaud, B., and Michelakis, E.D. (2007). A

mitochondria-K+ channel axis is suppressed in cancer and its normalization promotes apoptosis and inhibits cancer growth. Cancer Cell 11, 37-51.

Bonuccelli, G., Tsirigos, A., Whitaker-Menezes, D., Pavlides, S., Pestell, R.G., Chiavarina, B., Frank, P.G., Flomenberg, N., Howell, A., Martinez-Outschoorn, U.E., Sotgia, F., and Lisanti, M.P. (2011). Ketones and lactate "fuel" tumor growth and metastasis: Evidence that epithelial cancer cells use oxidative mitochondrial metabolism. Cell Cycle 9, 3506-3514.

Cavalli, L.R., Varella-Garcia, M., and Liang, B.C. (1997). Diminished tumorigenic phenotype after depletion of mitochondrial DNA. Cell growth & differentiation : the molecular biology journal of the American Association for Cancer Research 8, 1189-1198.

Chen, D.N. (1988). [Content of LDH isoenzyme and immunoglobulin in tears of patients with epidemic hemorrhagic conjunctivitis]. Zhonghua Yan Ke Za Zhi 24, 277-278.

Choi, H.H., Gully, C., Su, C.H., Velazquez-Torres, G., Chou, P.C., Tseng, C., Zhao, R., Phan, L., Shaiken, T., Chen, J., Yeung, S.C., and Lee, M.H. (2011). COP9 signalosome subunit 6 stabilizes COP1, which functions as an E3 ubiquitin ligase for 14-3-3sigma. Oncogene 30, 4791-4801.

Cong, L.N., Chen, H., Li, Y., Zhou, L., McGibbon, M.A., Taylor, S.I., and Quon, M.J. (1997). Physiological role of Akt in insulin-stimulated translocation of GLUT4 in transfected rat adipose cells. Mol Endocrinol 11, 1881-1890.

Dang, C.V. (1999). c-Myc target genes involved in cell growth, apoptosis, and metabolism. Mol Cell Biol 19, 1-11.

Dang, C.V. (2009). MYC, microRNAs and glutamine addiction in cancers. Cell Cycle 8, 3243-3245.

Dang, C.V. (2010a). Glutaminolysis: supplying carbon or nitrogen or both for cancer cells? Cell Cycle 9, 3884-3886.

Dang, C.V. (2010b). Rethinking the Warburg effect with Myc micromanaging glutamine metabolism. Cancer Res 70, 859-862.

Dang, C.V., Le, A., and Gao, P. (2009). MYC-induced cancer cell energy metabolism and therapeutic opportunities. Clin Cancer Res 15, 6479-6483.

Dang, C.V., Lewis, B.C., Dolde, C., Dang, G., and Shim, H. (1997). Oncogenes in tumor metabolism, tumorigenesis, and apoptosis. Journal of bioenergetics and biomembranes 29, 345-354.

Dang, C.V., and Semenza, G.L. (1999). Oncogenic alterations of metabolism. Trends in biochemical sciences 24, 68-72.

Dann, S.G., and Thomas, G. (2006). The amino acid sensitive TOR pathway from yeast to mammals. FEBS letters 580, 2821-2829.

Davis, A.C., Wims, M., Spotts, G.D., Hann, S.R., and Bradley, A. (1993). A null c-myc mutation causes lethality before 10.5 days of gestation in homozygotes and reduced fertility in heterozygous female mice. Genes & development 7, 671-682.

DeBerardinis, R.J., Lum, J.J., Hatzivassiliou, G., and Thompson, C.B. (2008a). The biology of cancer: metabolic reprogramming fuels cell growth and proliferation. Cell Metab 7, 11-20.

DeBerardinis, R.J., Mancuso, A., Daikhin, E., Nissim, I., Yudkoff, M., Wehrli, S., and Thompson, C.B. (2007). Beyond aerobic glycolysis: transformed cells can engage in glutamine metabolism that exceeds the requirement for protein and nucleotide synthesis. Proc Natl Acad Sci U S A 104, 19345-19350.

Deberardinis, R.J., Sayed, N., Ditsworth, D., and Thompson, C.B. (2008b). Brick by brick: metabolism and tumor cell growth. Curr Opin Genet Dev 18, 54-61.

Desjardins, P., Frost, E., and Morais, R. (1985). Ethidium bromide-induced loss of mitochondrial DNA from primary chicken embryo fibroblasts. Mol Cell Biol 5, 1163-1169.

Eng, C.H., Yu, K., Lucas, J., White, E., and Abraham, R.T. (2010). Ammonia derived from glutaminolysis is a diffusible regulator of autophagy. Sci Signal 3, ra31.

Facchini, L.M., and Penn, L.Z. (1998). The molecular role of Myc in growth and transformation: recent discoveries lead to new insights. FASEB journal : official publication of the Federation of American Societies for Experimental Biology 12, 633-651.

Ferguson, A.T., Evron, E., Umbricht, C.B., Pandita, T.K., Chan, T.A., Hermeking, H., Marks, J.R., Lambers, A.R., Futreal, P.A., Stampfer, M.R., and Sukumar, S. (2000). High frequency of hypermethylation at the 14-3-3 sigma locus

leads to gene silencing in breast cancer. Proc Natl Acad Sci U S A 97, 6049-6054.

Feron, O. (2009). Pyruvate into lactate and back: from the Warburg effect to symbiotic energy fuel exchange in cancer cells. Radiother Oncol 92, 329-333.

Fox, H.L., Kimball, S.R., Jefferson, L.S., and Lynch, C.J. (1998). Amino acids stimulate phosphorylation of p70S6k and organization of rat adipocytes into multicellular clusters. The American journal of physiology 274, C206-213.

Funasaka, T., Hu, H., Yanagawa, T., Hogan, V., and Raz, A. (2007). Down-regulation of phosphoglucose isomerase/autocrine motility factor results in mesenchymal-to-epithelial transition of human lung fibrosarcoma cells. Cancer Res 67, 4236-4243.

Funasaka, T., and Raz, A. (2007). The role of autocrine motility factor in tumor and tumor microenvironment. Cancer Metastasis Rev 26, 725-735.

Gao, P., Tchernyshyov, I., Chang, T.C., Lee, Y.S., Kita, K., Ochi, T., Zeller, K.I., De Marzo, A.M., Van Eyk, J.E., Mendell, J.T., and Dang, C.V. (2009). c-Myc suppression of miR-23a/b enhances mitochondrial glutaminase expression and glutamine metabolism. Nature 458, 762-765.

Gatenby, R.A., and Gillies, R.J. (2004). Why do cancers have high aerobic glycolysis? Nature reviews. Cancer 4, 891-899.

Golman, K., in 't Zandt, R., and Thaning, M. (2006). Real-time metabolic imaging. Proc Natl Acad Sci U S A 103, 11270-11275.

Green, D.R., and Chipuk, J.E. (2006). p53 and metabolism: Inside the TIGAR. Cell 126, 30-32.

Gruning, N.M., Rinnerthaler, M., Bluemlein, K., Mulleder, M., Wamelink, M.M., Lehrach, H., Jakobs, C., Breitenbach, M., and Ralser, M. (2011). Pyruvate kinase triggers a metabolic feedback loop that controls redox metabolism in respiring cells. Cell Metab 14, 415-427.

Hanahan, D., and Weinberg, R.A. (2011). Hallmarks of cancer: the next generation. Cell 144, 646-674.

Hara, K., Yonezawa, K., Weng, Q.P., Kozlowski, M.T., Belham, C., and Avruch, J. (1998). Amino acid sufficiency and mTOR regulate p70 S6 kinase and eIF-4E BP1 through a common effector mechanism. J Biol Chem 273, 14484-14494.

Harris, T., Eliyahu, G., Frydman, L., and Degani, H. (2009). Kinetics of hyperpolarized 13C1-pyruvate transport and metabolism in living human breast cancer cells. Proc Natl Acad Sci U S A 106, 18131-18136.

Henriksson, M., and Luscher, B. (1996). Proteins of the Myc network: essential regulators of cell growth and differentiation. Advances in cancer research 68, 109-182.

Hermeking, H., Lengauer, C., Polyak, K., He, T.C., Zhang, L., Thiagalingam, S., Kinzler, K.W., and Vogelstein, B. (1997). 14-3-3 sigma is a p53-regulated inhibitor of G2/M progression. Molecular cell 1, 3-11.

Hsu, P.P., and Sabatini, D.M. (2008). Cancer cell metabolism: Warburg and beyond. Cell 134, 703-707.

Ide, T., Brown-Endres, L., Chu, K., Ongusaha, P.P., Ohtsuka, T., El-Deiry, W.S., Aaronson, S.A., and Lee, S.W. (2009). GAMT, a p53-inducible modulator of apoptosis, is critical for the adaptive response to nutrient stress. Molecular cell 36, 379-392.

Jones, R.G., and Thompson, C.B. (2009). Tumor suppressors and cell metabolism: a recipe for cancer growth. Genes & development 23, 537-548.

Kennedy, K.M., and Dewhirst, M.W. (2010). Tumor metabolism of lactate: the influence and therapeutic potential for MCT and CD147 regulation. Future Oncol 6, 127-148.

Kim, J.W., Gao, P., Liu, Y.C., Semenza, G.L., and Dang, C.V. (2007). Hypoxia-inducible factor 1 and dysregulated c-Myc cooperatively induce vascular endothelial growth factor and metabolic switches hexokinase 2 and pyruvate dehydrogenase kinase 1. Mol Cell Biol 27, 7381-7393.

Kim, J.W., Zeller, K.I., Wang, Y., Jegga, A.G., Aronow, B.J., O'Donnell, K.A., and Dang, C.V. (2004). Evaluation of myc E-box phylogenetic footprints in glycolytic genes by chromatin immunoprecipitation assays. Mol Cell Biol 24, 5923-5936.

King, M.P., and Attardi, G. (1989). Human cells lacking mtDNA: repopulation with exogenous mitochondria by complementation. Science 246, 500-503.

Kohn, A.D., Summers, S.A., Birnbaum, M.J., and Roth, R.A. (1996). Expression of a constitutively active Akt Ser/Thr kinase in 3T3-L1 adipocytes stimulates glucose uptake and glucose transporter 4 translocation. J Biol Chem 271, 31372-31378.

Lee, M.H., and Lozano, G. (2006). Regulation of the p53-MDM2 pathway by 14-3-3 sigma and other proteins. Seminars in cancer biology 16, 225-234.

Lemaitre, J.M., Buckle, R.S., and Mechali, M. (1996). c-Myc in the control of cell proliferation and embryonic development. Advances in cancer research 70, 95-144.

Li, F., Wang, Y., Zeller, K.I., Potter, J.J., Wonsey, D.R., O'Donnell, K.A., Kim, J.W., Yustein, J.T., Lee, L.A., and Dang, C.V. (2005). Myc stimulates nuclearly encoded mitochondrial genes and mitochondrial biogenesis. Mol Cell Biol 25, 6225-6234.

Magda, D., Lecane, P., Prescott, J., Thiemann, P., Ma, X., Dranchak, P.K., Toleno, D.M., Ramaswamy, K., Siegmund, K.D., and Hacia, J.G. (2008). mtDNA depletion confers specific gene expression profiles in human cells grown in culture and in xenograft. BMC genomics 9, 521.

Majewski, N., Nogueira, V., Robey, R.B., and Hay, N. (2004). Akt inhibits apoptosis downstream of BID cleavage via a glucose-dependent mechanism involving mitochondrial hexokinases. Mol Cell Biol 24, 730-740.

Marcu, K.B., Bossone, S.A., and Patel, A.J. (1992). myc function and regulation. Annual review of biochemistry 61, 809-860.

Matoba, S., Kang, J.G., Patino, W.D., Wragg, A., Boehm, M., Gavrilova, O., Hurley, P.J., Bunz, F., and Hwang, P.M. (2006). p53 regulates mitochondrial respiration. Science 312, 1650-1653.

Mazurek, S., Boschek, C.B., and Eigenbrodt, E. (1997). The role of phosphometabolites in cell proliferation, energy metabolism, and tumor therapy. Journal of bioenergetics and biomembranes 29, 315-330.

Meng, M., Chen, S., Lao, T., Liang, D., and Sang, N. (2010). Nitrogen anabolism underlies the importance of glutaminolysis in proliferating cells. Cell Cycle 9, 3921-3932.

Morais, R., Zinkewich-Peotti, K., Parent, M., Wang, H., Babai, F., and Zollinger, M. (1994). Tumor-forming ability in athymic nude mice of human cell lines devoid of mitochondrial DNA. Cancer Res 54, 3889-3896.

Nicklin, P., Bergman, P., Zhang, B., Triantafellow, E., Wang, H., Nyfeler, B., Yang, H., Hild, M., Kung, C., Wilson, C., Myer, V.E., MacKeigan, J.P., Porter, J.A., Wang, Y.K., Cantley, L.C., Finan, P.M., and Murphy, L.O. (2009). Bidirectional transport of amino acids regulates mTOR and autophagy. Cell 136, 521-534.

Pastorino, J.G., Hoek, J.B., and Shulga, N. (2005). Activation of glycogen synthase kinase 3beta disrupts the binding of hexokinase II to mitochondria by phosphorylating voltage-dependent anion channel and potentiates chemotherapy-induced cytotoxicity. Cancer Res 65, 10545-10554.

Pastorino, J.G., Shulga, N., and Hoek, J.B. (2002). Mitochondrial binding of hexokinase II inhibits Bax-induced cytochrome c release and apoptosis. J Biol Chem 277, 7610-7618.

Potter, V.R. (1958). The biochemical approach to the cancer problem. Fed Proc 17, 691-697.

Prendergast, G.C., and Ziff, E.B. (1991). Methylation-sensitive sequence-specific DNA binding by the c-Myc basic region. Science 251, 186-189.

Schwartzenberg-Bar-Yoseph, F., Armoni, M., and Karnieli, E. (2004). The tumor suppressor p53 down-regulates glucose transporters GLUT1 and GLUT4 gene expression. Cancer Res 64, 2627-2633.

Semenza, G.L. (2008). Tumor metabolism: cancer cells give and take lactate. J Clin Invest 118, 3835-3837.

Sheiness, D., Fanshier, L., and Bishop, J.M. (1978). Identification of nucleotide sequences which may encode the oncogenic capacity of avian retrovirus MC29. Journal of virology 28, 600-610.

Spencer, C.A., and Groudine, M. (1991). Control of c-myc regulation in normal and neoplastic cells. Advances in cancer research 56, 1-48.

Urano, T., Saito, T., Tsukui, T., Fujita, M., Hosoi, T., Muramatsu, M., Ouchi, Y., and Inoue, S. (2002). Efp targets 14-3-3 sigma for proteolysis and promotes breast tumour growth. Nature 417, 871-875.

Vander Heiden, M.G., Cantley, L.C., and Thompson, C.B. (2009). Understanding the Warburg effect: the metabolic requirements of cell proliferation. Science 324, 1029-1033.

Verdoodt, B., Benzinger, A., Popowicz, G.M., Holak, T.A., and Hermeking, H. (2006). Characterization of 14-3-3sigma dimerization determinants:

requirement of homodimerization for inhibition of cell proliferation. Cell Cycle 5, 2920-2926.

Vousden, K.H., and Ryan, K.M. (2009). p53 and metabolism. Nature reviews. Cancer 9, 691-700.

Wallace, D.C. (2012). Mitochondria and cancer. Nature reviews. Cancer 12, 685-698.

Warburg, O. (1930). On metabolism of tumors. London: Constable.

Warburg, O. (1956a). On respiratory impairment in cancer cells. Science 124, 269-270.

Warburg, O. (1956b). On the origin of cancer cells. Science 123, 309-314.

Weinberg, F., Hamanaka, R., Wheaton, W.W., Weinberg, S., Joseph, J., Lopez, M., Kalyanaraman, B., Mutlu, G.M., Budinger, G.R., and Chandel, N.S. (2010). Mitochondrial metabolism and ROS generation are essential for Kras-mediated tumorigenicity. Proc Natl Acad Sci U S A 107, 8788-8793.

Welcker, M., Orian, A., Grim, J.E., Eisenman, R.N., and Clurman, B.E. (2004). A nucleolar isoform of the Fbw7 ubiquitin ligase regulates c-Myc and cell size. Current biology : CB 14, 1852-1857.

Wen, Y.Y., Chou, P.C., Pham, L., Su, C.H., Chen, J., Hsieh, Y.C., Xue, Y.-W., Qu, C.-J., Gully, C., Parreno, K., Teng, C., Hsu, S.L., Yeung, S.C., Wang, H.M., and Lee, M.H. (2012). DNA damage-mediated c-Myc degradation requires 14-3-3 sigma. Cancer Hallmarks in press.

Wieman, H.L., Wofford, J.A., and Rathmell, J.C. (2007). Cytokine stimulation promotes glucose uptake via phosphatidylinositol-3 kinase/Akt regulation of Glut1 activity and trafficking. Mol Biol Cell 18, 1437-1446.

Wilker, E.W., Grant, R.A., Artim, S.C., and Yaffe, M.B. (2005). A structural basis for 14-3-3sigma functional specificity. J Biol Chem 280, 18891-18898.

Wise, D.R., DeBerardinis, R.J., Mancuso, A., Sayed, N., Zhang, X.Y., Pfeiffer, H.K., Nissim, I., Daikhin, E., Yudkoff, M., McMahon, S.B., and Thompson, C.B. (2008). Myc regulates a transcriptional program that stimulates mitochondrial glutaminolysis and leads to glutamine addiction. Proc Natl Acad Sci U S A 105, 18782-18787.

Wise, D.R., and Thompson, C.B. (2010). Glutamine addiction: a new therapeutic target in cancer. Trends in biochemical sciences 35, 427-433.

Wu, M., Neilson, A., Swift, A.L., Moran, R., Tamagnine, J., Parslow, D., Armistead, S., Lemire, K., Orrell, J., Teich, J., Chomicz, S., and Ferrick, D.A. (2007). Multiparameter metabolic analysis reveals a close link between attenuated mitochondrial bioenergetic function and enhanced glycolysis dependency in human tumor cells. Am J Physiol Cell Physiol 292, C125-136.

Xu, G., Kwon, G., Marshall, C.A., Lin, T.A., Lawrence, J.C., Jr., and McDaniel, M.L. (1998). Branched-chain amino acids are essential in the regulation of PHAS-I and p70 S6 kinase by pancreatic beta-cells. A possible role in protein translation and mitogenic signaling. J Biol Chem 273, 28178-28184.

Yada, M., Hatakeyama, S., Kamura, T., Nishiyama, M., Tsunematsu, R., Imaki, H., Ishida, N., Okumura, F., Nakayama, K., and Nakayama, K.I. (2004).

Phosphorylation-dependent degradation of c-Myc is mediated by the F-box protein Fbw7. The EMBO journal 23, 2116-2125.

Yang , H., Wen , Y.Y., Zhao, R., Lin, Y.L., Fournier , K., Yang, H.Y., Wu, H.B., Qiu, Y., Diaz, J., Laronga, C., and Lee, M.H. (2006). DNA damage-induced protein 14-3-3 sigma inhibits protein kinase B/Akt activation and suppresses Akt-activated cancer. Cancer Res 66, 3096-3105.

Yang, H., Zhao, R., and Lee, M.H. (2006). 14-3-3sigma, a p53 regulator, suppresses tumor growth of nasopharyngeal carcinoma. Mol Cancer Ther 5, 253-260.

Yang, H.Y., Wen, Y.Y., Chen, C.H., Lozano, G., and Lee, M.H. (2003). 14-3-3sigma Positively Regulates p53 and Suppresses Tumor Growth. Mol Cell Biol 23, 7096-7107.

Yang, H.Y., Wen, Y.Y., Lin, Y.I., Pham, L., Su, C.H., Yang, H., Chen, J., and Lee, M.H. (2007). Roles for negative cell regulator 14-3-3sigma in control of MDM2 activities. Oncogene 26, 7355-7362.

Yeh, E., Cunningham, M., Arnold, H., Chasse, D., Monteith, T., Ivaldi, G., Hahn, W.C., Stukenberg, P.T., Shenolikar, S., Uchida, T., Counter, C.M., Nevins, J.R., Means, A.R., and Sears, R. (2004). A signalling pathway controlling c-Myc degradation that impacts oncogenic transformation of human cells. Nature cell biology 6, 308-318.

Yeung, S.J., Pan, J., and Lee, M.H. (2008). Roles of p53, MYC and HIF-1 in regulating glycolysis - the seventh hallmark of cancer. Cell Mol Life Sci 65, 3981-3999.

Ying, W., Alano, C.C., Garnier, P., and Swanson, R.A. (2005). NAD+ as a metabolic link between DNA damage and cell death. Journal of neuroscience research 79, 216-223.

Yuneva, M., Zamboni, N., Oefner, P., Sachidanandam, R., and Lazebnik, Y. (2007). Deficiency in glutamine but not glucose induces MYC-dependent apoptosis in human cells. The Journal of cell biology 178, 93-105.

Chapter 6. Vita

Liem Minh Phan was born in Nha Trang City, Vietnam on January 30th, 1983, the son of Mr. Chanh Minh Phan and Mrs. Hong Thi-Cam Tran. After graduating from Nguyen Van Troi High School in Nha Trang in 2001, he entered Vietnam National University College of Natural Sciences in Ho Chi Minh City, Vietnam. In 2005, he received a graduate fellowship from Vietnam Education Foundation, a US-Congress foundation established to promote the relationship between US and Vietnam by enhancing the development of science and technology in Vietnam. He enrolled The University of Texas Graduate School of Biomedical Sciences in September 2005, where he conducted his PhD degree project under the guidance of Dr. Mong-Hong Lee, Ph.D., at the Department of Molecular and Cellular Oncology, The University of Texas MD Anderson Cancer Center. He was awarded the degree of Doctor of Philosophy in December 2012.

Publications:

1. **Liem Phan**, Ping-Chieh Chou, Guermarie Velazquez-Torres, Ismael Samudio, Kenneth Parreno, Yaling Huang, Chieh Tseng, Thuy Vu, Chris Gully, Chun-Hui Su, Edward Wang, Jian Chen, Hyun-Ho Choi, Enrique Fuentes-Mattei, Ji-Hyun Shin, Christine Shiang, Brian Grabiner, Marzenna Blonska, Yiping Shao, Dianna Cody, Jorge Delacerda, Charles Kingsley, Douglas Webb, Colin Carlock, Zhongguo Zhou, Yun-Chih Hsieh, Jaehyuk Lee, Andrew Elliott, Marc Ramirez, Jim Bankson, John Hazle, Yongxing Wang, Lei Li, Shaofan Weng, Xin Lin, Hua Wang, Huamin Wang, Aijun Zhang, Xuefeng Xia, Yun Wu, Wei Yang, Lajos Pusztai, Sai-Ching Yeung, and Mong-Hong Lee. The tumor suppressor 14-3-3sigma is a new regulator of cancer metabolism. **Cell Metabolism** (2012) (in revision).

2. Chieh-Lin Teng, Yun-Chi Hsieh, **Liem Phan**, Jihyun Shin, Chris Gully, Guermarie Velazquez-Torres, Stephen Skerl, Sai-Ching J. Yeung, Shih-Lan Hsu and Mong-Hong Lee. FBXW7 is involved in Aurora B degradation. **Cell Cycle** 11:21, 1–10; November 1, 2012

3. Chun Chi Wu, Tsung-Ying Yang, Chang-Tze Ricky Yu, **Liem Phan**, Cristina Ivan, Anil K. Sood, Shih-Lan Hsu, Mong-Hong Lee. p53 negatively regulates Aurora-A and is involved in centrosome formation. **Cell Cycle (2012)** (accepted for publication)

4. YY Wen, P Chou, **L Phan**, J Chen, G Velazquez-Torres, CH Su, SC Yeung, and MH Lee. The role of 14-3-3sigma in Myc regulation. **Cancer Hallmark** (2012) (in press).

5. C Gully, G Velazquez-Torres, JH Shin, C Carlock, E Fuentes-Mattei, E Wang, J Chen, D Rothenberg, H Adams, HH Choi, S Guma**, L Phan**, P Chou, CH Su, F Zhang, SC Yeung and MH Lee. Aurora B kinase phosphorylates and instigages degradation of p53. **Proceedings of National Academy of Sciences** (2012). May 18, 2012, doi: 10.1073/pnas.1110287109

6. J Chen, R Zhao, JH Shin, **L Phan**, H Wang, Y Xue, P Chou, S Post, Z Zhou, C Gully, G Velazquez-Torres, E Fuentes-Mattei, CH Su, G Yeung, K Ohshiro, Y Qiao, T Shaikenov, HM Wang, SC Yeung, MH Lee. Role of COP 9 signalosome in lymphomagenesis. **Cancer Cell** (2012) (in revision).

7. MH Lee, R Zhao, **L Phan**, SC Yeung. Roles of COP9 signalosome in cancer. **Cell Cycle**. 2011. 10(18) : 3057-3066.

8. H-H Choi, C Gully, C-H Su, G Velazquez-Torres, P-C Chou, C Tseng, R. Zhao, **L Phan**, T Shaikenov, J Chen, S-C Yeung, M-H Lee. COP 9 Signalosome Subunit 6 Stabilizes COP1, a novel E3 Ubiquitin Ligase for 14-3-3 sigma. **Oncogene**. (2011) 30: 4791-4801.

9. C-H Su, R Zhao, F Zhang, C Qu, B Chen, YH Feng, **L Phan**, J Chen, H Wang, HM Wang, SC Yeung, MH Lee. 14-3-3sigma exerts tumor-suppressor activity mediated by regulation of COP1 stability. **Cancer Research** (2011). 71(3):884-894.

10. M McKeller, R Rangel, C Cande, J Sims-Mourtada, B Ortiz-Quintero, W Ma, **L Phan**, S Herrera-Rodriguez, C Kashi, V Melnikova, S Shishodia, B Aggarwal, M Blackburn, G Kroemer, K Singh and H Martinez-Valdez. Vital function of PRELI and essential requirement of its LEA motif. **Cell Death and Disease** (2010) 1, 10.1038.

11. H-Y Yang, Y-Y Wen, Y-I Lin, **L Phan**, C-H Su, H Yang, J Chen and M-H Lee. Roles of negative cell regulator 14-3-3σ in control of MDM2 activities. **Oncogene** (2007) 26, 73557362.